

**Parvoviral Interactions with the Cytoskeleton:
Exposing Vimentin – the Forgotten Player**

by

Nikta Fay

B.Sc., The University of British Columbia, 2008

A THESIS SUBMITTED IN PARTIAL FULFILLMENT OF
THE REQUIREMENTS FOR THE DEGREE OF

DOCTOR OF PHILOSOPHY

in

THE FACULTY OF GRADUATE AND POSTDOCTORAL STUDIES
(Zoology)

THE UNIVERSITY OF BRITISH COLUMBIA

(Vancouver)

October 2014

© Nikta Fay, 2014

Abstract

There are three structurally and functionally distinct cytoskeleton components: actin filaments, microtubules, and intermediate filaments (IFs). Among the three cytoskeleton networks IFs are understudied; consequently, there is a lack of information about the role of IFs during early viral infection. IFs have long been known to serve structural functions within the cell, and recently, additional functions have been elucidated, including novel roles during infection by many viruses. During early infection with the parvovirus minute virus of mice (MVM), prior to viral replication, I have found that the virus induces dramatic morphological changes in mouse fibroblast cells. This observed change in the shape of infected cells may be a result of the virus using the host cytoskeleton to aid in the mechanism of intracellular trafficking. Thus, this thesis focuses on MVM and its effects on the cytoskeleton components, especially IFs, during infection. Using fluorescence microscopy techniques, I found that during early infection with MVM, after endosomal escape, the vimentin IF network was considerably altered, yielding collapsed immunofluorescence staining near the nuclear periphery. Furthermore, I found that vimentin plays an important role in the infection cycle of MVM. The number of cells successfully replicating MVM was reduced in infected cells in which the vimentin network was pharmacologically modified or in cells lacking a vimentin network; viral endocytosis, however, remained unaltered. Perinuclear accumulation of MVM-containing vesicles and progression of MVM through the endocytic pathway was reduced in cells lacking vimentin. Cells lacking vimentin, accumulated virions in early endosomes up to 2 h post-infection compared to wild type cells. Thus, my data supports

a model where vimentin facilitates a productive MVM infection, presenting possibly a dual role: (1) during progression of MVM through the endocytic pathway and (2) following MVM escape from endosomes.

Preface

Sections of Chapters 3 and 4 have been published in a peer-reviewed journal:

- **Nikta Fay** and Panté N. (2013). The intermediate filament network protein, vimentin, is required for parvoviral infection. *Virology* **444**: 181-90
doi: 10.1016/j.virol.2013.06.009
<http://www.sciencedirect.com/science/article/pii/S0042682213003589>

Some of the work during my PhD was performed in collaboration with people within and outside the Panté lab. Dr. Igor Etingov, a post-doctoral fellow, assisted with optimization of the *in situ* hybridization experiments as presented in Chapter 3 and 4. The atomic force microscopy study, presented in Chapter 3, was done in collaboration with the lab of Dr. Christopher Yip at the University of Toronto. Dr. Amy Won, a post-doctoral fellow in his lab, performed the AFM measurements.

I also supervised, Janet Xu, an NSERC-USRA funded undergraduate student, who assisted in repeating the immunofluorescence studies of actin filaments (Fig. 3-10).

I designed, performed, and analyzed the data from all experiments with the guidance of my supervisor Dr. Nelly Panté. I wrote the first draft of the manuscript presented in Chapters 3 and 4, which was then further revised by Dr. Nelly Panté. Chapter 1 contains work that I plan to submit in the near future. The data presented is most up-to-date at the time of thesis completion.

The research presented in this thesis was approved by the UBC Bio-Safety Committee (Certificate B10-0057).

Table of Contents

Abstract	ii
Preface	iv
Table of Contents	v
List of Tables	x
List of Figures	xi
List of Abbreviations	xiii
Acknowledgements	xv
Dedication	xvii
Chapter 1 – Introduction	1
1.1 Virus interactions with actin filaments and microtubules	2
1.1.1 Actin filaments promote viral cell entry	2
1.1.2 The formation of actin tails aid viral transport	5
1.1.3 Microtubules provide tracks for viral cytoplasmic transport	6
1.2 Viruses and the forgotten player: intermediate filaments	9
1.2.1 Viruses interact with cell surface-expressed vimentin	13
1.2.2 Viruses use vimentin to form protective cages and replication complexes resembling aggresomes	17
1.2.3 Viruses require an intact vimentin network, likely for cytoplasmic trafficking	22
1.3 Parvovirus	24
1.3.1 Introduction to parvoviruses	24
1.3.2 Associated parvoviral disease	25
1.3.3 Parvovirus organization of genome and viral proteins	26
1.3.4 Parvovirus infection cycle	28
1.3.5 Parvovirus and the cytoskeleton	32
1.3.6 Therapeutic applications	33
1.4 Thesis objectives	35

1.4.1 Aim 1: To determine the morphological effects on the cytoskeleton upon infection with MVM.....	36
1.4.2 Aim 2: To determine whether vimentin has an effect on the MVM infection cycle	36
1.4.3 Aim 3: To determine the specific role of the vimentin network during MVM infection	37
Chapter 2 – Materials and Methods.....	38
2.1 Cells and tissue culture tissue culture	38
2.2 Antibodies	38
2.3 Purification of MVM and infection.....	40
2.3.1 MVM purification	40
2.3.2 MVM infection	42
2.4 Fluorescence microscopy	42
2.4.1 Immunofluorescence microscopy	42
2.4.2 Fluorescence <i>in situ</i> hybridization of MVM DNA combined with immunostaining of MVM capsid and lamin-B.....	44
2.5 2D-Fluorescence difference gel electrophoresis (2D-DIGE) analysis	48
2.6 Western blot of vimentin.....	48
2.7 Atomic force microscopy	49
2.8 Drug treatments	50
2.8.1 Acrylamide treatment.....	50
2.8.2 Bafilomycin A1 treatment.....	51
2.9 Cell growth curves.....	51
2.10 Statistical analysis	52
Chapter 3 – MVM Induces Morphological Changes to the Host Cell During Infection	53
3.1 Introduction	53
3.2 Results	54
3.2.1 MVM causes morphological changes in the cell and alters the vimentin filament network 2 h P.I.	54
3.2.2 MVM persists to rearrange the vimentin network 2, 4 and 6 h P.I.	58

3.2.3 Late infection of mouse fibroblast cells with MVM collapses the vimentin network.....	62
3.2.4 Cell type and vimentin network symmetry determine the effect on vimentin during MVM infection.....	64
3.2.5 Vimentin is not significantly cleaved in MVM-infected cells.....	69
3.2.6 MVM rearranges the microtubule network at 2 h P.I., however the microtubule network is stabilized by 24 h P.I.....	71
3.2.7 The rearrangements to the microtubule network are due to trafficking of MVM-containing vesicles.....	76
3.2.8 The actin network is unaltered during early MVM infection, however exhibits patchiness 24 h P.I.....	76
3.2.9 Lamin B network is disrupted during early infection with MVM.....	77
3.2.10 MVM decreases stiffness of fibroblast cells during early infection.....	80
3.3 Discussion.....	84
Chapter 4 – Vimentin Facilitates a Productive MVM Infection.....	89
4.1 Introduction.....	89
4.2 Results.....	90
4.2.1 The vimentin network of LA9 mouse fibroblasts collapses and forms aggregates after acrylamide treatment.....	90
4.2.2 ACR treatment is reversible after 12 hours.....	92
4.2.3 An intact vimentin cytoskeleton facilitates MVM replication.....	92
4.2.4 Endosomal uptake of MVM is not inhibited by pre-treatment with acrylamide.....	95
4.2.5 LA9 cells incubated for 8 h with 5 mM ACR exhibit no effect on cell growth.....	95
4.2.6 MVM replication is significantly reduced in vimentin-null cells.....	96
4.2.7 Vimentin null cells seem to progress through the S-phase similar to the vimentin wild type cells.....	101
4.2.8 Cell growth is unaltered in MVM-infected vimentin-null cells as compared to MVM-infected control cells.....	101

4.2.9 Absence of vimentin does not affect endosomal uptake, but leads to reduced accumulation of MVM capsid immunostaining on one side of the nucleus	102
4.3 Discussion	106
Chapter 5 – Vimentin Plays a Role in the Progression of MVM Through the Endocytic Pathway	109
5.1 Introduction	109
5.2 Results	110
5.2.1 Late endosome/lysosome immunostaining is altered in vim ^{-/-} cells compared to vim ^{+/+} cells.....	110
5.2.2 Cells lacking vimentin show an increased amount of MVM in early endosomes at 1 and 2 h P.I. compared to vim ^{+/+} cells.....	112
5.2.3 MVM capsid immunostaining is reduced in late endosomes and lysosomes in vim ^{-/-} MEF cells	114
5.3 Discussion	120
Chapter 6 – General Discussion and Future Directions.....	123
6.1 The role of the vimentin network in the progression of MVM through the endocytic pathway.....	125
6.2 Possible roles for vimentin rearrangements after MVM escape from endosomes.....	127
6.2.1 Vimentin rearrangements may be involved in MVM utilizing the aggresome/proteasome pathway	127
6.2.2 Vimentin rearrangements could facilitate nuclear entry of MVM	128
6.2.3 Vimentin may be involved in the trafficking of MVM toward the nucleus	129
6.3 Possible mechanisms for vimentin rearrangement during MVM infection	130
6.4 Future directions	131
6.4.1 Is acidification of endosomes affected in MVM-infected cells lacking vimentin?	132
6.4.2 Do cells lacking vimentin become susceptible to MVM infection when transfected with vimentin?	133

6.4.3 Does vimentin facilitate the partial uncoating of MVM DNA progressing toward the nucleus?.....	134
6.4.4 What is the mechanism for vimentin rearrangement during MVM infection?	134
6.4.5 Is the MVM-induced vimentin rearrangement involved in forming aggresomes?	135
6.5 Concluding remarks	136
Bibliography	138

List of Tables

Table 1-1: Animal viruses that require vimentin for cell entry.	15
Table 1-2: Viruses that require vimentin for formation of a vimentin cage to structurally aid the viral replication site.	19
Table 1-3: Viruses that require an intact vimentin network, likely for cytoplasmic trafficking.	23
Table 2-1: Forward and reverse primer sequences used for generation of DNA probes	45

List of Figures

Figure 1-1: Different viruses utilize actin filament-involved processes for cell entry and rapid transport within and between cells	4
Figure 1-2: Microtubules provide tracks for viral cytoplasmic transport	8
Figure 1-3: The roles for vimentin during viral infection	12
Figure 1-4: MVM replication cycle.....	29
Figure 2-2: Agarose gel electrophoresis of the biotin labeled hybridization probes.	47
Figure 3-1: MVM causes morphological changes in the cell and alters the vimentin filament network 2 h P.I.....	56
Figure 3-2: MVM co-localizes with MTOC protein pericentrin 2 h P.I.....	59
Figure 3-3: Early infection of mouse fibroblasts with MVM rearranges the vimentin filament network	60
Figure 3-4: Late infection of mouse fibroblast cells with MVM collapses the vimentin filament network	63
Figure 3-5: Early infection of NIH-3T3 mouse fibroblasts with MVM rearranges the vimentin filament network.....	66
Figure 3-6: Early infection of NEB324k human kidney fibroblast cells with MVM does not alter the vimentin filament network, despite a productive infection.	68
Figure 3-7: Vimentin is not cleaved in MVM-infected cells.....	70
Figure 3-8: MVM rearranges the microtubule network at 2 h P.I., however the MT network is stabilized by 24 h P.I.	72
Figure 3-9: The rearrangements to the microtubule network are due to trafficking of MVM-containing vesicles.....	74
Figure 3-10: The actin filament network is unaltered during early MVM infection, however exhibits patchiness 24 h P.I.	78
Figure 3-11: Lamin B immunostaining is disrupted during early infection with MVM. ...	79
Figure 3-12: Atomic force microscopy can record FD curves and provide the elastic modulus of a cell	82
Figure 3-13: Atomic force microscopy shows decrease in stiffness of MVM-infected mouse fibroblast cells.....	83
Figure 3-14: MVM induces morphological changes to the host cell 2 h P.I.....	88

Figure 4-1: The vimentin network of LA9 mouse fibroblasts collapses and forms perinuclear aggregates after acrylamide treatment.....	91
Figure 4-2: ACR treatment is reversible after 12 hours	93
Figure 4-3: An intact vimentin cytoskeleton facilitates MVM replication	94
Figure 4-4: Endosomal uptake of MVM is not inhibited by pre-treatment with acrylamide.	97
Figure 4-5: Growth curve of LA9 cells untreated or treated with 5 mM and 10 mM acrylamide.	98
Figure 4-6: MVM replication is significantly reduced in vimentin-null cells	99
Figure 4-7: MVM DNA replication is significantly reduced in vimentin-null cells	100
Figure 4-8: Growth curve for LA9, vim ^{+/+} and vim ^{-/-} MEF cells	103
Figure 4-9: Cell growth is unaltered in MVM-infected vimentin-null cells as compared to MVM-infected control cells..	104
Figure 4-10: The absence of vimentin does not affect endosomal uptake, but leads to the reduction of perinuclear accumulation of MVM capsid immunostaining on one side of the nucleus	105
Figure 4-11: Vimentin facilitates productive MVM infection.....	108
Figure 5-1: Late endosome/Lysosome immunostaining is altered in vim ^{-/-} cells compared to vim ^{+/+} cells.	111
Figure 5-2: Vim ^{-/-} cells show an increased amount of MVM remaining in early endosomes at 1 and 2 h P.I. as compared to MVM-infected vim ^{+/+} cells.	113
Figure 5-3: MVM capsid immunostaining in late endosomes/lysosomes appears reduced in vim ^{-/-} cells at 1 h and 2 h P.I. as compared to MVM-infected vim ^{+/+} cells..	116
Figure 5-4: MVM does not reach late endosomes/lysosomes in vim ^{-/-} cells treated with BafilomycinA as compared to vim ^{+/+} cells	119
Figure 5-5: Lack of vimentin in cells leads to alteration of the progression of MVM through the endocytic pathway.....	122
Figure 6-1: The dual role of vimentin during MVM infection cycle.....	124

List of Abbreviations

2D-DIGE: 2D-Fluorescence difference gel electrophoresis
AAV: adeno-associated virus
ACR: acrylamide
AFM: atomic force microscopy
AFs: actin filaments
Arp2/3: actin-related protein 2/3
APAR: autonomous parvovirus-associated replication
BafA1: Bafilomycin A1
BSA: bovine serum albumin
CaMK-II: calcium/calmodulin kinase II
CLIC/GEEC: clathrin-independent carriers/GPI-AP enriched early endosomal compartment
CPV: canine parvovirus
CRM1: chromosome maintenance region 1
DMEM: Dulbecco's modified Eagle's medium
F-actin: filamentous actin
FBS: fetal bovine serum
FD: force-distance
FPV: feline parvovirus
G-actin: globular actin
GAPDH: glyceraldehyde 3-phosphate dehydrogenase
GFAP: glial fibrillary acidic protein
HIV-1: human immunodeficiency virus type 1
HSV-1: herpes simplex virus type 1
IFs: intermediate filaments
LINC: linker of nucleoskeleton and cytoskeleton
MEF: mouse embryonic fibroblast
MEM: minimum essential medium
MOI: multiplicity of infection

MTOC: microtubule organizing center
MTs: microtubules
MVM: minute virus of Mice
NPC: nuclear pore complex
ORF: open reading frame
PS: penicillin/streptomycin
PBS: phosphate buffered saline
PFA: paraformaldehyde
PFU: plaque-forming units
P.I.: post-infection
PI3-K: phosphatidylinositide 3-kinase
PKC: protein kinase C
PLA2: phospholipase A2 domain
PIC: pre-integration complex
RanBP2/Nup358: Ran binding protein 2/nucleoporin 358
ROCK: rho-associated protein kinase
SSC: saline-sodium citrate
VP1u: VP1 unique
WASP: Wiskott–Aldrich Syndrome protein
WIP: WASP interacting protein

Acknowledgements

My mighty 10-year journey in higher education and research has been filled with much discovery and self-growth. These moments would not have been possible without a number of fundamental people who helped me see the big picture, offered endless support, and helped me become a successful scientist at the end of this tunnel.

I would like to express my very great appreciation to my supervisor Dr. Nelly Panté, who initially took me on as an undergraduate in her lab. Her scientific guidance, encouragement to pursue varied opportunities, and unwavering support have helped me get through the PhD program and graduate as successful a scientist as possible. While an undergraduate in her lab I was fortunate to have as my direct supervisor, Dr. Sarah Cohen, a successful scientist and PhD candidate at the time. I extend my thanks to her for the continued mentorship and guidance throughout my PhD program.

I thank all of my committee members, Dr. Don Moerman, Dr. David Theilmann, and Dr. Wayne Vogl for the suggestions, guidance, and encouragement. Thank you for making the journey a challenging yet enjoyable and satisfying experience. Thank you also to our collaborators, Dr. Laura Hertel (Children's Hospital Oakland Research Institute), Dr. David Pintel (University of Missouri School of Medicine), Dr. Peter Tattersall (Yale University School of Medicine), Dr. Amy Wun (University of Toronto), and Dr. Chris Yip (University of Toronto), who have provided ideas, tools, and reagents.

I have been fortunate during my PhD to experience the synergy between research and teaching while part of the Biology Program at UBC. I would like to personally thank all of

the instructors in the Biology Program, as well as Dr. Sunita Chowrira, Kathy Nomme, Dr. Carol Pollock, and Dr. Lacey Samuels for encouraging and valuing my teaching skills, and being great role models.

I would like to thank all the current and past members of the Panté lab for the suggestions and fun adventures, and Dr. Richard Adeyemi (currently post-doctoral fellow in the lab of Dr. Steve Elledge, Harvard Medical School) for the many long chats about parvovirus and his invaluable friendship.

Without the help of my supportive friends I could not have stood tall every step of this journey – my warmest hugs and thank you go to Kayleigh M. and her family (Karen, Peter and Zayne), Jesi L., Thomas G., Mojan S., Adam P., Alex L., and Ross P. A special thank you to Francis Arevalo for understanding and believing in me, standing by me through a tough journey, and inspiring many epiphanies at pivotal moments.

My most wholehearted and strongest thank you goes to my family: my mother, for enthusiastically supporting all of my endeavors, my father, for his dedicated guidance, encouragement and continuous support, and my sister, for always putting up with my eclectic ways – your fine feathered friend has finally made it!

Financial support for this work has been provided by grants awarded to Dr. Nelly Panté from the Canadian Institutes of Health Research (CIHR), the Natural Sciences and Engineering Research Council of Canada (NSERC), and the Michael Smith Foundation for Health Research (MSFHR).

To all those who have ever asked 'why' and eagerly searched for the answers.

Chapter 1 – Introduction

All viruses are dependent on the host cell for many aspects of their infection cycle from cytoplasmic transport, to genome replication, to capsid protein synthesis and assembly. As a fundamental component of the cell involved in many cellular processes, such as endocytosis, cellular trafficking, and cell division, the host cytoskeleton and its associated proteins are required by many viruses for a successful infection. There are three known structurally and functionally distinct cytoskeleton components in the host cell: actin filaments (AFs), microtubules (MTs), and intermediate filaments (IFs). Of the cytoskeleton components, the roles of AFs and MTs during viral infection have been extensively studied (reviewed by Greber & Way, 2006; Radtke *et al.*, 2006; Taylor *et al.*, 2011; Welch & Way, 2013). However, due to the unique properties of IFs, studies on the novel roles of IFs during viral infection have only just begun to be revealed over the last decade (reviewed by Spripada & Dayaraj, 2010). The aims of this chapter are to introduce the reader more generally to studies on the role of AFs and MTs during viral infection (Section 1.1), introduce in detail the newly discovered roles of IFs during viral infection (Section 1.2), and introduce parvoviruses and the roles of the cytoskeleton during early parvoviral infection (Section 1.3). In general, studies on the role of the cytoskeleton during viral infection have opened the doors to potential novel therapeutics and continue to broaden our understanding of the role of the cytoskeleton, especially IFs, within the cell.

1.1 Virus interactions with actin filaments and microtubules

1.1.1 Actin filaments promote viral cell entry

For any virus the first step to a successful infection is gaining access to the host cell. Depending on their properties, viruses utilize many of the already existing cellular mechanisms to gain entry into the host cell such as receptor-mediated endocytosis, membrane fusion, or macropinocytosis (reviewed by Grove & Marsh, 2011; Marsh & Helenius, 2006; Mercer *et al.*, 2010a; Yamauchi & Helenius, 2013). Among other cellular processes, such as cell division, adhesion and migration, AFs play an important role in cellular uptake mechanisms as well as in the transport of cargo within the cell (reviewed by Blanchoin *et al.*, 2014). Filamentous actin (F-actin) is created by polymerization of monomeric or globular actin (G-actin), from nucleation complexes such as actin-related protein 2/3 (Arp2/3) (reviewed by Dominguez & Holmes, 2011). AFs are polar and dynamic filaments, containing a rapidly growing and shrinking plus-end and a stable minus-end. AFs are known to create networks and arrays near the cell cortex by polymerizing and depolymerizing F-actin to specific structures such as stress fibers, filopodia, and lamellipodia (reviewed by Chhabra & Higgs, 2007; Le Clainche & Carlier, 2008). In order to extend cytoplasmic protrusions, filopodia form from parallel actin bundles that polymerize toward sites at the plasma membrane, often containing receptors, integrins, and cadherins (reviewed by Blanchoin *et al.*, 2014; Mattila & Lappalainen, 2008). On the other hand, lamellipodia contain highly branched networks of AFs occurring at the plasma membrane, often forming membrane ruffles and comprising the leading edge of migrating cells (reviewed by Bisi *et al.*, 2013; Chhabra & Higgs, 2007). Several viruses induce membrane ruffling and macropinocytosis for

cellular uptake (reviewed by Mercer & Helenius, 2012). The roles that AFs play in cellular entry mechanisms during viral infection have also been well studied (reviewed by Roberts & Baines, 2011; Taylor *et al.*, 2011).

Among the many different viruses that utilize AF-involved processes for cell entry, vaccinia virus and herpes simplex virus type 1 (HSV-1) are two good examples. As illustrated in Fig. 1-1, vaccinia virus mature virions enter cells by macropinocytosis (Huang *et al.*, 2008; Mercer & Helenius, 2008; Mercer *et al.*, 2010b). Other supporting data indicate that these steps are dependent on AF rearrangements and several key signaling molecules that are involved in macropinocytosis, including rac1, pak1, protein kinase C (PKC), and phosphatidylinositide 3-kinase (PI3-K) (Izmailyan *et al.*, 2012; Locker *et al.*, 2000; Mercer & Helenius, 2008; Schroeder *et al.*, 2012). In the case of HSV-1 (Fig. 1-1), one role for AF remodeling during entry of the virus is for the virus to “surf” along filopodia to efficiently reach cell entry sites (reviewed by Van den Broeke & Favoreel, 2011). The term “surfing” indicates movement of virus on filopodia protrusions toward the cell body before cell entry. Additionally, various kinases such as Rho GTPase, RhoA, PI3-K, and cdc42 have been shown to trigger the reorganization of the AF network, and induce receptor clustering and surfing of HSV-1 virus particles along filopodia (Clement *et al.*, 2006; Petermann *et al.*, 2009; Tiwari & Shukla, 2010).

While many viruses breach the barrier posed by the actin cortex by entering the cell by endocytosis or other AF-involved processes, viruses that fuse their membrane with the

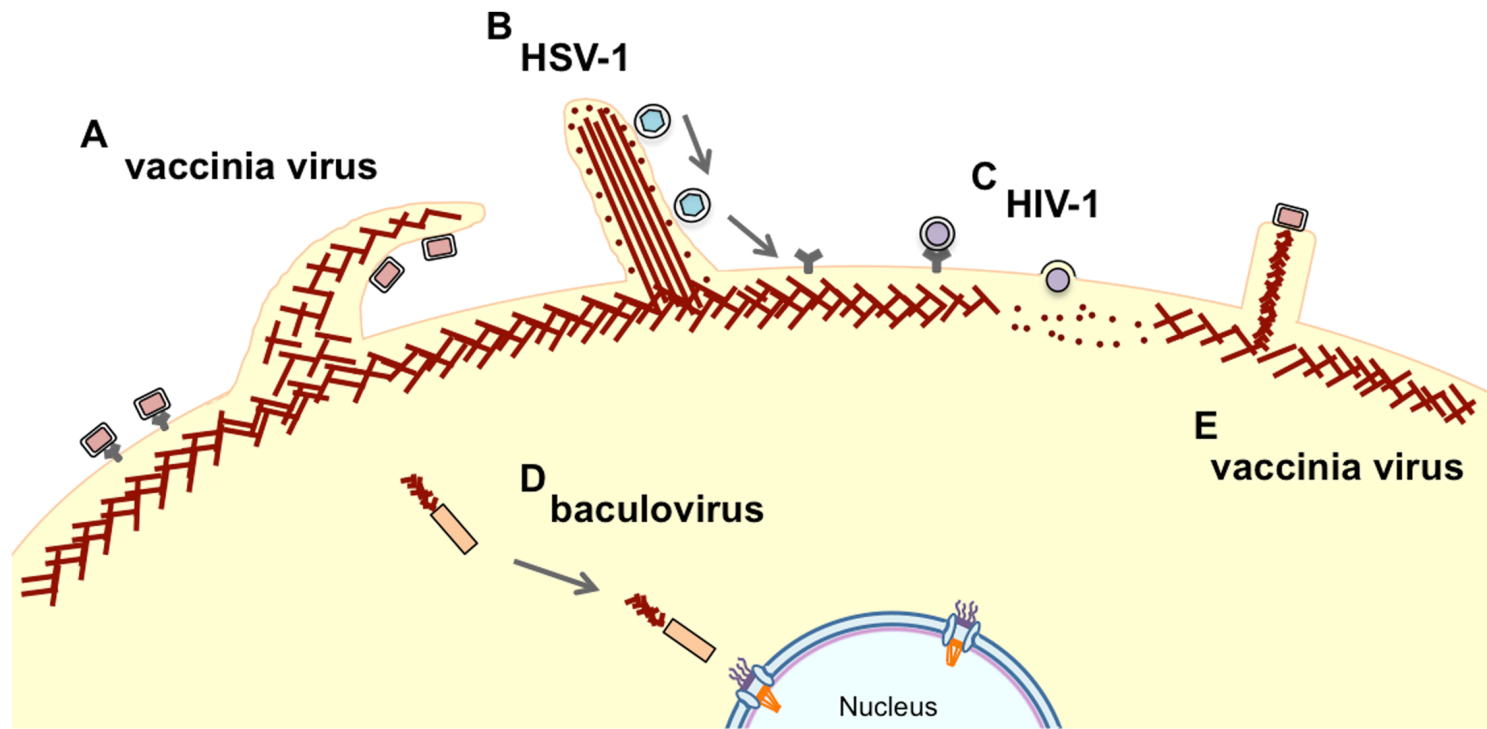


Figure 1-1: Different viruses utilize actin filament-involved processes for cell entry, rapid transport within cells and cell-cell transmission. AFs play an important role in cellular uptake mechanisms, as well as in the transport of cargo within the cell. The roles that AFs play in cellular entry mechanisms during viral infection have been well studied. Several viruses, such as vaccinia virus and HSV-1, overcome the cell cortex as a barrier to cell entry by using AF-involved processes: A) Vaccinia virus mature virions enter cells by macropinocytosis involving AF rearrangements; B) HSV-1 causes remodeling of the AF network to “surf” along filopodia to efficiently reach cell entry sites. Other viruses, such as HIV-1 that fuses with the plasma membrane for cell entry, need a way to remove the actin cortex as a barrier to entry: C) HIV-1, activates cofilin, an AF depolymerization factor, which subsequently leads to AF depolymerization and loosening of the actin cortex, allowing for easier passage of the viral core into the cytoplasm. AFs have also been implicated in trafficking of viruses within cells and cell-cell transmission, such as baculovirus and vaccinia virus : D) Baculovirus forms actin tails at one end of the viral capsid to aid with trafficking toward the nucleus; E) Vaccinia virus uses the process of actin tail formation for cell-cell transmission.

plasma membrane face the actin cortex as a barrier for passage of the viral core into the cytoplasm. Thus, many of these viruses have evolved a mechanism to promote cell signaling and remodeling of the AF network at the cell cortex. This mechanism is best known for human immunodeficiency virus 1 (HIV-1) (Fig. 1-1). Binding of HIV-1 to its receptor, CXCR4, promotes extensive signaling and AF remodeling (reviewed by Stolp & Fackler, 2011). For HIV-1, cofilin, an AF depolymerization factor, is activated and subsequently leads to AF depolymerization (Yoder *et al.*, 2008). This ultimately loosens the actin cortex allowing for easier passage of the viral core into the cytoplasm.

1.1.2 The formation of actin tails aid viral transport

While some viruses are able to induce and utilize AF-involved processes in the cell such as macropinocytosis, other viruses can hijack the AF polymerization process itself to propel many essential viral activities (reviewed by Goldberg, 2001; Welch & Way, 2013). AFs form rapidly from nucleation complexes such as Arp2/3 (reviewed by Goley & Welch, 2006). Viruses, such as baculovirus and vaccinia virus, hijack this process and create actin tails in order to mediate rapid transport of virions within or between cells (reviewed by Ohkawa *et al.*, 2010; Welch & Way, 2013). For baculovirus (Fig. 1-1), actin-based motility is required for intracellular migration and replication during infection (reviewed by Ohkawa *et al.*, 2010). Actin tails form at one end of the viral capsid to aid with trafficking toward the nucleus (Charlton & Volkman, 1991, 1993; Lanier & Volkman, 1998). Furthermore, in order to trigger AF polymerization, the viral protein VP78/83 acts similar to the host Wiskott–Aldrich Syndrome protein (WASP), which activates the Arp2/3 complex (Goley *et al.*, 2006; Machesky *et al.*, 2001). For vaccinia virus (Fig. 1-1),

the viral protein A36R recruits WASP, WASP interacting protein (WIP), and other related proteins through tyrosine phosphorylation, in order to interact with the Arp2/3 complex for the process of actin tail formation in cell-cell transmission of the virus (Frischknecht *et al.*, 1999; Katz *et al.*, 2003; Moreau *et al.*, 2000; Newsome *et al.*, 2006; Scaplehorn *et al.*, 2002).

1.1.3 Microtubules provide tracks for viral cytoplasmic transport

For most viruses, especially DNA viruses, an efficient infection requires the virus to overcome barriers in the cytoplasm in order to reach the replication site and replicate its genome. Transport in the viscous cytoplasm by diffusion would take far too long. For example, it has been calculated that the HSV-1 capsid would take 231 years to diffuse 10 mm in the axonal cytoplasm (Sodeik, 2000). Therefore, many viruses use the host's organized network of MTs for intracellular trafficking, either for cytosolic transport of naked viral particles or for transport inside vesicles. The role of MTs and their associated motor proteins have already been extensively studied for the transport of many viruses within the host cytoplasm (reviewed by Greber & Way, 2006; Hsieh *et al.*, 2010; Radtke *et al.*, 2006; Slonska *et al.*, 2012; Ward, 2011). MTs are polar, hollow cylinders of α - and β -tubulin subunits that exhibit dynamic instability (reviewed by Desai & Mitchison, 1997; Heald & Nogales, 2002), whereby the plus end is rapidly growing and shrinking usually near the cell periphery, and the minus end is stably anchored to the centrosome at the microtubule organizing center (MTOC) (reviewed by Wade, 2009). Many motor proteins mediate the transport of cargo on MTs. Dynein motors mediate the minus-end directed movement, while a large group of kinesin motors

mediate plus-end directed movement (reviewed by Vale, 2003). Dynein is composed of light, intermediate and heavy chains, and is often associated with another protein complex, dynactin, which consists of dynamitin, among other proteins (reviewed by Allan, 2011; Jacquot *et al.*, 2010; Schroer, 2004; Vallee *et al.*, 2004). Dynamitin overexpression dissociates the dynactin complex and affects all dynein-mediated transport processes in the cell such as the positioning of several organelles (Burkhardt *et al.*, 1997; Valetti *et al.*, 1999). Thus, dynamitin overexpression has become a valuable tool to determine the requirement for dynein in a given cellular process. The kinesin motor proteins are a much larger group of motor proteins than dyneins, are composed of light and heavy chains, and are involved in cellular processes such as organelle positioning (reviewed by Hirokawa *et al.*, 2009; Vale, 2003).

Many viruses have been observed in close association with MTs and MT associated motor proteins (reviewed by Dodding & Way, 2011; Dohner *et al.*, 2005; Merino-Gracia *et al.*, 2011). As illustrated in Fig. 1-2, adenovirus and HSV-1 are two good examples of viruses that use MTs and dynein for transport toward the nucleus. For example, experiments that use drugs to depolymerize MTs or inhibit dynein by using anti-dynein antibodies or dynamitin overexpression, have shown that MTs and dynein are required for the trafficking of adenovirus and HSV-1 (Dohner *et al.*, 2002; Engelke *et al.*, 2011; Leopold *et al.*, 2000; Sodeik *et al.*, 1997; Suomalainen *et al.*, 1999). In addition, adenovirus interacts directly with the dynein intermediate chain (Bremner *et al.*, 2009), while HSV-1 proteins UL34, UL35, and UL46 interact directly with dynein light and intermediate chains (Douglas *et al.*, 2004; Ye *et al.*, 2000). Immuno-gold electron

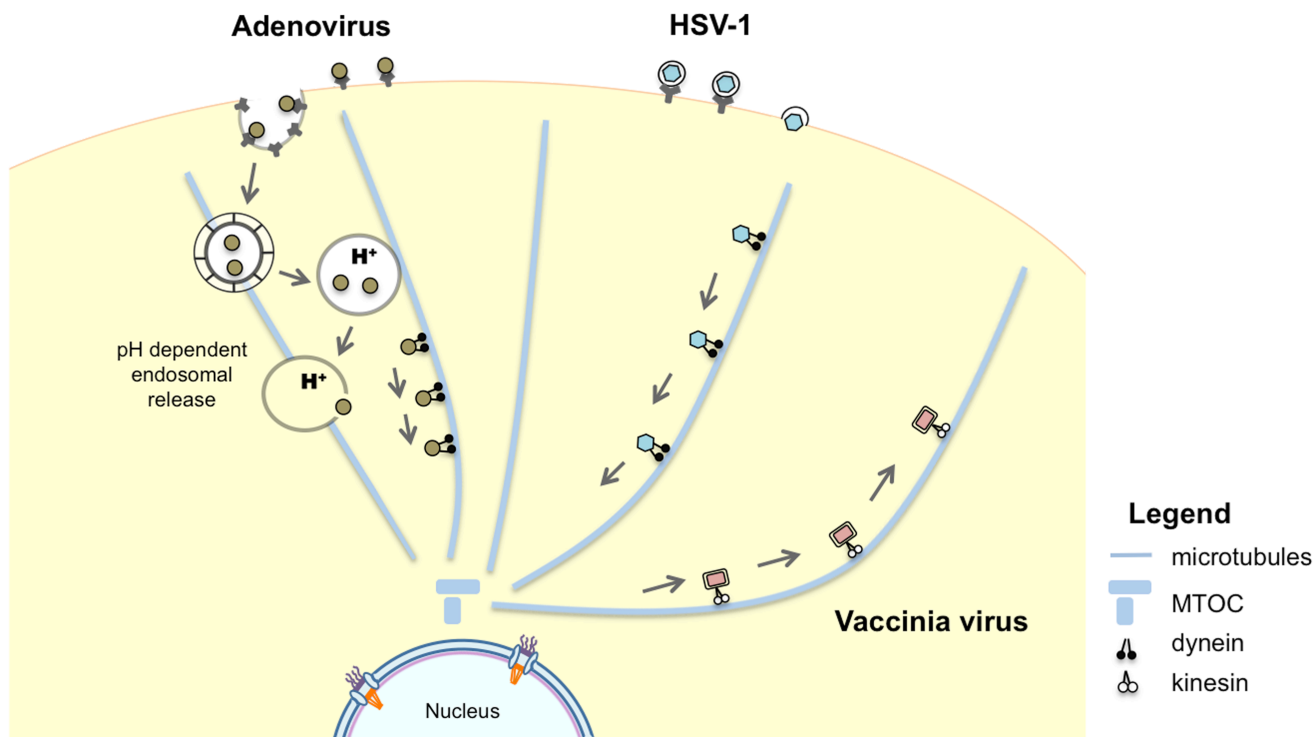


Figure 1-2: Microtubules provide tracks for viral cytoplasmic transport. Many viruses have been observed in close association with MTs, and MT associated motor proteins. DNA viruses, such as adenovirus and HSV-1, use MTs and dynein for transport toward the nucleus. Other viruses, such as vaccinia virus, use the motor protein kinesin in order to move in the opposite direction, from the nucleus toward the cell periphery for cellular egress.

microscopy of HSV-1-infected cells has also shown dynein near incoming viral capsids in the vicinity of MTs (Sodeik *et al.*, 1997). Other viruses, such as vaccinia virus, use the motor protein kinesin in order to move in the opposite direction from the nucleus toward the cell periphery for cellular egress (reviewed by Ward, 2011).

Many viruses use MTs for trafficking toward the MTOC and the nucleus. However, how viral capsids move between the gap from the MTOC to the nuclear pore complex (NPC) is not yet well understood. Studies have shown that the nuclear export factor chromosome maintenance region 1 (Crm1) is required for adenovirus transport from the MTOC to the nucleus (Strunze *et al.*, 2005). In addition, kinesins may catalyze the plus-end directed MT transport from the MTOC to the nucleus and Crm1 interacts with the NPC protein Ran binding protein 2/nucleoporin 358 (RanBP2/Nup358) (Singh *et al.*, 1999), which in turn can bind kinesin-1 (Cai *et al.*, 2001). Therefore, this suggests a model where viral capsids interact with kinesin, which interact with RanBP2/Nup358, which in turn interacts with Crm1 (Strunze *et al.*, 2011). However, more studies need to be conducted to make a conclusive model.

1.2 Viruses and the forgotten player: intermediate filaments

While the roles of AFs and MTs have been widely studied with respect to virus infection, very little is known about the role of IFs during viral infection. Over 70 genes in humans code for a variety of IF proteins that assemble as subunits of the 10-12 nm filaments. IF proteins are grouped into five types based on their amino acid sequence identity (reviewed by Herrmann *et al.*, 2007). Type 1 and 2 are comprised of the acidic and

basic keratins, type 3 includes vimentin, desmin and glial fibrillary acidic protein (GFAP), type 4 are the neurofilament proteins, and type 5 are the nuclear lamins. Of the cytoplasmic IF proteins, vimentin is the most abundant, expressed in a wide variety of cell types, ranging from fibroblasts to macrophages and lymphocytes; however, it is predominantly expressed in cells of mesenchymal origin (reviewed by Goldman *et al.*, 2012) (Steinert & Parry, 1985). In terms of structure, vimentin and all other IF proteins, have a well-conserved long central α -helical 'rod' domain that is flanked by variable non- α -helical N- and C-terminal 'head' and 'tail' domains (Reviewed by Herrmann *et al.*, 2007).

Within the cell, IFs have long been known to serve structural functions. More recently, however, we are beginning to understand that they are more than just structural proteins (reviewed by Goldman *et al.*, 2012; Herrmann *et al.*, 2007). For example, the type 3 IF protein, vimentin, has been implicated in cell adhesion, migration, and wound healing (reviewed by Dave & Bayless, 2014; Ivaska *et al.*, 2007), as well as in the cellular positioning of several organelles such as the Golgi network and late endosomal/lysosomal complexes (reviewed by Styers *et al.*, 2005; Toivola *et al.*, 2005). Vimentin interactions with a peripherally associated Golgi protein, formiminotransferase cyclodeaminase, is involved in the distribution of the Golgi network (Gao & Sztul, 2001). On the other hand, distribution and acidification of the endosomal-lysosomal compartments involves vimentin binding to the adapter protein AP-3, a heterotetrameric adaptor complex that carries vesicles between endosomal-lysosomal compartments and regulates sorting of lysosomes (Styers *et al.*, 2004). Vimentin has also been used

as a marker for cells of mesenchymal origin, and has been proposed to play a key role in the epithelial-mesenchymal transition, a hallmark for tumour invasiveness (reviewed by Thiery, 2002). A role of vimentin in the growth and invasiveness of cancer cells has already been indicated for a number of cancers, including breast, prostate, colon, and lung (reviewed by Satelli & Li, 2011).

Interestingly, vimentin may also play important roles during viral infection. There are now several viruses that have been shown to require the host vimentin network for a successful infection, from cell entry to viral egress (reviewed by Spripada & Dayaraj, 2010). As illustrated in Fig. 1-3, the roles for vimentin during viral infection, using three viruses as examples are:

- A) Viral attachment and entry, as shown by Japanese encephalitis virus (described in Section 1.2.1).
- B) Structural support for protective cages and replication complexes where viral replication occurs, as shown by African swine fever virus (Stefanovic *et al.*, 2005) (described in Section 1.2.2).
- C) Cellular trafficking, as shown by cytomegalovirus (CMV) (Reviewed by Hertel, 2011) (Miller & Hertel, 2009) (described in Section 1.2.3).

Other viruses have been shown to cause rearrangement or post-translational modifications to the vimentin network, although the function for these modifications during the virus infection cycle is, as yet, uncharacterized. For example, rotavirus infection causes vimentin reorganization (Weclawicz *et al.*, 1994), and microinjection of

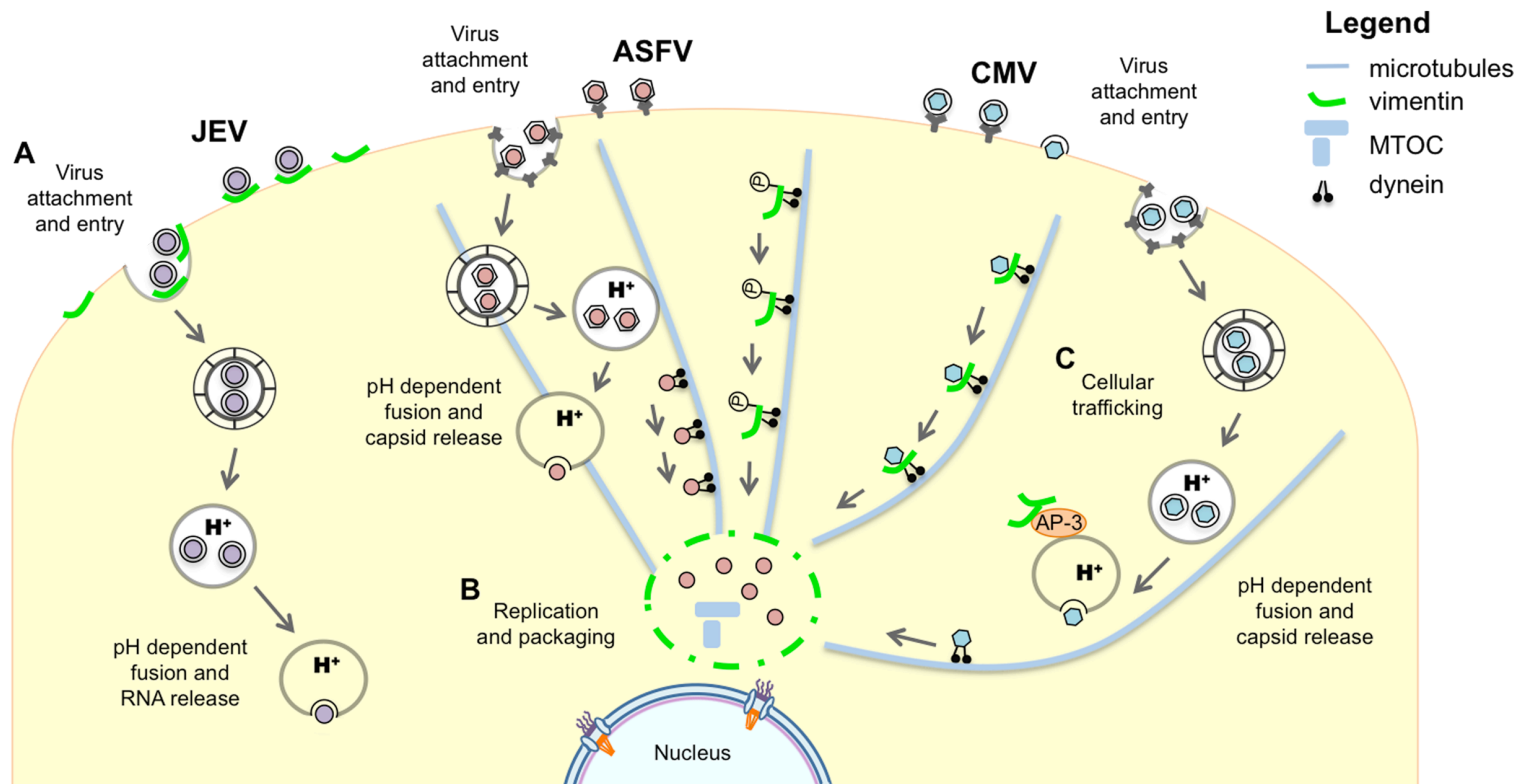


Figure 1-3: The roles for vimentin during viral infection. There are now several viruses that have been shown to require the host vimentin network for a successful infection. The roles for vimentin during viral infection, using three viruses as examples are: A) viral attachment and entry, as shown by Japanese encephalitis virus (JEV). The virus binds to surface expressed vimentin in order to enter the cell; B) structural support for protective cages and replication complexes where viral replication occurs, as shown by African swine fever virus (ASFV). Phosphorylated vimentin is seen transported using the MT network toward the MTOC in order to form the protective cage; and C) cellular trafficking, as shown by cytomegalovirus (CMV). After viral entry, either by fusion or endocytosis, viral capsids can be seen either trafficking along MTs using dynein and vimentin interaction, or requiring vimentin for trafficking within endosomes and endosomal release.

cells with HIV-1 protease or cells infected with adenovirus result in cleavage of vimentin and collapse of the vimentin network (Belin & Boulanger, 1987; Honer *et al.*, 1991; Shoeman *et al.*, 1990). The function of this cleavage is unclear; however, the N-terminal cleavage products of vimentin, which are liberated as a result of cleavage by the HIV-1 protease, dramatically affect nuclear architecture and chromatin structure (Shoeman *et al.*, 2001). In addition, the vimentin N-terminus is highly active and shows a high affinity for lipids, especially for negatively charged and nonpolar lipids (Perides *et al.*, 1987). Thus, it is thought that the vimentin cleavage products may translocate into the nucleus, by an unknown mechanism, and affect host gene expression (Honer *et al.*, 1991; Shoeman *et al.*, 2001). The role of vimentin during HIV-1 infection could also be similar to infection with Epstein-Barr virus (EBV), where the EBV protein LMP1 causes disruption of the vimentin network to modulate cell signaling (Meckes *et al.*, 2013). With other viruses, an increase of vimentin expression is observed, such as infection with hepatitis C virus (Ghosh *et al.*, 2011) and T-cell leukemia virus type I (Lilienbaum *et al.*, 1990). Nevertheless, with increasing studies on the role of IFs during viral infection, the mechanisms for the rearrangement and cleavage of vimentin during the infection cycle of these viruses will undoubtedly soon be uncovered.

1.2.1 Viruses interact with cell surface-expressed vimentin

Vimentin has long been known to be located in the cytoplasm, but surprisingly, extracellular vimentin has recently been found. Cell surface-expressed or secreted vimentin has been reported in several cell types, including activated macrophages, apoptotic neutrophils, and endothelial cells (Moisan & Girard, 2006; Mor-Vaknin *et al.*,

2003). Cell surface-expressed vimentin may be involved in cell-cell interactions and migrating cells, or it may participate in the formation of cell adhesion complexes (reviewed by Ivaska *et al.*, 2007). How vimentin is targeted to the secretory pathway or is recruited to the cell surface remains an unanswered and interesting question. Vimentin lacks any signal sequence for secretion; however, it has been proposed that the vimentin N-terminus, which is highly active and shows a high affinity for negatively charged and nonpolar lipids, could serve in directing it toward membranes and aiding in binding of the protein to the lipid bilayer (Perides *et al.*, 1987). Yet, the mechanism for transport of vimentin to the cell surface still remains unclear. It has been proposed to possibly require β 3 integrin, plectin, and the MT network (Bhattacharya *et al.*, 2009).

Studies are now beginning to show that viruses, such as porcine reproductive and respiratory syndrome virus, enterovirus 71, and Japanese encephalitis virus (summarized in Table 1-1), require cell surface-expressed vimentin as one of the important cellular proteins responsible for cell attachment and entry. These are animal viruses; however, cowpea mosaic virus, which normally infects plant cells, also uses vimentin for cellular attachment when binding to mammalian cells (Koudelka *et al.*, 2007; Koudelka *et al.*, 2009). This suggests a conserved role for cell surface-expressed vimentin as a general attachment factor for viral entry among different groups of viruses.

Table 1-1: Animal viruses that require vimentin for cell entry.

Virus name, family, and composition	Main findings	Citation(s)
<p>Porcine Reproductive and Respiratory Syndrome Virus (PRRSV)</p> <p><i>Arteriviridae</i> ssRNA genome Enveloped</p>	<ul style="list-style-type: none"> - PRRSV binds vimentin (virus overlay protein binding assay and western blot analysis). - Anti-vimentin antibodies block PRRSV infection (immunofluorescence microscopy of FITC-conjugated SDOW-17, a MAb against PRRSV nucleocapsid protein). - The expression of vimentin on the cell surface is changed by PRRSV infection. The expression level of vimentin is reduced by half compared to uninfected cells at 2 days P.I., but is restored to the same level as uninfected cells at 3 days P.I. (flow cytometric analysis). - Delivery of simian vimentin to non-susceptible cells makes the cells susceptible to PRRSV infection (fluorescence microscopy of FITC-conjugated SDOW-17, a mAb against PRRSV nucleocapsid protein). 	<p>Kim <i>et al.</i>, 2006</p>
<p>Enterovirus (EV71)</p> <p><i>Picornaviridae</i> ssRNA genome Non-enveloped</p>	<ul style="list-style-type: none"> - EV71 VP1 protein binds cell surface-expressed vimentin (immunoprecipitation and western blot analysis, as well as pull-down assays). - Soluble vimentin or an anti-vimentin antibody inhibits binding of EV71 to host cells, and reduces viral yields (competitive inhibition assays). - Reducing vimentin expression on the cell surface decreases the binding of EV71 to cells and decreases viral yields (vimentin knockdown cell line using retrovirus-based RNAi vectors). - The N-terminus of vimentin is responsible for the interaction between EV71 and vimentin (pull-down assays with vimentin truncates). 	<p>Du <i>et al.</i>, 2014</p>

Table 1-1: Animal viruses that require vimentin for cell entry.

Virus name, family, and composition	Main findings	Citation(s)
<p>Japanese Encephalitis Virus (JEV)</p> <p><i>Flaviviridae</i> ssRNA genome Enveloped</p>	<p>- A cell surface molecule of approximately 57 kDa interacts with a JEV virulent strain (RP-9), but not an attenuated strain (RP-2ms) in BHK-21 cells (<i>in vitro</i> virus-protein binding pull-down assay).</p>	<p>Chen <i>et al.</i>, 1996</p>
	<p>- Vimentin is recognized as a possible receptor for JEV in porcine kidney cells (virus overlay protein binding assay and mass spectrometry).</p> <p>- Vimentin on porcine kidney cells binds JEV-E protein (co-immunoprecipitation assay).</p> <p>- Anti-vimentin monoclonal antibodies block JEV cell entry into porcine kidney cells.</p>	<p>Das <i>et al.</i>, 2011</p>
	<p>- Vimentin binds to RP-9 and weakly to RP-2ms (pull down assay and mass spectroscopy).</p> <p>- Anti-vimentin antibodies and recombinant-expressed vimentin in human and mouse neuroblastoma cells block infection by RP2 but not RP-2ms (detected by western blot analysis of viral nonstructural protein).</p> <p>- Cells with reduced vimentin expression (vimentin-knockdown using shRNA), bind less RP-9 and produced lower levels of RP-9 viral proteins and progeny.</p> <p>- The vimentin interaction is likely with the JEV-E protein, and E-E138K mutation is resistant to anti-vimentin blockage.</p> <p>- RP-2ms becomes dependent on vimentin only when cell surface glycosaminoglycans are blocked.</p>	<p>Liang <i>et al.</i>, 2011</p>

1.2.2 Viruses use vimentin to form protective cages and replication complexes resembling aggresomes

Among the ways that viruses can utilize vimentin during infection, the requirement of vimentin for efficient replication of viruses within defined replication complexes has been the mechanism most widely studied. There are a number of studies on large DNA and RNA viruses, such as African swine fever virus, vaccinia virus, foot-and-mouth disease virus, dengue virus, and enterovirus 71, that have shown that vimentin and tubulin rearrange during infection to provide a mechanical scaffold for viral proteins as a part of the viral replication factory in the cytoplasm (summarized in Table 1-2). These structures often resemble cellular aggresomes, which are located close to centrosomes and are enclosed in a characteristic vimentin cage (Heath *et al.*, 2001). The ability of aggresomes to concentrate proteins and cellular chaperones (Kopito, 2000) make them highly suitable for facilitating virus assembly (reviewed by Wileman, 2006, 2007). Viruses that do not replicate in the cytoplasm, such as adenovirus, also use aggresome formation. This is to protect the viral DNA from cellular proteins that target viral proteins and inhibit viral replication, and is done by sequestering host cellular proteins in the cytoplasm and greatly accelerating their degradation by proteosomes (Liu *et al.*, 2005) (reviewed by Schreiner *et al.*, 2012).

The observed vimentin rearrangements stated above could either involve a direct interaction between viral proteins and vimentin, or the phosphorylation of the vimentin N-terminal domain by cellular kinases. The latter would lead to filament disassembly and transport of vimentin along MTs (reviewed by Helfand *et al.*, 2004). Indeed, for

several of these viruses, interactions between a viral protein and vimentin have been observed. Several viral proteins of foot-and-mouth disease virus, dengue virus, and enterovirus 71 directly interact with vimentin via co-immunoprecipitation and/or pull-down studies (Gladue *et al.*, 2013; Haolong *et al.*, 2013; Kanlaya *et al.*, 2010; Teo & Chu, 2014). Phosphorylation of vimentin also occurs in cells infected by several of these viruses. The vimentin network rearrangement observed during African swine fever virus and enterovirus 71 infection involves phosphorylation of vimentin at serine 38 or serine 82 by Calcium/Calmodulin Kinase II (CaMK-II) (Haolong *et al.*, 2013; Stefanovic *et al.*, 2005), while dengue virus infection involves activation of rho-associated protein kinase (ROCK) in addition to phosphorylation of vimentin at serine 38 by CaMK-II (Lei *et al.*, 2013; Teo & Chu, 2014).

Interestingly, the cell uses aggresomes and the autophagy pathway to degrade and destroy misfolded and unwanted material. Thus, it is intriguing how viruses that use these aggresome-like structures prevent their own degradation by such complexes in the cell. Understanding how a virus could utilize and simultaneously avoid the cellular autophagy pathway for its own survival is an interesting field of study (reviewed by Chiramel *et al.*, 2013; Kudchodkar & Levine, 2009).

Table 1-2: Viruses that require vimentin for formation of a vimentin cage to structurally aid the viral replication site.

Virus name, family, and composition	Main findings	Citation(s)
<p>African Swine Fever Virus</p> <p><i>Asfarviridae</i> dsDNA genome Enveloped</p>	<ul style="list-style-type: none"> - Aggresomes and African swine fever virus assembly sites cause redistribution of vimentin (GFP-250 or viral protein co-immunostaining with vimentin). - Vimentin is recruited into virus assembly sites early during infection, before DNA replication and late gene expression (immunofluorescence staining). - The movement of vimentin toward the virus assembly site is dependent on MTs (immunofluorescence staining in p50/dynamitin expressing cells). - Once viral DNA replication is initiated, vimentin is phosphorylated by CaMK-II, moves to the edge of the viral factory and forms a cage around the assembly site (immunofluorescence staining, western blot analysis, and use of an inhibitor of CaMK-II). 	<p>Heath <i>et al.</i>, 2001</p> <p>Stefanovic <i>et al.</i>, 2005</p>
<p>Vaccinia Virus</p> <p><i>Poxviridae</i> dsDNA genome Enveloped</p>	<ul style="list-style-type: none"> - Vimentin is found around viral factories. Vimentin and the vaccinia virus core protein p39 co-localize (immuno-gold electron microscopy and confocal microscopy). 	<p>Risco <i>et al.</i>, 2002</p>
<p>Foot-and-Mouth Disease Virus (FMDV)</p> <p><i>Picornaviridae</i> ssRNA genome Non-enveloped</p>	<ul style="list-style-type: none"> - Vimentin and FMDV nonstructural protein, 2C, interact, via 2C amino acids 78-91 (yeast 2 hybrid, co-immunoprecipitation, immunofluorescence). - Vimentin cage structure surrounds FMDV 2C (immunofluorescence staining of FMDV-infected cells), and vimentin is cleaved during infection producing products 50, 46, and 29 kDa (western blot analysis). - Expression of a dominant-negative form of vimentin, or disruption of vimentin by acrylamide (ACR) decreases viral yield (immunofluorescence staining). - Changes to amino acid residues of 2C responsible for binding vimentin, amino acid 78-91, produce nonviable virus (reverse genetics). 	<p>Gladue <i>et al.</i>, 2013</p> <p>Armer <i>et al.</i>, 2008</p>

Table 1-2: Viruses that require vimentin for formation of a vimentin cage to structurally aid the viral replication site.

Virus name, family, and composition	Main findings	Citation(s)
<p>Dengue Virus (DENV)</p> <p><i>Flaviviridae</i> ssRNA genome Enveloped</p>	<ul style="list-style-type: none"> - Direct interaction between vimentin and DENV nonstructural protein 4A (NS4A), a known component of the viral replication complex (Tandem affinity purification and mass spectroscopy and co-immunoprecipitation and western blot analysis). - DENV infection induces a significant change in the morphology of vimentin; vimentin co-localized with ER, NS4A, and dsRNA (immunofluorescence, confocal 3D construction and SEM). - The first 50 amino acid residues at the cytosolic N-terminal domain of NS4A (N50 region) interact with vimentin (molecular cloning of different fragments of DENV NS4A and subcellular localization studies). - Vimentin reorganization and phosphorylation occurs by caMK-II (western blot analysis, caMK-II siRNA). - Gene silencing of vimentin by siRNA induces a significant alteration in the distribution of replication complexes in DENV-infected cells. 	<p>Teo & Chu, 2014</p>
	<ul style="list-style-type: none"> - DENV infection leads to vimentin and ER reorganization to the perinuclear area (immunofluorescence); ER redistribution is blocked by a ROCK inhibitor (Y-27632). - DENV antigens co-localize with vimentin (immunofluorescence). - Disruption of vimentin leads to reduction in DENV infection (ACR treatment, immunofluorescence). - DENV infection induces ROCK activation and phosphorylation of vimentin at serine 71 (immunofluorescence, ELISA, and western blot analysis); DENV infection is blocked with a ROCK inhibitor (Y-27632). 	<p>Chen <i>et al.</i>, 2008; Lei <i>et al.</i>, 2013</p>
	<ul style="list-style-type: none"> - Vimentin interacts with DENV-2 hnRNP C1/C2 and K proteins (2D-PAGE, mass spectrometry, immunoprecipitation, western blot analysis, and immunofluorescence). - Disruption of vimentin by ACR dissociates these complexes and reduces nuclear hnRNPs expression. - Vimentin is also associated with DENV NS1 (immunofluorescence). - Disruption of vimentin by ACR dissociates this complex, reduces DENV NS1 expression (immunofluorescence), as well as viral replication and release (cell associated and viral titers in supernatant). 	<p>Kanlaya <i>et al.</i>, 2010</p>

Table 1-2: Viruses that require vimentin for formation of a vimentin cage to structurally aid the viral replication site.

Virus name, family, and composition	Main findings	Citation(s)
<p>Enterovirus (EV71)</p> <p><i>Picornaviridae</i> ssRNA genome Non-enveloped</p>	<ul style="list-style-type: none"> - Vimentin is important for EV71 replication in human astrocytoma cells and influences the distribution of EV71: virus replication decreased in a vimentin knockdown cell line (VK-U251 cells) compared to normal U251 cells (lower level of virus proteins and decrease in virus titers in the cell supernatants). The distribution of EV71 VP1 protein in VK-U251 cells was different compared to U251 cells (immunofluorescence). - EV71 VP1 and 3C proteins directly interact with vimentin (sub-cellular fractionation, pull-down assays and co-immunoprecipitation). - EV71 infection causes the rearrangement of vimentin in human astrocytoma cells, and together with various EV71 components, forms aggresome-like structures in the perinuclear region (confocal microscopy and electron microscopy). - Aggresomes are virus replication sites since most of the EV71 particles and the newly synthesized viral RNA are concentrated here (electron microscopy and viral RNA labeling). - EV1 VP1 activates CaMK-II, which phosphorylates the N-terminal domain of vimentin on serine 82 (immunofluorescence and western blot analysis), and is required for the replication of EV1 (shown by using KN93, a CaMK-II inhibitor). 	<p>Haolong <i>et al.</i>, 2013</p>

1.2.3 Viruses require an intact vimentin network, likely for cytoplasmic trafficking

The role that MTs and AFs play in mediating transport of viruses within cells has been well established; more recently, however, an intact vimentin network has also been shown to be important for trafficking of viruses such as blue tongue virus, CMV, and junin virus (summarized in Table 1-3). There are currently no commercially available inhibitors of IF polymerization. Acrylamide (ACR) has instead been widely used to selectively and reversibly disrupt the IF network, without disrupting the MT network (Aggeler & Seely, 1990; Durham *et al.*, 1983; Miller & Hertel, 2009). In these studies it has been documented using indirect immunofluorescence microscopy, that after treatment of cells with ACR, the IF network forms aggregates and eventually collapses. Studies on the role of vimentin during infection by blue tongue virus, CMV, and junin virus have all used ACR in order to disrupt the vimentin IF network and further study its role during infection (summarized in Table 1-3). For blue tongue virus infection, disruption of the vimentin network leads to an accumulation of intracellular virus particles and a reduction in viral release. Therefore, the role for vimentin has been proposed to occur after replication, and for egress of the virus to the cell surface (Bhattacharya *et al.*, 2007). In contrast, for CMV and Junin virus, vimentin is possibly involved in trafficking of the virus toward the nucleus (Cordo & Candurra, 2003; Miller & Hertel, 2009). Disruption of the vimentin IF network in both Junin virus and CMV infection leads to lack of viral protein production and protein expression. Furthermore, with CMV infection, the virus remained in the cytoplasm longer in cells lacking vimentin as compared to wild type cells. Thus, it was concluded that viral trafficking toward the nucleus was delayed in cells lacking an intact vimentin network (Miller & Hertel, 2009).

Table 1-3: Viruses that require an intact vimentin network, likely for cytoplasmic trafficking.

Virus name, family, and composition	Main findings	Citation(s)
<p>Blue Tongue Virus</p> <p><i>Reoviridae</i> dsRNA genome Non-enveloped</p>	<ul style="list-style-type: none"> - Blue tongue virus VP2 binds vimentin (sub-fractionation and immunofluorescence studies). - VP2 amino acids 1–118 are sufficient for association with vimentin, and deletion of VP2 residues 65–114 or mutation of amino acids 70–72 to DVD are sufficient to abolish vimentin interaction. - Disruption of the vimentin filament network by ACR leads to a decrease in virus titers in culture medium, and an increase in cell associated virus. 	<p>Bhattacharya <i>et al.</i>, 2007</p>
<p>Cytomegalovirus</p> <p><i>Herpesviridae</i> dsDNA genome Enveloped</p>	<ul style="list-style-type: none"> - Viral entry does not alter vimentin organization (immunofluorescence). - Disruption of vimentin by ACR inhibits viral protein production. - Viral gene expression is reduced in cells lacking vimentin. - In vimentin null cells, viral particles remained in the cytoplasm longer than in vimentin wild type cells (immunofluorescence microscopy). 	<p>Miller & Hertel, 2009</p>
<p>Junin Virus</p> <p><i>Arenaviridae</i> ssRNA genome Enveloped</p>	<ul style="list-style-type: none"> - Disrupting vimentin filament network with ACR, inhibits viral production, and the expression of viral proteins (cell viability test, plaque assay, immunofluorescence) - Recovery experiments show that viral production is partially increased when medium containing ACR is replaced by normal medium (plaque assay). - The binding and internalization steps are not affected by IF disruption. 	<p>Cordo & Candurra, 2003</p>

1.3 Parvovirus

1.3.1 Introduction to parvoviruses

The *Parvoviridae* family includes non-enveloped, icosahedral viruses that are 26-30 nm in diameter and contain a single-stranded linear 5 kb DNA genome. This family is divided into two subfamilies, *Parvovirinae* and *Densovirinae* that can infect a diverse range of hosts from vertebrates to insects, respectively (reviewed by Cotmore *et al.*, 2014). Those that naturally infect vertebrates are divided into eight genera based on the protein and sequence alignment of two viral proteins, VP1 and NS1 (reviewed by Cotmore *et al.*, 2014). Within the *Parvovirinae* subfamily, the genus *Dependoparvovirus* includes those that are replication-defective, such as adeno-associated virus (AAV), that depend entirely on adenovirus or herpesvirus co-infection for their replication (reviewed by Berns & Parrish, 2013).

A second notable genus within the subfamily is *Protoparvovirus*, which includes viruses such as minute virus of mice (MVM), canine parvovirus (CPV), and feline parvovirus (FPV). These viruses are capable of replication without the aid of a helper virus but require cellular S-phase for their DNA replication (reviewed by Cotmore & Tattersall, 2013). Once the cell has entered S-phase, however, they cause DNA damage response and cell cycle arrest at various points depending on the virus (reviewed by Chen & Qiu, 2010). For MVM, the virus induces host DNA damage response (Adeyemi *et al.*, 2010; Ruiz *et al.*, 2011), which then leads to S/G2 cell cycle arrest prior to mitosis (Op De Beeck *et al.*, 2001). The proteins and kinases that are usually responsible for DNA damage responses and cell cycle arrest in the cell, such as p21 and ChK1 are not

responsible for MVM-induced DNA damage response (Adeyemi & Pintel, 2012; Adeyemi *et al.*, 2010). Instead MVM activates an ataxia telangiectasia mutated (ATM) - dependent, rather than an ataxia telangiectasia and Rad3-related protein (ART)- dependent, DNA damage signaling cascade involving phosphorylation of histone H2AX, nibrin, Chk2, and p53, among other DNA damage response proteins (Adeyemi & Pintel, 2012; Adeyemi *et al.*, 2010; Ruiz *et al.*, 2011). It has further been shown that Chk2 activation by MVM leads to a transient S-phase block, and degradation of CDC25A (Adeyemi & Pintel, 2014). Additionally, MVM-induced DNA damage response leads to an inhibition of the cyclin-B1-CDK1 complex, which prevents mitotic entry and causes cell cycle arrest (Adeyemi & Pintel, 2014).

There are currently two strains of MVM, the prototype virus MVMp (in this thesis referred to as MVM, unless otherwise specified) and the immunosuppressive strain MVMi. *In vitro* these two strains exhibit varying cell tropisms; MVMp infects cells of fibroblast origin (Spalholz & Tattersall, 1983; Tattersall & Bratton, 1983), while MVMi infects erythropoietic progenitors and T-lymphocytes (McMaster *et al.*, 1981). These two strains are 97% homologous at the genomic level (Astell *et al.*, 1986), but differ in 14 amino acids on the viral capsid, which cause minor structural differences that are responsible for the distinct observed differences in cell tropism between MVMp and MVMi (Kontou *et al.*, 2005; Nam *et al.*, 2006).

1.3.2 Associated parvoviral disease

The diseases caused by parvoviruses range in severity from sub-clinical to severe and even fatal infections, depending on the virus and host factors such as age and

susceptibility. The transmission routes of many parvoviruses are inhalation or contact with infectious sputum, feces, or urine (reviewed by Berns & Parrish, 2013). The parvovirus B19, belonging to the genus *Erythroparvovirus*, was the only parvovirus known to cause disease in humans up until 2005 when a new parvovirus, human bocavirus belonging to the genus *Bocaparvovirus*, was discovered from nasopharyngeal aspirate specimens by large-scale molecular virus screening (Allander *et al.*, 2005). The B19 virus leads to childhood fifth disease, arthropathy in adults, and rare fetal infections (reviewed by Broliden *et al.*, 2006), while human bocavirus is a probable cause of lower respiratory tract infections and gastroenteritis (reviewed by Jartti *et al.*, 2012; Vicente *et al.*, 2007). Infection with MVMp in mice is asymptomatic with virus replicating minimally in several organs; high levels of virus can only be found in the intestine (Brownstein *et al.*, 1992). However, infection with MVMi causes a variety of diseases and death, mostly in neonates and older animals, and exhibits multiple tissue tropisms (Brownstein *et al.*, 1991). Despite this, MVM remains a high prevalence in laboratory animal facilities and can have detrimental impacts on biomedical research (reviewed by Janus & Bleich, 2012). Thus, good surveillance practices and frequent serological testing is recommended in all laboratory animal facilities.

1.3.3 Parvovirus organization of genome and viral proteins

Unlike other viruses, the small size of the parvoviral genome means parvoviruses only express a small number of genes and viral proteins to help complete their infection cycle. The parvovirus genome contains two large open reading frames (ORFs). The 3' ORF codes for two nonstructural proteins, NS1 (83 kDa) and NS2 (25 kDa), while the 5'

ORF codes for the capsid proteins (reviewed by Cotmore & Tattersall, 2006a). The nonstructural proteins are the first genes to be expressed during infection, with NS1 expressed three times as much as NS2. Subsequently, NS1 plays a role in initiating DNA replication and activating expression of VP1 and VP2 (reviewed by Cotmore & Tattersall, 2006b). Thus, NS1 is commonly used as readout for MVM replication in experimental studies. However, the role of NS1 is not just limited to initiating DNA replication; NS1 is also involved in inducing cell cycle arrest and DNA-damage response, in triggering apoptosis, and in the release/egress of progeny virus (Adeyemi *et al.*, 2010; Bar *et al.*, 2008; Hristov *et al.*, 2010; Nuesch & Rommelaere, 2006; Op De Beeck *et al.*, 2001). On the other hand, NS2 is essential for MVM DNA replication in cells of murine origin (Brownstein *et al.*, 1992; Naeger *et al.*, 1990; Ruiz *et al.*, 2006), viral protein synthesis (Li & Rhode, 1991; Naeger *et al.*, 1993), and capsid assembly and egress of progeny virions from the nucleus (Cotmore *et al.*, 1997; Eichwald *et al.*, 2002).

The MVM capsid is composed of 60 copies of only three structural proteins: VP-1 (84 kDa), VP-2 (63 kDa), and VP-3 (61 kDa) (reviewed by Parrish, 2010). VP1 and VP2 are translated from alternatively spliced message RNAs, while VP3 is formed in full capsids by the cleavage of a peptide from the N-terminus of VP2 exposed outside the capsid (reviewed by Berns & Parrish, 2013). VP1 contains the complete sequence of VP2 and a unique 143-residue long N-terminal sequence, called the VP1 unique (VP1u) region, that is necessary for viral infectivity but not for capsid formation (Tullis *et al.*, 1993).

1.3.4 Parvovirus infection cycle

Parvoviruses use a variety of cellular mechanisms for successful cell infection, from endocytosis to initiation of replication (reviewed by Vihinen-Ranta & Parrish, 2006). In order to gain entry into their host cells, parvoviruses in general use receptor-mediated endocytosis (Fig. 1-4, step 1) (reviewed by Cotmore & Tattersall, 2007). CPV and FPV both use transferrin receptor for cellular entry by endocytosis (Cureton *et al.*, 2012; Parker & Parrish, 2000; Parker *et al.*, 2001). AAV, on the other hand, uses heparan sulphate proteoglycan as its receptor, as well as $\alpha\text{V}\beta\text{5}$ integrin as a co-receptor (Asokan *et al.*, 2006; Summerford & Samulski, 1998; Summerford *et al.*, 1999). Many parvoviruses, including MVM, use host sialic acid and its derivatives as a direct ligand for cell attachment (Halder *et al.*, 2014; Lopez-Bueno *et al.*, 2006; Nam *et al.*, 2006; Wu *et al.*, 2006). More recently, CPV and FPV have also been shown to bind non-human sialic acid *N*-glycolylneuraminic acid (Lofling *et al.*, 2013). Virions are then endocytosed, usually by clathrin-mediated endocytosis (Fig. 1-4, step 2), and enter the endosomal pathway (Harbison *et al.*, 2009; Parker & Parrish, 2000). Recent studies have revealed that parvoviruses can use several endocytic pathways. For example: AAV type 2 uses the clathrin-independent carriers/GPI-AP enriched early endosomal compartment (CLIC/GEEC) pathway (Nonnenmacher & Weber, 2011), AAV type 5 uses caveolae-dependent endocytosis (Bantel-Schaal *et al.*, 2009), and porcine parvovirus uses macropinocytosis (Boisvert *et al.*, 2010). Nevertheless, acidification of endosomes has been shown to be essential for infection by parvoviruses (Ros *et al.*, 2002) (Fig. 1-4, step 3). Low pH triggers a required conformational change in the capsid, which exposes

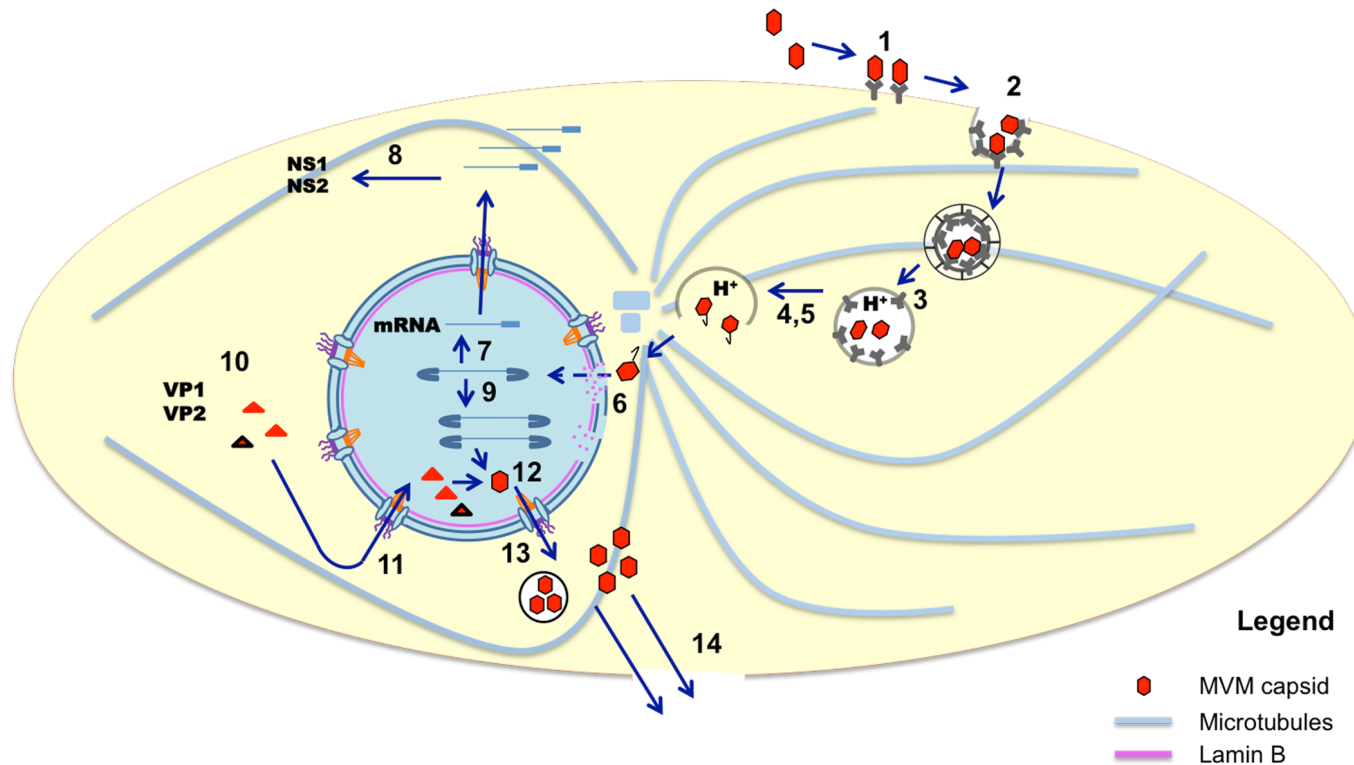


Figure 1-4: MVM infection cycle. [1]: Virus attachment to cellular receptor. [2]: Cellular entry through clathrin mediated endocytosis. [3]: Acidification of endosomes, leading to [4]: conformational changes in the MVM capsid, exposure of the unique VP1 region containing the PLA2 motif, and endosomal release of MVM. [5]: MVM trafficking toward the perinuclear region either while still in vesicles or once virions have lysed out of the endosomes. [6]: MVM enters the nucleus through breaks in the nuclear envelope. [7]: DNA transcription. [8]: Protein translation. [9]: DNA replication. [10]: Capsid protein assembly into trimers. [11]: Nuclear import of capsid proteins. [12]: Assembly of viral progeny. [13]: Nuclear export of viral progeny through the NPCs. [14]: Cellular exit either by cell lysis or transport in vesicles and fusion with the plasma membrane.

the VP1u region containing the phospholipase A2 domain (PLA2) of MVM (Mani *et al.*, 2006; Ros *et al.*, 2002; Farr *et al.*, 2005). This PLA2 domain is essential for viral infectivity, specifically for triggering the endosomal release of virions from endosomes to the cytoplasm in the low pH environment (Fig. 1-4, Step 4) (Zadori *et al.*, 2001). MVM-containing endosomes then travel and accumulate at the perinuclear region, near the MTOC (Fig 1-4, step 5) (Ros & Kempf, 2004). However, the viral release process into the cytoplasm has been shown to be inefficient for parvoviruses, including MVM and CPV, with many virions remaining in endosomal compartments up to 8 hours after the virus has entered endosomes (Mani *et al.*, 2006; Ros *et al.*, 2002; Suikkanen *et al.*, 2002; Vihinen-Ranta *et al.*, 2000).

The few virions that escape the endosomes to the cytoplasm, then enter the nucleus (Fig. 1-4, step 6) by a mechanism that, due to their small size, has been speculated to involve transport through the NPC. However, evidence for the use of the NPC by MVM has not been demonstrated. Instead, there is experimental evidence that MVM gains access to the nucleus through caspase-mediated transient lamin A/C and nuclear envelope disruptions (Cohen & Pante, 2005; Cohen *et al.*, 2006; Cohen *et al.*, 2011). A second mechanism has been proposed for the process of MVM-induced nuclear envelope breakdown that involves activated PKC and cdk2 (Porwal *et al.*, 2013). Once inside the nucleus, viral DNA is released, and the virus must then wait for the cell to enter S-phase before beginning viral DNA replication (reviewed by Cotmore & Tattersall, 2013).

For parvoviruses, the mechanism of DNA replication and gene expression are very well understood (reviewed by Cotmore & Tattersall, 2013). Parvoviral DNA replication involves a “rolling hairpin” mechanism. The 100 to 300 terminal bases at both the genomic 3’ and 5’ ends of parvovirus DNA are self complementary and folded into stable hairpin structures (reviewed by Cotmore & Tattersall, 2006b). Extension of the fold-back 3’ terminus by DNA polymerase delta yields a double stranded replicative form of DNA early in infection, which then acts as a template for transcription (Fig. 1-4, step 7) (reviewed by Cotmore & Tattersall, 2006b). The first gene to be expressed is NS1, which then plays a role in initiating DNA replication and inducing cell cycle arrest (Fig. 1-5, steps 8 and 9) (Clemens & Pintel, 1988) (reviewed by Berns & Parrish, 2013). MVM DNA replication occurs in nuclear structures termed autonomous parvovirus-associated replication (APAR) bodies (Bashir *et al.*, 2001). NS1 co-localizes with replicating viral DNA in APAR bodies, where other cellular proteins essential for DNA replication and cell cycle arrest also accumulate, such as proliferating nuclear cell antigen, replication protein A, DNA polymerase alpha and delta, and cyclin A, among others (Bashir *et al.*, 2001; Christensen & Tattersall, 2002; Christensen *et al.*, 1997). VP1 and VP2 capsid proteins of MVM are then translated in the cytoplasm and form two types of trimers, which are then transported into the nucleus through the NPC (Fig. 1-4, steps 10 and 11) (Lombardo *et al.*, 2002; Riolobos *et al.*, 2006). Progeny virions are then assembled in the nucleus (Fig. 1-4, step 12), and subsequently exported from the nucleus using a nuclear export signal at the VP2 N-terminus through the NPC (Fig. 1-4, step 13); an interaction between NS2 and the nuclear export receptor Crm1 has also

been implicated in this process (Engelsma *et al.*, 2008; Maroto *et al.*, 2004; Miller & Pintel, 2002).

To complete its infection cycle, virions must exit the cell and enter the extracellular environment. It has long been thought that virions do so by cell lysis; however, there is recent evidence showing that vesicular transport through the ER and Golgi and gelsolin-induced modulation of AFs is essential for MVM virus egress (Fig. 1-4, step 14) (Bar *et al.*, 2013; Bar *et al.*, 2008). This provides evidence that progeny virions may move to the cell periphery through vesicular transport, being released into the extracellular milieu even before cellular collapse.

1.3.5 Parvovirus and the cytoskeleton

Not surprisingly, many of the above-mentioned steps of parvovirus endocytosis, endosomal or viral trafficking, and nuclear entry, depend on and impact the host cytoskeleton. For parvoviruses in general, the cytoskeleton networks of MTs and AFs have been implicated in the viral infection cycle. For example, CPV and the AAV both exploit MTs and dynein for the process of trafficking toward the nucleus (Kelkar *et al.*, 2006; Suikkanen *et al.*, 2003; Xiao & Samulski, 2012). However, other studies contradict this idea and suggest a passive process for the movement of MVM toward the nucleus that does not depend on active movement on the cytoskeletal network (Hirosue *et al.*, 2007; Lyi *et al.*, 2014). Furthermore, a previous study showed that during late infection with MVM, for the process of viral egress, the AF network and the vimentin IF network are disrupted, while the MT network remains intact (Nuesch *et al.*,

2005). The AF network has been shown to regulate MVM egress through MVM-induced actin degradation, and the function of the actin-severing protein gelsolin (Bar *et al.*, 2008). Of the IFs, the nuclear lamina, a type 5 IF network protein that provides structural support for the nucleus, is disrupted with MVM and parvovirus H1 infection, aiding the nuclear entry of the virus (Cohen *et al.*, 2006; Cohen *et al.*, 2011; Porwal *et al.*, 2013).

1.3.6 Therapeutic applications

Parvoviruses have several unique and advantageous properties that give them great therapeutic potential. Rodent parvoviruses have oncotropic properties that make them interesting candidates for potential cancer therapies (reviewed by Nuesch *et al.*, 2012). As mentioned previously, parvoviruses require S-phase to begin replication; however, unlike other tumor causing viruses, parvoviruses are unable to promote the progression of cell cycle into S-phase (reviewed by Cotmore & Tattersall, 2013). Once the cell has entered S-phase, however, parvoviruses cause cell cycle arrest at various points depending on the virus (reviewed by Chen & Qiu, 2010), and induce host DNA damage responses (Adeyemi & Pintel, 2014; Adeyemi *et al.*, 2010). Furthermore, other important features of rodent parvoviruses for cancer therapy are that they reduce the occurrence of tumours in laboratory animals, target and kill rapidly dividing cancer cells, and are small enough to spread through tumours (reviewed by Nuesch *et al.*, 2012). One reason behind the virus specifically targeting cancer cells is that these cells lack innate antiviral mechanisms, such as the type I interferon (IFN) response. Some viruses, such as parvoviruses, are either naturally, or engineered to, lack the ability to evade these

antiviral immune responses of the cell. MVM and the rat parvovirus H1 have been shown to only replicate in tumours or transformed mouse and human cells, since these cells lack the key factors of the antiviral response and INF response (Grekova *et al.*, 2010a; Mattei *et al.*, 2013; Raykov *et al.*, 2013). A recent study has also shown that parvoviruses may replicate in a variety of other human cells irrespective of INF responses (Paglino *et al.*, 2014). In addition to this, parvoviruses enhance anti-tumour immune responses by stimulating the release of danger signals and tumour-associated antigens (Grekova *et al.*, 2010b). In the last decades, many other oncolytic viruses have already been used in advanced stages of clinical trials for cancer therapy (reviewed by Russell *et al.*, 2012). The rat parvovirus H1 has already been used in animal models for the study of several cancers such as pancreas, cervical, and breast carcinomas (Angelova *et al.*, 2009a; Angelova *et al.*, 2009b; Faisst *et al.*, 1998; Grekova *et al.*, 2012), and recently, a phase I clinical trial has begun using parvovirus H1 for the first time as a treatment for patients with recurring glioblastoma (Geletneky *et al.*, 2012).

Additionally, parvoviruses in the genus *Dependoparvovirus*, such as AAV, have potential use in gene therapy. The commonly used viruses for gene therapy in the past have included recombinant vectors based on retrovirus, lentivirus, adenovirus, or AAV (reviewed by Bouard *et al.*, 2009). However, AAV-based vectors have gained popularity due to their low immunogenicity and pathogenicity (reviewed by Kaufmann *et al.*, 2013). Currently, AAV is already being used as a vector in human clinical trials for the gene therapy of many diseases, such as cystic fibrosis, muscular dystrophy, Batten's disease, and Parkinson's disease, among others (reviewed by Asokan *et al.*, 2012).

1.4 Thesis objectives

Of the cytoskeleton components, the roles of AFs and MTs during viral infection have been extensively studied. However, due to the unique properties of IFs, studies on the novel roles of IFs during viral infection have only just begun to be revealed over the last decade. For MVM, cytoskeleton networks of MTs and AFs have been implicated in the viral infection cycle. However, the role of IFs during parvoviral infection remains to be characterized. A previous study showed that during late infection with MVM, for the process of viral egress, the AF network and the vimentin IF network are disrupted, while the MT network remains intact (Nuesch *et al.*, 2005). However, the role of the vimentin network during early infection with MVM has yet to be determined.

For my PhD project, I aim to address four major questions about the MVM infection cycle, immediately after viral cell entry:

1. What are the morphological effects on the cytoskeleton upon infection with MVM?
2. Does MVM affect the mechanical properties of cells during infection?
3. Does vimentin have an effect on MVM infection cycle?
4. What is the specific role of vimentin during MVM infection?

I have used cell biology imaging techniques, as well as biochemical assays and atomic force microscopy in order to answer these questions. The following are the specific objectives of my PhD project.

1.4.1 Aim 1: To determine the morphological effects on the cytoskeleton upon infection with MVM

During early infection with MVM, before any viral replication, I have found that the virus induces dramatic morphological changes in mouse fibroblast cells. My hypothesis is that this observed change in the shape of infected cells is a result of changes in the host's organized network of three filaments, AFs, IFs, and MTs during MVM infection. To test this hypothesis I used immunofluorescence microscopy and atomic force microscopy to observe and quantify the distribution of all three components of the cytoskeleton, and the morphological changes to the cell during MVM infection. The results of these experiments are described in Chapter 3.

1.4.2 Aim 2: To determine whether vimentin has an effect on the MVM infection cycle

There are now several viruses that have been shown to cause rearrangements to the vimentin network and require the IF protein vimentin for a successful infection (reviewed by Spripada & Dayaraj, 2010). The results from my experiments for Aim 1 (Chapter 3) document that during early infection with MVM at 2 h P.I. the vimentin immunostaining is dramatically altered, ultimately collapsing around the nucleus by 24 h P.I. Therefore, I hypothesized that the vimentin network has an effect on the MVM infection cycle. There are currently no commercially available inhibitors of IF polymerization. In order to selectively and reversibly disrupt the IF network, ACR has been used in many studies (Aggeler & Seely, 1990; Durham *et al.*, 1983; Miller & Hertel, 2009). Thus, to test my hypothesis, the experiments described in Chapter 4 determined whether the IF network

has an effect on a productive MVM infection by using cells that had an artificially disrupted vimentin IF network using ACR. In addition, I also examined MVM infection of vimentin null cells, *vim*^{-/-} mouse embryonic fibroblasts (MEFs).

1.4.3 Aim 3: To determine the specific role of the vimentin network during MVM infection

Although the traffic and cellular position of organelles of the endocytic pathway have long been known to require MTs, AFs, and their motor proteins (Caviston & Holzbaur, 2006; Vale, 2003), there is now increasing evidence for the involvement of the vimentin filament network in membrane bound organelle transport and cellular distribution (Chang *et al.*, 2009; Nekrasova *et al.*, 2011; Styers *et al.*, 2004). Since MVM uses the endocytic pathway to infect cells, I hypothesized that vimentin is involved in the progression of MVM through the endocytic pathway. To test this hypothesis I infected *vim*^{-/-} MEF cells with MVM and used multiple markers of endocytic organelles. The results of these experiments are described in Chapter 5.

Chapter 2 – Materials and Methods

2.1 Cells and tissue culture tissue culture

Adherent immortalized vim^{+/+} and vim^{-/-} MEFs derived from wild type and knockout mice (courtesy of Dr. Robert Evans, University of Colorado Health Sciences Center; and Dr. Laura Hertel, Children's Hospital Oakland Research Institute; (Holwell *et al.*, 1997)), NIH-3T3 human fibroblast cells and NEB324k newborn human kidney fibroblast cells (courtesy of Dr. David Pintel, University of Missouri), and LA9 mouse fibroblast cells were maintained at 5% CO₂ and 37 °C in complete Dulbecco's modified Eagle's medium (DMEM) supplemented with 10% Fetal Bovine Serum (FBS) and penicillin/streptomycin (PS).

2.2 Antibodies

The monoclonal antibodies used to detect MVM were against intact MVM capsids (1:300, MAb B7) (Kaufmann *et al.*, 2007), and against the C-terminus of MVM NS1 (1:100) (Yeung *et al.*, 1991) (both monoclonal antibodies were kindly provided by Dr. Peter Tattersall, Yale University). The polyclonal antibody against MVM was a custom made antibody (Pacific Immunity Corp.) raised against the MVM VP1u region containing the PLA2 domain of VP1, with the following amino acid sequence:

NH₂ – SDAAAKEHDEAYDQYIKSGKN – COOH

This antibody was previously characterized by Dr. Sarah Cohen and was confirmed to accurately detect the VP1u region of MVM capsids by dot blot, after heat shock

treatment of full capsids. However, when it is used for immunofluorescence microscopy, it gives a general background. To eliminate this background, this antibody was pre-absorbed against mouse fibroblast cells prior to use. Cells were seeded on 100-mm dishes, fixed (3% paraformaldehyde (PFA), 10 min), permeabilized (0.2% Triton X-100, 5 min), blocked (1% bovine serum albumin (BSA), 15 min), and incubated with the custom made polyclonal antibody against MVM VP1u region (1:5000) at 4 °C for 24 h. The supernatant was removed and used in immunofluorescence studies or stored at 4 °C for future use.

Commercial primary antibodies used were for vimentin (rabbit polyclonal antibody, 1:20, Santa Cruz Biotechnology, H-84; or mouse monoclonal antibody, 1:400, Sigma, V9), alpha-tubulin (1:500, Sigma, DM1A), pericentrin (1:300, Abcam, ab44448), Glyceraldehyde 3-phosphate dehydrogenase (GAPDH; 1:1000, Sigma), lamin-B (1:200, Santa Cruz Biotechnology, C-20), EEA1 (1:200, Cell Signaling Technology, C45B10), M6PR (1:100, Abcam, ab134153), or LAMP1 (1:400, Abcam, ab24170). Phalloidin-FITC (1:1000, Sigma, P5282) was used to detect F-actin and Streptavidin-FITC (15 ug/ml, Vector Laboratories SA-5001) was used to detect biotin labeled DNA.

Fluorophore-conjugated antibodies were from Invitrogen: Alexa Fluor 568 Goat Anti-Mouse IgG (Invitrogen, A-11004), Alexa Fluor 568 Goat Anti-Rabbit IgG (Invitrogen, A-11011), Alexa Fluor 448 Goat Anti-Rabbit IgG (Invitrogen, A-11008), Alexa Fluor 647 Goat Anti-Rabbit IgG (Invitrogen A-21244), and Fluorescein Goat Anti-Mouse IgG (Invitrogen, F-2761).

2.3 Purification of MVM and infection

2.3.1 MVM purification

The MVM prototype strain MVMp (in this thesis referred to as MVM) was purified as previously developed (Tattersall *et al.*, 1976; Williams *et al.*, 2004) and described (Au *et al.*, 2010). Empty capsids were purified by the same protocol and separated from full capsids on the basis of their buoyant density.

LA9 cells were grown in suspension and maintained in 5% CO₂ at 37°C at a concentration of 2×10^5 cells/ml for at least 2 weeks prior to infection. The growth medium consisted of minimum essential medium (MEM) supplemented with 5% FBS and 1% PS. For infection, approximately 200 ml of cells were infected with MVM at a multiplicity of infection (MOI) of 1×10^3 plaque-forming units (PFU) per cell. The cells were then diluted daily to maintain the concentration at 2×10^5 cells/ml (generating a final volume of 2 L), and were monitored for cell death by light microscopy. Cell death usually occurred five days after infection and the cells were harvested immediately.

Rather than collecting released virus from the culture medium, cells were lysed and MVM was purified from the infected cells. To avoid proteolytic activity, all steps for purification of MVM were performed with chilled, sterile buffers, either at 4 °C or on ice. Infected cells were first pelleted by centrifugation at 1,600 x g at 4°C and washed with 100 ml TNE buffer (50 mM Tris, 150 mM NaCl, 0.5 mM EDTA, pH 8.7). Cells were then pelleted a second time, and the pellet was re-suspended in 20 ml TE. To release virus from the infected cells, cells were then lysed by sonication on a low setting (by 3-4 brief

bursts). The cells debris was first pelleted by centrifugation at 17,800 c g for 30 minutes at 4 °C, and then discarded. Virus particles were precipitated in 25 mM CaCl₂ and incubated on ice for 30 minutes. The precipitated virus was then pelleted by centrifugation at 3,100 x g for 25 minutes, and re-suspended by gentle sonication (3-4 bursts) in 20 ml T20E buffer (50 mM Tris, 20mM EDTA, pH 8.7). This suspension was then centrifuged again at 12,300 x g for 10 minutes, and the supernatant was loaded onto a continuous CsCl gradient.

The CsCl gradient was created in four Beckman ultraclear centrifuge tubes (14 mm x 89 mm), and first filled with 5 ml CsCl (0.53 g/ml in TE), then a 0.75 ml 1 M sucrose cushion in TE, and last, 5 ml of virus-containing supernatant. The gradients were centrifuged at 96,800 x g for 20 hours. Three bands were visible the next day, and were removed from the centrifuge tubes with a syringe. The most apparent band was a doublet of empty capsids; 1 cm below was a single band of full (genome containing) capsids. In order to remove the CsCl, the virus containing solution was then dialysed against TE 4 over 48 h replacing the TE4 several times.

The virus preparation titer was then determined by plaque assay as previously described (Tattersall, 1972) and usually yielded titers of 1×10^8 - 1×10^9 pfu/ml. Virus preparations were then either used immediately, or aliquoted and frozen at -80 °C for long term storage.

2.3.2 MVM infection

Unless otherwise specified, LA9 cells were grown in monolayers on glass coverslips and infected with the MVM prototype strain MVMp (in this thesis referred to as MVM) at a MOI of 4 PFU per cell in DMEM supplemented with 1% FBS. Cells were then incubated at room temperature or 4 °C for 1 h to allow binding of the virus, followed by incubation at 37 °C for the duration of the infection time.

For mock-infected cells, cells were incubated with DMEM supplemented with 1% FBS. For experiments with empty capsids, these were used at an equivalent MOI of 4 PFU per cell in DMEM supplemented with 1% FBS. For both mock-infected and empty capsid-treated cells, cells were incubated and manipulated in the same way as indicated above for the infected cells.

2.4 Fluorescence microscopy

2.4.1 Immunofluorescence microscopy

For all immunofluorescence experiments, cells were seeded on coverslips 24 hours prior to the experiment.

For NS1, MVM capsid, and MVM Vp1u region immunostaining experiments, cells were fixed (3% PFA, 10 min), permeabilized (0.2% Triton X-100, 5 min), blocked (1% bovine serum albumin (BSA), 15 min), and incubated with a custom made polyclonal antibody against MVM VP1u region (1:5000) or monoclonal antibodies against the intact viral capsid (1:300, MAb B7) (Kaufmann *et al.*, 2007) or NS1 (1:100) (Yeung *et al.*, 1991) at

room temperature for 1 h), followed by several washes with phosphate buffered saline (PBS) and incubation with an appropriate fluorescently labeled secondary antibody, Alexa Fluor 568 Goat Anti-Mouse IgG (Invitrogen, A-11004) for NS1 and MVM capsid immunostaining, or Alexa Fluor 568 Goat Anti-Rabbit IgG (Invitrogen, A-11011) for MVM VP1u region immunostaining.

For immunostaining of vimentin, cells were fixed (3% PFA, 10 min), permeabilized (0.003% digitonin, 15 min on ice), blocked (1% BSA, 15 min), and incubated with a rabbit polyclonal antibody against vimentin (1:20, Santa Cruz Biotechnology, H-84) at room temperature for 1 h, followed by several washes with PBS and incubation with an appropriate fluorescently labeled secondary antibody, Alexa Fluor 448 Goat Anti-Rabbit IgG (Invitrogen, A-11008).

For immunostaining of alpha-tubulin and pericentrin, cells were fixed (3% PFA, 10 min), permeabilized (0.2% Triton X-100, 5 min), blocked (1% BSA, 15 min), and incubated with antibodies against alpha-tubulin (1:500, Sigma, DM1A), or pericentrin (1:300, Abcam, ab4448) at room temperature for 1 h, followed by several washes with PBS and incubation with an appropriate fluorescently labeled secondary antibody, Fluorescein Goat Anti-Mouse IgG (Invitrogen, F-2761) for alpha-tubulin immunostaining, or Alexa Fluor 448 Goat Anti-Rabbit IgG (Invitrogen, A-11008) for pericentrin immunostaining.

For immunostaining of AFs, cells were fixed (3% PFA, 10 min), permeabilized (0.2% Triton X-100, 5 min), blocked (1% BSA, 15 min), and incubated with phalloidin-FITC (1:1000, Sigma, P5282) for 40 min.

For immunostaining of endosomal markers EEA1, M6PR, and LAMP1, cells were fixed (3% PFA, 10 min), permeabilized (0.2% Triton X-100, 5 min), blocked (1% BSA, 15 min), and incubated with antibodies against EEA1 (1:200, Cell Signaling Technology, C45B10), M6PR (1:100, Abcam, ab134153), or LAMP1 (1:400, Abcam, ab24170) at room temperature for 1 h, followed by several washes with PBS and incubation with an appropriate fluorescently labeled secondary antibody, Alexa Fluor 448 Goat Anti-Rabbit IgG (Invitrogen, A-11008).

All coverslips were then washed several times with PBS, mounted using Prolong Gold Anti-fade with DAPI (Invitrogen), and visualized using a Zeiss Axioplan 2 upright fluorescent microscope or an Olympus Fluoview FV1000 Laser Scanning Confocal Microscope.

2.4.2 Fluorescence *in situ* hybridization of MVM DNA combined with immunostaining of MVM capsid and lamin-B

Biotinylated probes specific for the MVM genome were first generated from PCR products. The PCR products for the biotinylation were obtained with two sets of primers against two specific regions of MVM DNA from nucleotide 259-740 and from nucleotide 1629-2590 (Table 2-1), and purified using Qiagen PCR purification kit. The sizes of the

Table 2-1: Forward and reverse primer sequences used for generation of DNA probes

Region of MVM DNA	Primer sequence	Length
Nucleotide 259-740	Forward: 5' – CCATGGCTGGAAATGCTTACTC – 3' Reverse: 5' – GGCTGTTACCAACCATCTGCTC – 3'	482 bp
Nucleotide 1629-2590	Forward: 5' – GCCATTTGCTCTGGTCAAACCTAT – 3' Reverse: 5' – TGGCGTCCTTGGTTTGGTCA – 3'	962 bp

hybridization probes were confirmed by agarose gel electrophoresis as normal for DNA analysis (Fig. 2-2) (Sambrook & Russell, 2001) as approximately 482 and 962 nucleotides in length, using a 100 bp DNA molecular weight standard (New England Biolabs). The DNA concentration and purity were determined with a spectrophotometer.

Cells were then mock-infected or infected with MVM on coverslips for 2 and 12 h (as described in Section 2.3.2), washed twice with PBS, fixed (4% PFA 15 min), permeabilized (0.2% Triton X-100, 5 min), and washed several times with 0.1 M glycine. The 12 h infection samples were denatured (95% deionized formamide, 10 min at 65 °C) and immediately placed on ice. Cells were then incubated with hybridization solution (50 % deionized formamide, 10% dextran sulfate, saline-sodium citrate buffer (SSC; 0.03 M sodium citrate, 0.3 M sodium chloride, pH 8), 1 mg/ml sheared herring DNA (denatured), 1 µg/ml labeled probe DNA (denatured)) overnight at 37 °C. Cells were then washed several times with 50% deionized formamide and SSC buffer solution, and several times with SSC buffer at 37 °C, followed by another several washes with SSC at room temperature. For immunostaining of lamin-B and MVM capsids, cells were then washed several times with 1.5% BSA in PBS (5 min each), blocked with 1.5% BSA in PBS (37 °C, 30 min), and incubated with antibodies against lamin-B (1:200, Santa Cruz Biotechnology, C-20) and MVM intact capsid (1:300, MAAb B7) at 37 °C for 1 h, followed by several washes with 1.5% BSA in PBS and incubation with appropriate fluorescently labeled secondary antibodies, Alexa Fluor 568 Goat Anti-Mouse IgG (Invitrogen, A-11004), Alexa Fluor 647 Goat Anti-Rabbit IgG (Invitrogen A-21244) and Streptavidin-FITC (15 µg/ml, Vector Laboratories SA-5001) at 37 °C for 1 h.

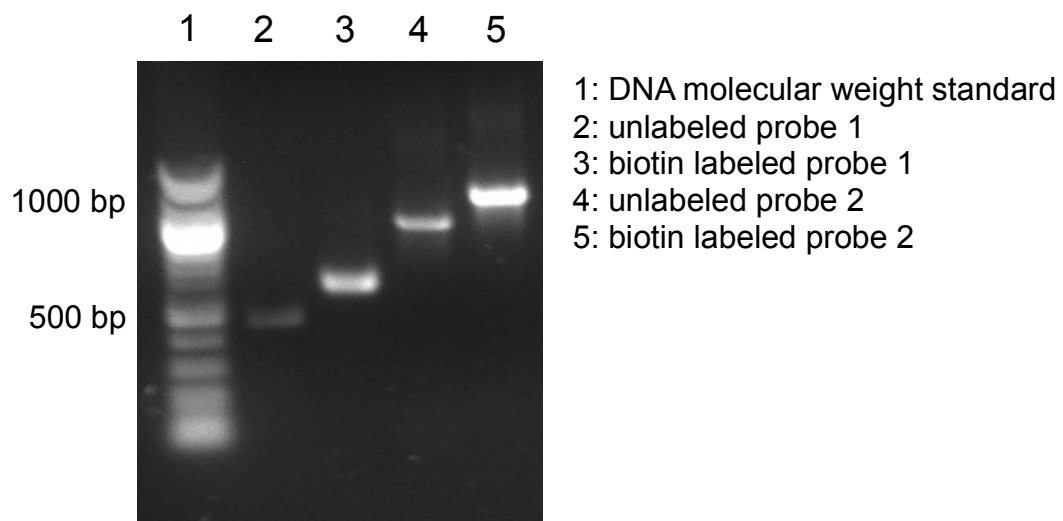


Figure 2-2: Agarose gel electrophoresis of the biotin labeled hybridization probes. Biotinylated probes specific for the MVM genome were first generated from PCR products. The PCR products for the biotinylation were obtained with two sets of primers against two specific regions of MVM DNA from nucleotide 259-740 (probe 1) and from nucleotide 1629-2590 (probe 2), as indicated in Table 2-1. They were then purified using Qiagen PCR purification kit. Shown are the unlabeled probes (lanes 2 and 4) and biotin-labeled probes (lanes 3 and 5) of both PCR products 1 and 2. The sizes of the hybridization probes were confirmed as approximately 482 and 962 nucleotides in length using the 100 bp DNA molecular weight standard (lane 1).

All coverslips were then washed several times with PBS, mounted using Prolong Gold Anti-fade with DAPI (Invitrogen), and visualized using an Olympus Fluoview FV1000 Laser Scanning Confocal Microscope.

2.5 2D-Fluorescence difference gel electrophoresis (2D-DIGE) analysis

LA9 cells were grown on 100-mm dishes and mock-infected or infected with MVM at an MOI of 4 and 10 PFU per cell for 2 h (as described in Section 2.3.2). Cells were collected by scraping (with PBS at 4°C), snap frozen (with liquid nitrogen), and sent to Applied Biomics Inc. for 2D-Fluorescence difference gel electrophoresis (2D-DIGE) analysis. At Applied Biomics Inc., cell lysates were prepared, and protein samples from mock- and MVM-infected cells were labeled with CyDye™ green and red fluorophores, respectively. Both samples were then loaded onto the same electrophoresis gel and resolved in 2D using isoelectric focusing and SDS polyacrylamide gel electrophoresis. Spots corresponding to vimentin cleavage products and MVM VP1 were excised from the gel and identified by MALDI-ToF mass spectrometry.

2.6 Western blot of vimentin

LA9 cells were grown on 100-mm dishes, infected with MVM (as described in Section 2.3.2), and then lysed in RIPA buffer (10 mM Tris base pH 7.2, 150 mM NaCl, 0.1% SDS, 5 mM EDTA, 1% Triton- X100) containing a protease inhibitor mixture (Roche Applied Sciences), 1 mM phenylmethylsulfonyl fluoride, 10 mM sodium fluoride, and 2 mM sodium orthovanadate on ice for 30 min. Lysates were cleared by centrifugation at 16 000 x g for 5 minutes at 4°C. The supernatants were mixed with Laemmli sample

buffer and aliquots with equal amounts of protein were loaded on an 8% SDS-polyacrylamide gel. Proteins were transferred to nitrocellulose membrane, and the proteins that were present in the lysates were detected by western blot, using antibodies against vimentin (1:400, Sigma, V9) or GAPDH (1:1000, Sigma) as a loading control.

2.7 Atomic force microscopy

These experiments were performed in collaboration with Dr. Amy Won (Post-doctoral fellow at the lab of Dr. Christopher Yip, University of Toronto). LA9 cells were grown on 35-mm dishes, mock-infected or infected with MVM at an MOI of 4 (as described in Section 2.3.2), and prepared for AFM 2 h P.I. The force distance (FD) curves of MVM-infected cells were recorded first in order to calculate Young's modulus (elastic modulus) accurately at 2 h P.I., after which the FD curves of mock-infected cells were recorded. All FD curves were obtained using a Bioscope scanning probe system (Digital Instruments) and a Nanoscope IIIA controller (Digital Instruments) with software version 5.30r3sr3. The Sharp Nitride Lever- 10 (SNL-10) tips (Bruker) and Bioscope fluid cells (Bruker) were first irradiated under UV light for 30 min, and the probe D of SNL-10 (nominal spring constant 0.06 N/m) was calibrated on a cell free region of the dishes for deflection sensitivity. To avoid cell damage and vertical deflection, the tip was raised at least 30 μm apart from the dish surface followed by gradual step down cycle at 1 μm increment with trigger force of about 3 nN. All measurements were done at scan rate of 0.500 Hz, ramp size of 2.5 μm , and in a temperature controlled environment at 37 $^{\circ}\text{C}$ using a petri dish heater (Bioscience Tools). All force curves were processed using

Bruker's Nanoscope Analysis software v140r3sr3 to calculate the Young's modulus (elastic modulus) of the cells with tip half angle of 18.00° and Poisson's Ratio of 0.50. The probe was cleaned with bleach in ethanol between MVM-infected and mock-infected cells. Note: No effect on elastic modulus was observed when the probe was gently cleaned with bleach and ethanol vs. using a new probe.

2.8 Drug treatments

2.8.1 Acrylamide treatment

ACR was used to disrupt the vimentin IF network. 5 mM ACR solutions were made by diluting ACR/bis-ACR solution (30% [wt/vol]; Bio-Rad) in culture medium. For characterizing the effect of ACR in LA9 cells, cells were incubated with DMEM (as controls) or ACR solutions for 2, 4, 6, or 8 h, and then washed twice with DMEM medium and immunostained for vimentin (as described in Section 2.4.1). To check whether the effect of ACR on vimentin was reversible, cells were incubated with DMEM (as controls) or ACR solutions for 8 h, washed twice with DMEM medium, and then incubated for 12 h with DMEM and immunostained for vimentin (as described in Section 2.4.1). For MVM endosomal uptake experiments, LA9 cells were incubated with DMEM or ACR solutions for 2, 4, 6, or 8 h, washed twice with DMEM medium, infected with MVM for 2 h (as described in Section 2.3.2), and immunostained for vimentin and MVM capsids (as described in Section 2.4.1). For onset of replication studies, LA9 cells were incubated with DMEM or ACR solutions for 2, 4, 6, or 8 h, washed twice with DMEM medium, infected with MVM for 12 h (as described in Section 2.3.2), and immunostained for NS1 (as described in Section 2.4.1).

2.8.2 Bafilomycin A1 treatment

The drug Bafilomycin A1 (BafA1; Sigma B1793) was used as an inhibitor of vacuolar-ATPase. MEF cells were incubated with 100 nM BafA1 (dissolved in DMSO) diluted in DMEM or DMEM with similar volume of DMSO (as a control) at 37 °C for 1 h, washed with DMEM, and infected with MVM (as described in Section 2.3.2) in the presence or absence of BafA1, and prepared for immunostaining 3 h P.I. (as described in Section 2.4.1).

2.9 Cell growth curves

For ACR experiments, LA9 cells were seeded on 12-well plates. 12 h after seeding, cells were treated with 5 mM and 10 mM ACR for 8 h (as described in Section 2.6.1). Cells were then trypsinized, stained with trypan blue solution, and counted using a light microscope and a hemocytometer at 6 h intervals over a 24 h period.

For cell growth experiments, LA9 and MEF cells were seeded on 12-well plates, and allowed 12 h to attach to the dish. Cells were then trypsinized, stained with trypan blue solution, and counted using a light microscope and a hemocytometer at 6 h intervals over a 24 h period.

For MVM-infection experiments, LA9 and MEF cells were seeded on 12-well plates, and mock-infected or infected with MVM (as described in Section 2.3.2) 12 h after seeding. Cells were then trypsinized, stained with trypan blue solution, and counted using a light microscope and a hemocytometer every 24 h over a period of 3 days.

2.10 Statistical analysis

For all experiments, mean values and standard error were measured for 3 independent experiments. Where indicated statistical significance was determined by unpaired Student *t* test (* $P < 0.05$, ** $P < 0.01$, *** $P < 0.001$). For experiments of MVM-infected cells and endosomal markers, quantification of co-localization between MVM capsid immunostaining and EEA1, M6PR or LAMP1 immunostaining was determined with a free, open source software package, BioImageXD (<http://www.bioimagexd.net/>). To quantify the level of co-localization, 25 cells from three independent experiments were randomly selected and optically sectioned using an Olympus Fluoview FV1000 Laser Scanning Confocal Microscope. Levels for the laser power, detector amplification, and optical sections were optimized for each channel before starting the quantification. Thresholds were adjusted automatically, using the BioImageXD software, to eliminate fluorescence background noise. The co-localization percentage shown represents the percent of MVM staining pixels co-localizing with endocytic marker staining pixels, using BioImageXD.

Chapter 3 – MVM Induces Morphological Changes to the Host Cell During Infection¹

3.1 Introduction

Like with other DNA viruses, an efficient infection with MVM requires the virus to overcome barriers within the cell, such as membranes and a viscous cytoplasm, in order to reach the nucleus and replicate its genome. Many steps of MVM infection that are important in overcoming these barriers, such as endocytosis, endosomal or viral trafficking, and nuclear entry, depend on and impact the host cytoskeleton. For parvoviruses in general, the cytoskeleton networks of MTs and AFs have been implicated in the viral infection cycle. For example, the CPV and the AAV both exploit MTs and dynein for the process of nuclear targeting (Kelkar *et al.*, 2006; Suikkanen *et al.*, 2003). As well, the AF network regulates MVM egress through MVM-induced actin degradation, and the function of the actin-severing protein gelsolin (Bar *et al.*, 2008). However, many aspects regarding the role of the cytoskeleton during parvoviral infection, including the role of IFs, remains to be characterized.

In this chapter I first characterized the effect of early MVM infection on the cytoskeleton. I studied the distribution of the cytoskeleton components, AFs, MTs and IFs, upon MVM infection, as well as changes to the nuclear lamina. I then determined if these

¹ Parts of this chapter have been published:

Nikta Fay and Panté N. (2013). The intermediate filament network protein, vimentin, is required for parvoviral infection. *Virology* **444**: 181-90, doi: 10.1016/j.virol.2013.06.009
<http://www.sciencedirect.com/science/article/pii/S0042682213003589>

morphological changes in the cytoskeleton are correlated with changes in the mechanical properties of the host cell during early MVM infection.

3.2 Results

3.2.1 MVM causes morphological changes in the cell and alters the vimentin filament network 2 h P.I.

In order to investigate the role of the cytoskeleton during early MVM infection, I used a morphological approach to initially visualize whether there are any changes to the overall shape of mouse fibroblast cells at 2 h P.I. Morphological changes during late infection, at 24 and 48 h P.I., have previously been studied (Nuesch *et al.*, 2005). In that study it was shown that the majority of the infected cells changed their overall shape, some with large protrusions, others rounded-up. I first wanted to determine whether these changes occur during earlier steps of infection with MVM and therefore visualized MVM-infected cells by bright field microscopy. In contrast to mock-infected cells, which present the characteristic star-like shape of mouse fibroblasts, LA9 mouse fibroblast cells at 2 h P.I. with MVM had a less distinct or more patchy cytoplasm on one side of the nucleus than the other (Fig. 3-1a). This observed change in the shape of infected cells may be a result of the virus altering the host's organized network of three filaments, AFs, IFs and MTs.

MVM infects fibroblasts of mesenchymal origin, in which the predominant IF is vimentin (Reviewed by Goldman *et al.*, 2012) (Steinert & Parry, 1985). Thus, I then went on to visualize by indirect fluorescence microscopy whether there are any changes in the

distribution of the vimentin, MT, and AF networks in MVM-infected cells. Of the three cytoskeleton filaments, the most notable changes were seen in the vimentin network. Mock-infected cells have the regular pattern of vimentin immunostaining with filaments distributed throughout the cell and extending from the perinuclear region to the plasma membrane (Fig. 3-1b). In contrast, this pattern was altered in cells infected with MVM for 2 h, yielding a vimentin network that has withdrawn from the cellular periphery and accumulated at the nuclear periphery (Fig. 3-1b, arrows). In most of the infected cells this vimentin immunostaining accumulation was on one side of the nucleus, in close proximity to the virus, which accumulate at the perinuclear region at 2 h P.I. (Fig. 3-1b). In order to quantify this effect, the percentage of cells that show accumulation of vimentin immunostaining on one side of the nucleus (as indicated with arrowheads in Fig. 3-1b) were counted in mock- and MVM-infected cells. The change in vimentin immunostaining pattern was found to be statistically significant, occurring in $62 \pm 4\%$ of infected-cells at 2 h P.I. (Fig. 3-1d).

Since endosomal release of MVM into the cytoplasm is inefficient with only few virions leaving this compartment and entering the cytosol (Mani *et al.*, 2006), it is possible that the rearrangement of the vimentin network detected 2 h P.I. may be due to an interaction between the viral containing endosomes with the vimentin network, rather than with the few free virions in the cytoplasm. To test this, I visualized by indirect fluorescence microscopy whether there are any changes in the distribution of the vimentin network in cells incubated with empty capsids (devoid of DNA) 2 h P.I. Empty capsids are able to enter cells similar to full MVM capsids, however, they are unable to escape from endosomes. Cells incubated with empty capsids have the same pattern of

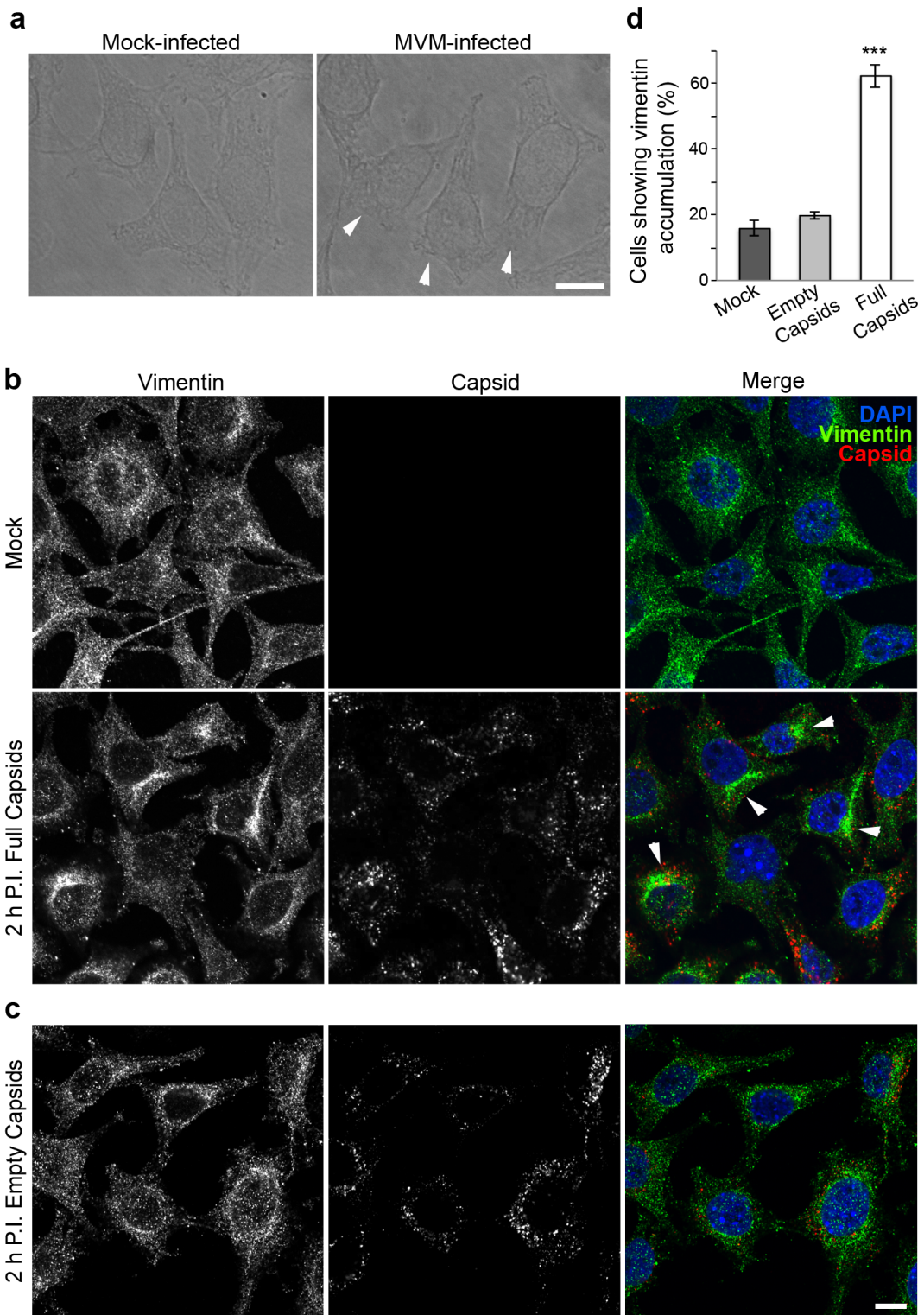


Figure 3-1: MVM causes morphological changes in the cell and alters the vimentin filament network 2 h P.I. LA9 cells were mock infected, infected with MVM (MOI of 4), or incubated with empty viral capsids and prepared for indirect immunofluorescence microscopy 2 h P.I. Cells were fixed with 3% PFA and permeabilized with 0.003% digitonin. (a) Representative bright field of cells mock infected or infected with MVM. Arrowheads point to cells that have morphological changes on one side of the cell. (b) Representative confocal microscopy images of cells mock infected or infected with MVM full capsids. (c) Representative confocal microscopy images of cells incubated with empty capsids. Cells were labeled with an anti-vimentin antibody (H84; green), an anti-capsid antibody (MAb B7; red), and with DAPI to detect DNA (blue). Arrowheads point to cells that show accumulation of the vimentin immunostaining at the perinuclear region. Scale bars, 10 μ m. (d) Bar graph of the proportion of cells showing accumulation of the vimentin immunostaining at the perinuclear region as a percentage of total cells. Shown are the mean values and standard error measured for 3 independent experiments (100 cells were counted for each condition). ***, $P < 0.001$ compared to mock infection (unpaired Student t test). (Figure reproduced with permission from Fay and Pante, 2013)

vimentin immunostaining as seen in mock-infected cells (Fig. 3-1, b and c), and similar quantification of the percentage of cells that show accumulation of vimentin immunostaining on one side of the nucleus (Fig. 3-1d). Since empty capsids are unable to escape the endosomal compartments (Farr *et al.*, 2005), this result suggests that the rearrangement of vimentin occurs after virions have left the endosomal compartment, even if only few virions escape the endosome.

As described above, in most of the infected cells the accumulation of vimentin immunostaining was on one side of the nucleus, in close proximity to the virus, which accumulated at the perinuclear region at 2 h P.I. The accumulation of MVM is likely at the MTOC because the virus traffics within endosomes toward one side of the nucleus (Ros & Kempf, 2004). To confirm that MVM is accumulated near the MTOC in infected cells, I visualized by indirect fluorescence microscopy MVM and pericentrin 2 h P.I. Pericentrin is one of the proteins responsible for MT nucleation and anchoring which makes up the centrosome as the main MTOC (Doxsey *et al.*, 1994; Rieder *et al.*, 2001), and thus was used as a MTOC marker. As expected, I found that in MVM-infected cells the immunostaining of MVM capsids was on one side of the nucleus, in close proximity to pericentrin immunostaining (Fig. 3-2).

3.2.2 MVM persists to rearrange the vimentin network 2, 4 and 6 h P.I.

To determine whether the rearrangements in vimentin immunostaining continued throughout MVM infection, I visualized vimentin by indirect fluorescence microscopy in cells infected with MVM at 4 and 6 h P.I., and found that this accumulation of the vimentin immunostaining continues to be prominent 4 and 6 h P.I. (Fig. 3-3). Similar to

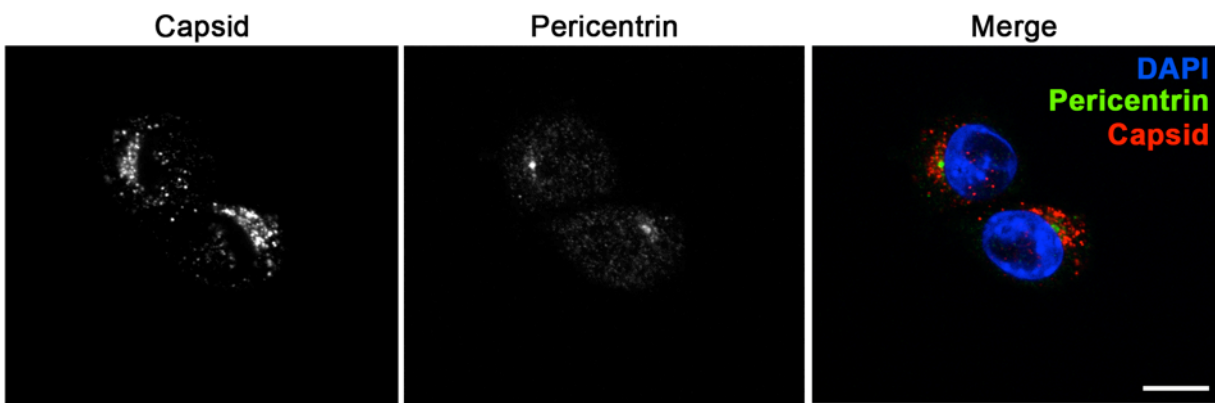


Figure 3-2: MVM co-localizes with MTOC protein pericentrin 2 h P.I. LA9 cells were infected with MVM (MOI of 4) and prepared for indirect immunofluorescence microscopy 2 h P.I. Cells were fixed and permeabilized with methanol and labeled with an anti-capsid antibody (MAb B7; red), and an anti-pericentrin antibody (ab4448; green) and with DAPI to detect DNA (blue). Shown are representative confocal microscopy images of cells infected with MVM. Scale bar, 10 μ m.

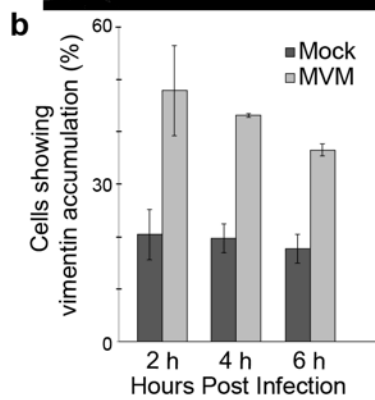
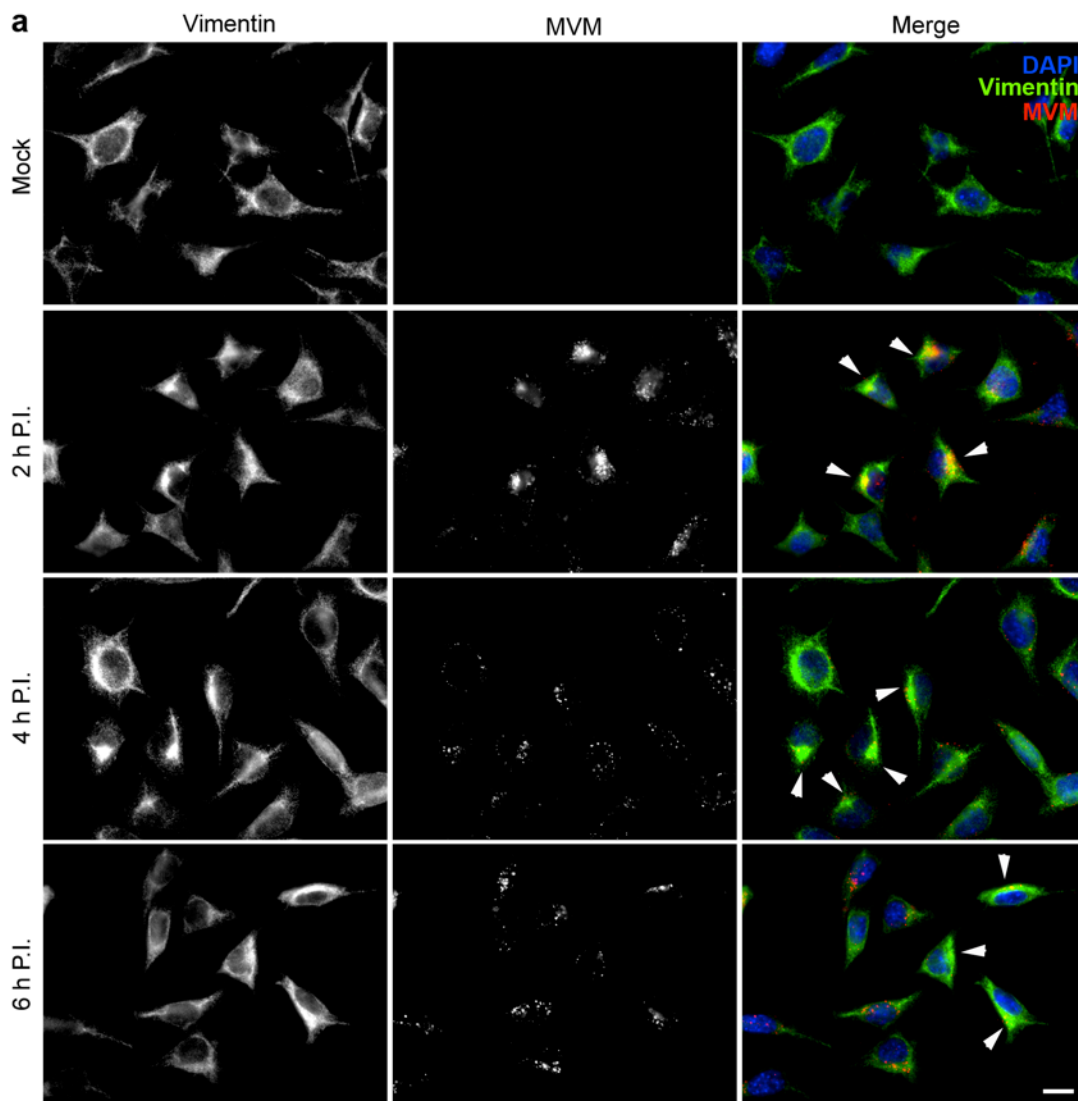


Figure 3-3: Early infection of mouse fibroblasts with MVM rearranges the vimentin filament network. LA9 cells were mock infected or infected with MVM (MOI of 4) and prepared for indirect immunofluorescence microscopy 2, 4, and 6 h P.I. Cells were fixed with 3% PFA, permeabilized with 0.003% digitonin and labeled with an anti-vimentin antibody (H84; green), an anti-capsid antibody (MAb B7; red), and with DAPI to detect DNA (blue). (a) Representative epifluorescence microscopy images of cells mock infected or infected with MVM. Arrowheads point to cells, which show accumulation of the vimentin immunostaining at the perinuclear region. Scale bar, 10 μ m. (b) Bar graph of the proportion of cells showing accumulation of the vimentin immunostaining at the perinuclear region as a percentage of total cells. Shown are the mean values and standard error measured for 3 independent experiments (85 cells were counted for each condition).

the observed results at 2 h P.I., in most of the infected cells the vimentin immunostaining accumulated on one side of the nucleus, in close proximity to the virus, which accumulated at the perinuclear region at 4 and 6 h P.I. (Fig. 3-3a). In order to quantify this effect, the percentage of cells that show accumulation of vimentin immunostaining on one side of the nucleus (as indicated with arrowheads in Fig. 3-3a) were counted in mock- and MVM-infected cells. The change in vimentin immunostaining pattern was found to be statistically significant, occurring in $48 \pm 9\%$, $43 \pm 0.4\%$, and $37 \pm 1\%$ of infected-cells at 2, 4, and 6 h P.I. respectively.

3.2.3 Late infection of mouse fibroblast cells with MVM collapses the vimentin network

To confirm the previous published observation that the vimentin network is completely disrupted at later time of MVM infection (Nuesch *et al.*, 2005), experiments were also performed at 24 h P.I. As illustrated in Fig. 3-4a, the vimentin immunostaining was more drastically altered at 24 h P.I.; instead of the accumulation on one side of the nucleus, the immunostaining was found forming a ring around the nucleus. This is an indication that the vimentin network collapsed entirely around the nucleus. This change is also statistically significant, occurring in $48 \pm 4\%$ of infected-cells at 24 h P.I. (Fig. 3-4b). This observed change in distribution of the vimentin immunostaining at 24 h agrees with previous results by Nüesch *et al.* (2005), showing that the vimentin network is disrupted during late MVM infection, collapsing around the nucleus like a ring. Thus, the vimentin network is rearranged during both the earlier and late stages of infection with MVM.

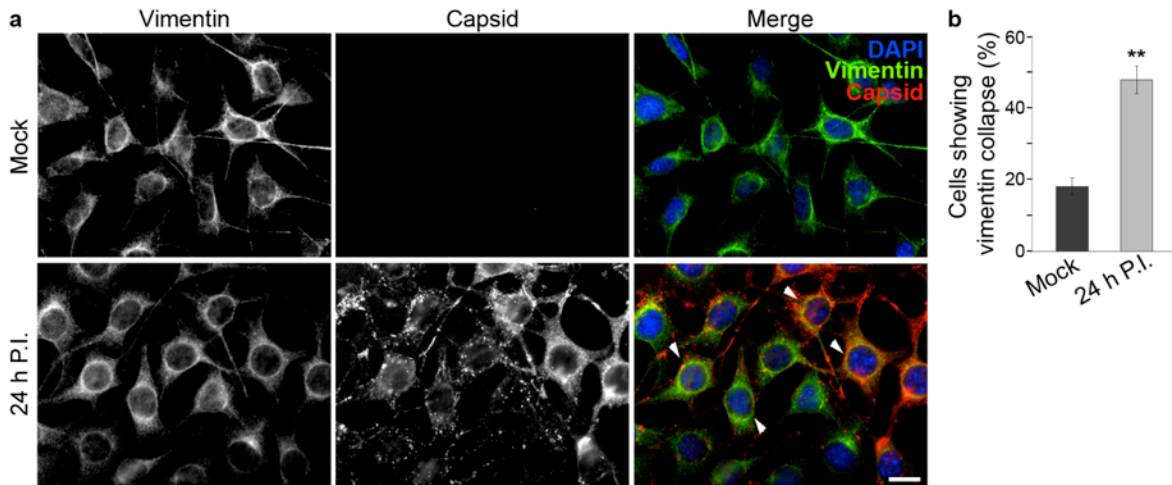


Figure 3-4: Late infection of mouse fibroblast cells with MVM collapses the vimentin filament network. LA9 cells were mock infected or infected with MVM (MOI of 4) and prepared for indirect immunofluorescence microscopy 24 h P.I. Cells were fixed with 3% PFA, permeabilized with 0.003% digitonin, and labeled with an anti-vimentin antibody (H84; green), an anti-capsid antibody (MAb B7; red), and with DAPI to detect DNA (blue). (a) Representative epifluorescence images of cells mock infected or infected with MVM. Arrowheads point to cells that show ring-like pattern of the vimentin immunostaining. Scale bar, 10 μ m. (b) Bar graph of the proportion of cells showing collapse of the vimentin filament network as a percentage of total cells. Shown are the mean values and standard error measured for 3 independent experiments (85 cells were counted for each condition). **, $P < 0.01$ compared to mock infection (unpaired Student t test). (Figure reproduced with permission from Fay and Pante, 2013)

3.2.4 Cell type and vimentin network symmetry determine the effect on vimentin during MVM infection

I then went on to investigate whether the rearrangements to vimentin observed at 2 h P.I. are cell type specific or are universal to other cell types. Other cell types that are often used in parvovirus research are NIH-3T3 and NB324k cells (Adeyemi *et al.*, 2010; Ventoso *et al.*, 2010). NIH-3T3 cells are susceptible to MVM infection, as they are a standard mouse fibroblast line, and I have shown this by immunostaining for NS1 12 h P.I. (data not shown). I performed immunostaining of vimentin 2 h P.I. in NIH-3T3 cells (Fig. 3-5) and found results similar to LA9 mouse fibroblast cells. MVM-infection of NIH-3T3 cells showed vimentin immunostaining accumulated on one side of the nucleus, in close proximity to the virus, which accumulated at the perinuclear region (Fig. 3-5). The percentage of cells that show accumulation of vimentin immunostaining on one side of the nucleus (as indicated with arrowheads in Fig. 3-5a) were counted in mock- and MVM-infected cells. The change in vimentin immunostaining pattern was found to be statistically significant, occurring in $41 \pm 2\%$ of infected-cells at 2 h P.I. (Fig. 3-5b).

Although NB324K cells are newborn human kidney fibroblast cells, they are simian virus 40-transformed and are able to rapidly replicate. However, MVM-infection of NB324k cells showed no difference in vimentin immunostaining compared to mock-infected cells (Fig. 3-6a). Due to this differing result among the LA9 and NIH-3T3 cells, and the NB324K cells, I next confirmed whether these cells were in fact susceptible to MVM infection by immunostaining of the viral nonstructural protein NS1 12 h P.I. (Fig. 3-6b). NS1 is the first non-structural protein to be expressed during MVM infection; however, it

is not incorporated into assembled capsids and only plays a role in initiating DNA replication and activating expression of VP1 and VP2 (reviewed by Cotmore & Tattersall, 2006b). Thus, NS1 was used as readout for MVM replication. The presence of NS1 immunostaining in NB324k cells indicates susceptibility to MVM. Additionally, the regular immunostaining of vimentin in mock-infected cells was different in this human cell line as compared to either LA9 or NIH-3T3 cells. Here, vimentin extended from a region close to the nucleus in a star-like manner in mock-infected cells; this same pattern was observed in MVM-infected cells (Fig. 3-6a). However, in MVM-infected cells, MVM was mostly seen only in the regions close to the nuclear periphery where a high amount of vimentin was found. This suggests that the pre-existing pattern of the vimentin network in a cell may determine how extensive the vimentin network is rearranged during MVM infection. Thus, although the vimentin arrangement did not differ between MVM-infected and mock-infected NB324k cells, there could exist a role for vimentin in the MVM-infected cells due to the close spatial arrangement of vimentin and MVM.

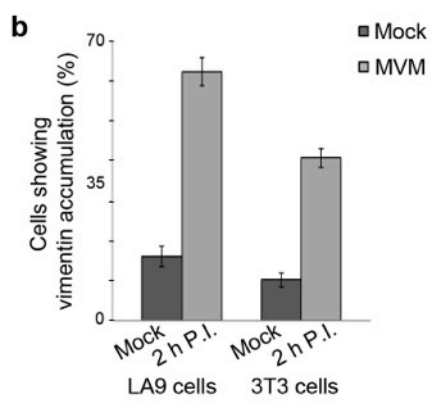
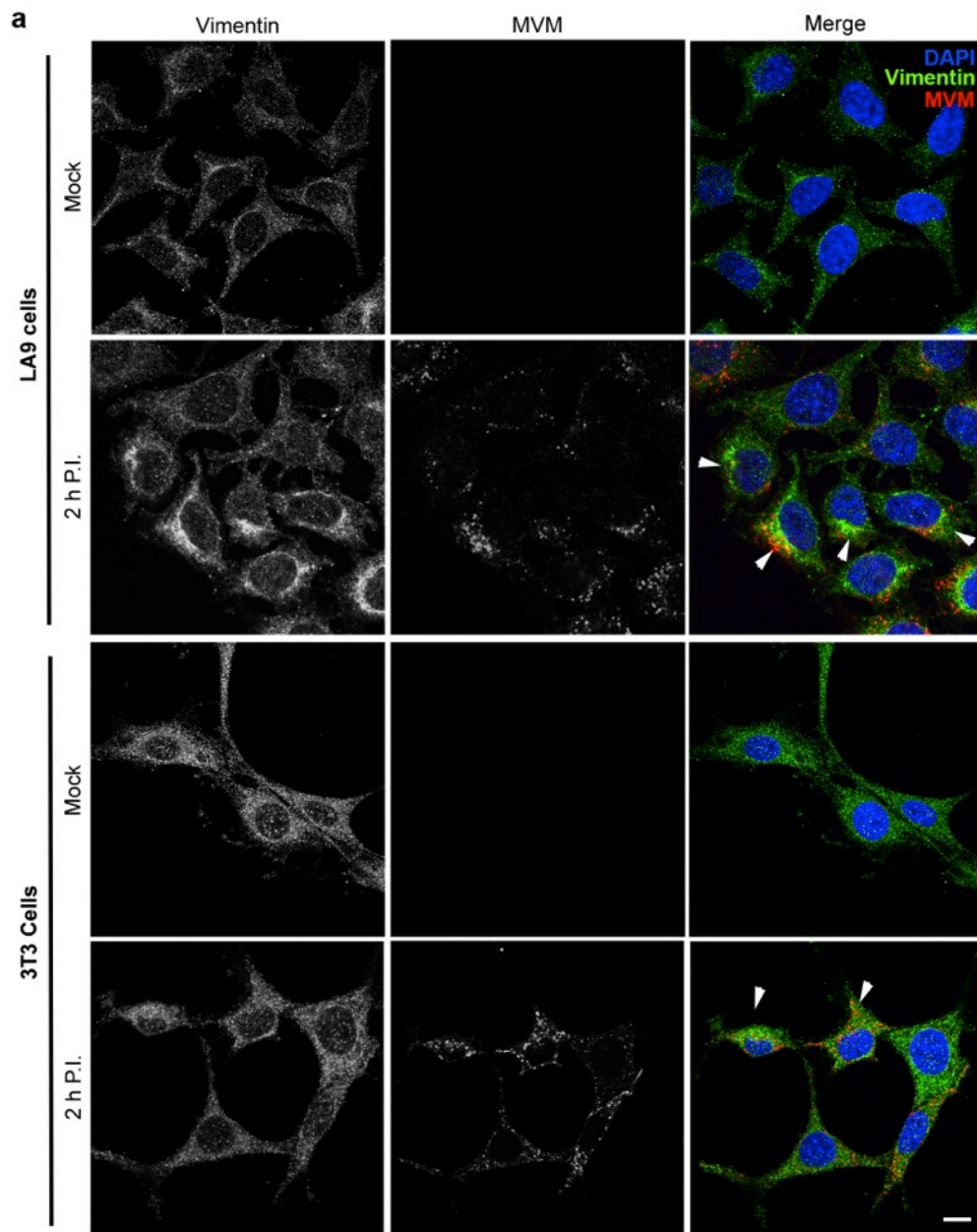


Figure 3-5: Early infection of NIH-3T3 mouse fibroblasts with MVM rearranges the vimentin filament network. LA9 cells (as a control) and NIH-3T3 cells were mock infected or infected with MVM (MOI of 4), prepared for indirect immunofluorescence microscopy 2 P.I. Cells were fixed with 3% PFA and permeabilized with 0.003% digitonin and labeled with an anti-vimentin antibody (H84; green), an anti-capsid antibody (MAb B7), and with DAPI to detect DNA (blue). (a) Representative confocal microscopy images of cells mock infected or infected with MVM. Arrowheads point to cells, which show accumulation of the vimentin immunostaining at the perinuclear region. Scale bar, 10 μ m. (b) Bar graph of the proportion of cells showing accumulation of the vimentin immunostaining at the perinuclear region as a percentage of total cells. Shown are the mean values and standard error measured for 3 independent experiments (100 cells were counted for LA9 cells; 50 cells were counted for 3T3 cells).

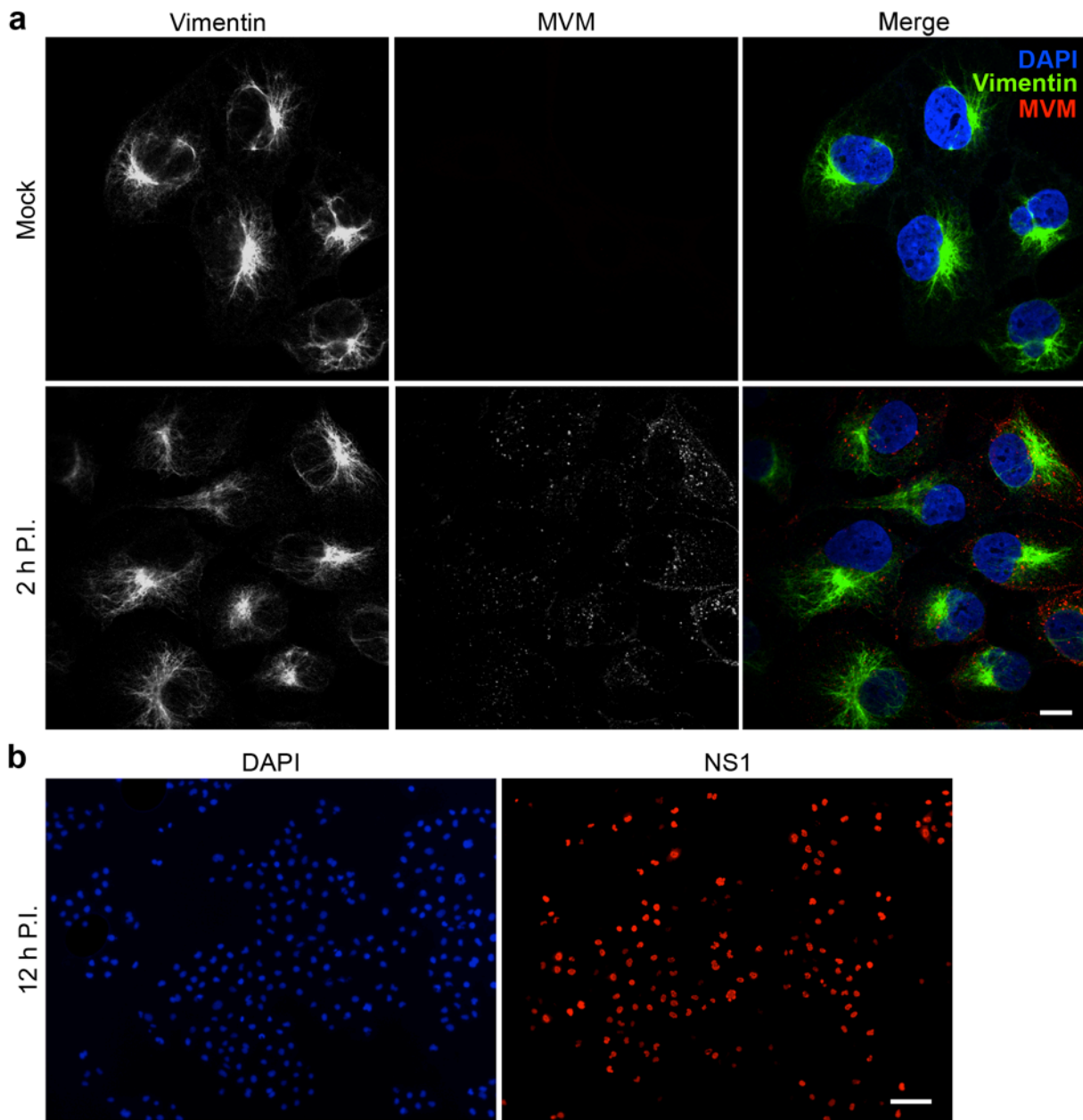


Figure 3-6: Early infection of NEB324k human kidney fibroblast cells with MVM does not alter the vimentin filament network, despite a productive infection. NEB324k cells were mock infected or infected with MVM (MOI of 4) and prepared for indirect immunofluorescence microscopy 2 h and 12 h P.I. (a) Representative confocal microscopy images of cells mock infected or infected with MVM for 2 h. Cells were fixed with 3% PFA and permeabilized with 0.003% digitonin and labeled with an anti-vimentin antibody (H84; green), an anti-capsid antibody (MAb B7; red), and with DAPI to detect DNA (blue). Scale bar, 10 μ m. (b) Representative epifluorescence microscopy images of cells mock infected or infected with MVM for 12 h. Cells were fixed with 3% PFA and permeabilized with 0.2% Triton, and labeled with an anti-NS1 antibody (red), and with DAPI to detect DNA (blue). Scale bar, 50 μ m.

3.2.5 Vimentin is not significantly cleaved in MVM-infected cells

Both cleavage and phosphorylation of vimentin could lead to rearrangements of the vimentin IF network and its eventual collapse that I observed in MVM-infected cells. For HIV-1 and adenovirus, which induce vimentin rearrangement during infection, it has been shown that it is a result of proteolytic cleavage of vimentin (Belin & Boulanger, 1987; Defer *et al.*, 1990; Shoeman *et al.*, 1990), which then results in the collapse or rearrangements of the vimentin IF network (Honer *et al.*, 1991). In the case of HIV-1, it has been demonstrated that a viral protease cleaves vimentin (Honer *et al.*, 1991; Shoeman *et al.*, 1990). For adenovirus, however, the data indicate that a cellular protease, rather than a viral protease may lead to the proteolytic processing of vimentin. MVM proteins have no known proteolytic activities, thus similar to adenovirus, a cellular protease may also be responsible for the cleavage of vimentin during MVM infection. Recently, it has been shown that during early MVM infection, caspase-3 cleaves lamin-B (Cohen *et al.*, 2011). Similar to lamin-B, vimentin may also be cleaved by caspase-3 during MVM infection, causing the rearrangement and further collapse of the vimentin IF network that I observed around the nucleus.

Thus, I investigated the cleavage of vimentin through 2D-DIGE analysis of mock- or MVM-infected mouse fibroblast cells 2 h P.I. These cells were then lysed, and the proteins from mock- and MVM-infected cells were fluorescently labeled, run on the same gel and analyzed by 2D-DIGE (Fig. 3-7a). Two of the three spots known to correspond to vimentin cleavage products were excised from the gel for confirmation of identification by MALDI-ToF mass spectrometry, and were identified correctly as vimentin cleavage products of size 48 and 50 kDa.

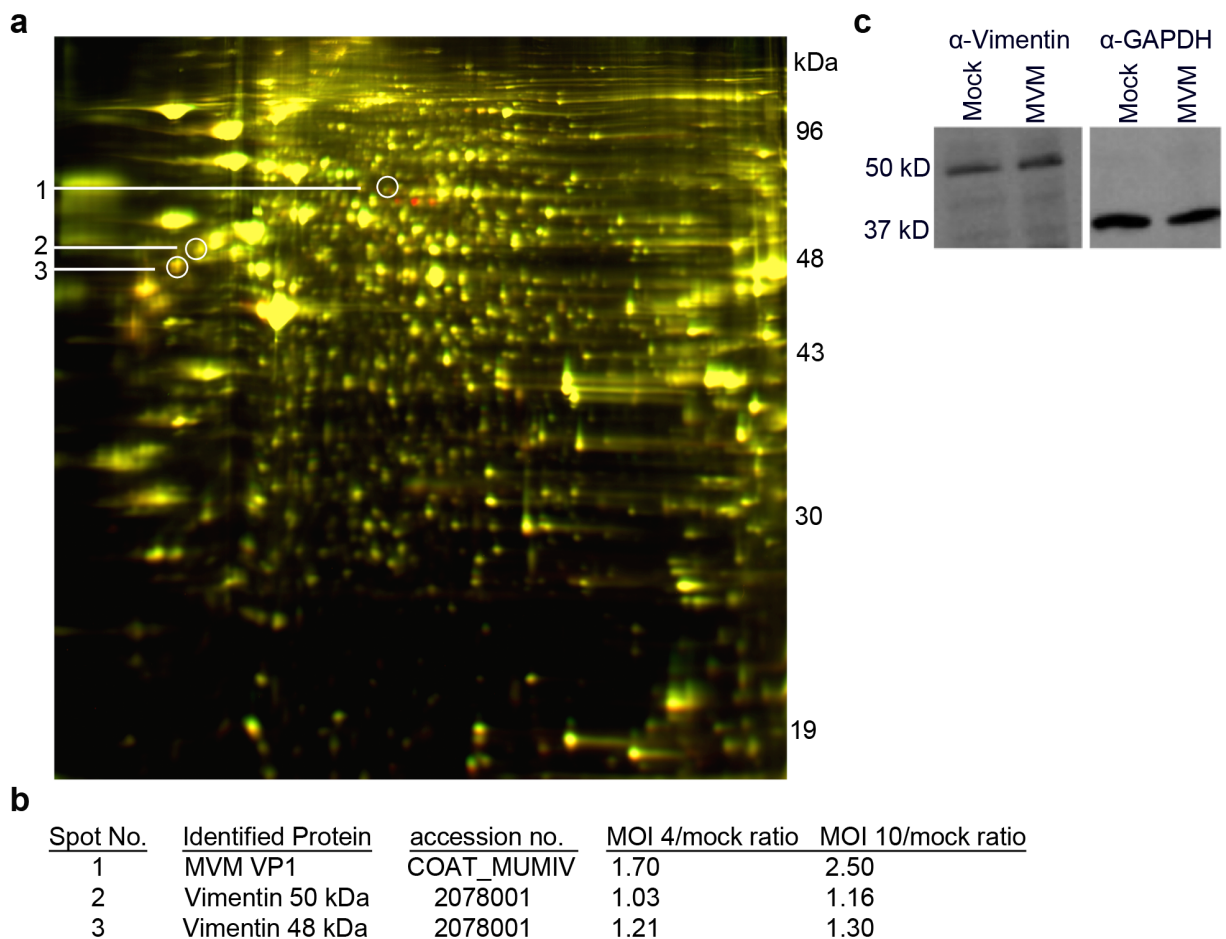


Figure 3-7: Vimentin is not cleaved in MVM-infected cells. 2D- DIGE analysis of mock-infected and MVM-infected cells 2 h P.I. (a) Proteins from mock-infected cells are shown in green, while proteins from MVM-infected cells (MOI of 4) are shown in red; where the two samples are similar, the gel appears yellow. The three spots (circled) were excised from the gel followed by MALDI-ToF mass spectrometry. (b) The ratios of the three spots are shown. (c) Lysates from cells mock- and MVM-infected (MOI of 4) were run on SDS-PAGE 2 h P.I., and analyzed by western blot with anti-vimentin (V9) and anti-GAPDH antibodies.

In addition, the MVM capsid protein, VP1, was also identified. The vimentin cleavage products had an MVM-infected to mock-infected volume ratio of 1.21 and 1.03 respectively for cells infected at a MOI of 4, which then increased to 1.30 and 1.16 for cells infected at a MOI of 10 (Fig. 3-7b). Values of 1.50 are considered significant. Thus, in this case I cannot confirm the significant presence of vimentin cleavage products in the MVM-infected cells. The MVM capsid protein, VP1, had an MVM-infected to mock-infected volume ratio of 1.70 for cells infected at a MOI of 4, which then increased to 2.50 for MOI of 10, thus confirming successful infection.

I further validated these results by western blot analysis. Lysates from cells mock- and MVM-infected were analyzed by western blot with an anti-vimentin antibody 2 h P.I., revealing a band of predicted molecular weight of 50 kDa (Fig. 3-7c). Although full-length vimentin is 57 kDa, it has been shown to run on western blots at around 50 kDa. No differences in bands were observed between mock- and MVM-infected lanes, similar to the control lanes analyzed with anti-GAPDH antibody. This indicates that vimentin is not cleaved during early infection with MVM.

3.2.6 MVM rearranges the microtubule network at 2 h P.I., however the microtubule network is stabilized by 24 h P.I.

The cytoskeleton components are connected into a network, specifically with IFs using MTs for their assembly (Helfand *et al.* 2002). To investigate whether there was any alterations to the MT network that were similar to the vimentin IF network, mouse fibroblast cells were mock infected or infected with MVM and were examined by immunofluorescence microscopy 2, 4, 6, and 24 h P.I. (Fig. 3-8). Noteworthy changes to

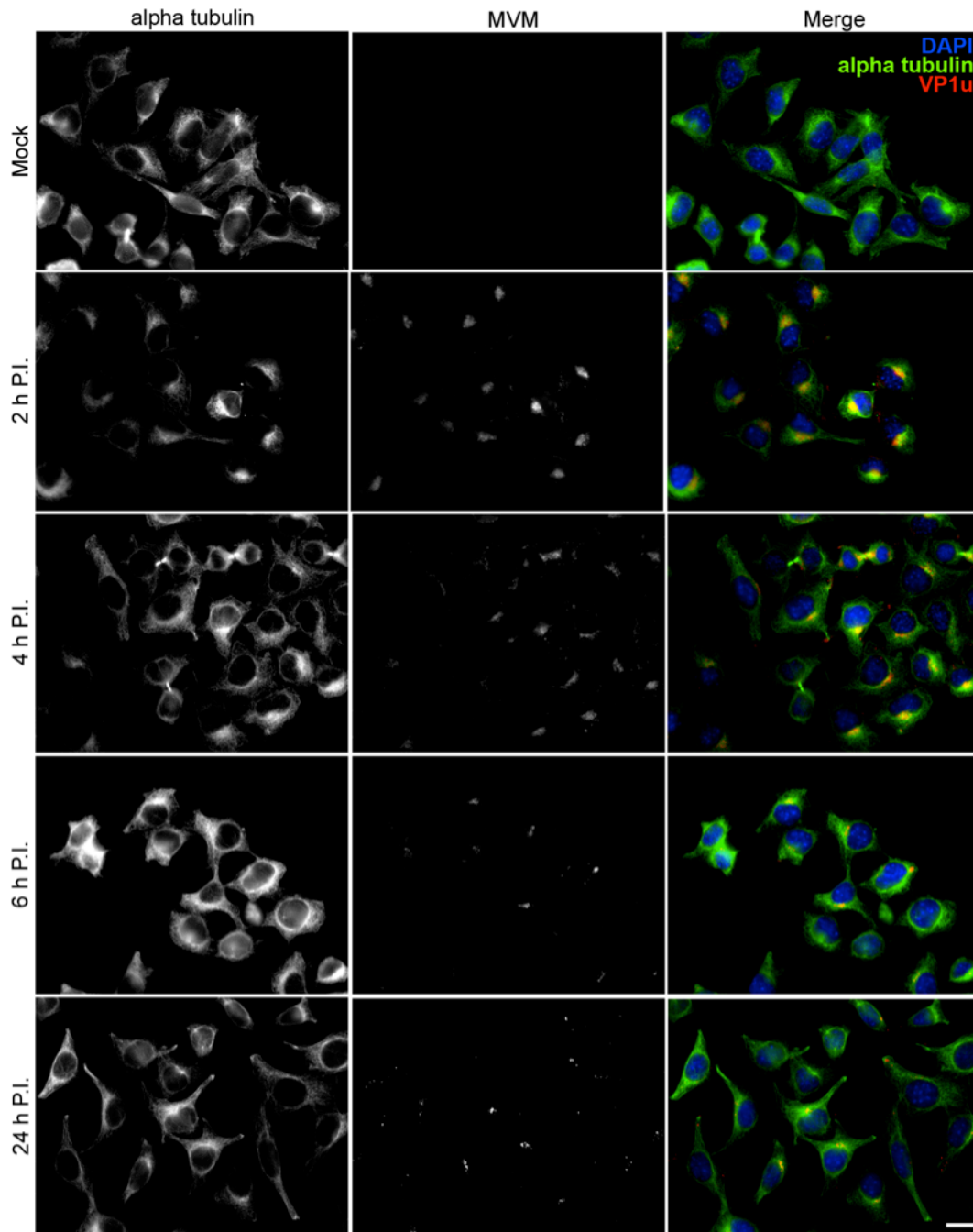


Figure 3-8: MVM rearranges the microtubule network at 2 h P.I., however the MT network is stabilized by 24 h P.I. LA9 cells were mock infected or infected with MVM (MOI of 4) and prepared for indirect immunofluorescence microscopy 2, 4, 6, and 24 h P.I. Cells were fixed with 3% PFA and permeabilized with 0.2% Triton and labeled with an anti-alpha tubulin antibody (DM1A; green), an anti-MVM antibody against the unique region of VP1 (VP1u; red), and with DAPI to detect DNA (blue). Shown are representative epifluorescence microscopy images of cells mock infected or infected with MVM. Scale bar, 10 μ m.

the MT network occur during early infection. Similar to the changes to the vimentin IF network, the MT network in mock-infected cells was distributed evenly throughout the cell, while in MVM-infected cells the MT network accumulated on one side of the nucleus in close proximity to the virus at 2 h P.I. (Fig. 3-8). These changes are no longer observed at 6 and 24 h P.I. and are consistent with the findings of Nüesch *et al.* (2005), which showed that during late infection with MVM 24-48 h P.I., the MT network is maintained.

The MVM immunostaining was more distinct and perinuclear at 24 h P.I. in Figure 3-8 as compared with Figure 3-4. This is because I used different antibodies for these experiments. In Fig. 3-4, I used a mouse antibody against MVM intact capsids (MAb B7) and a rabbit antibody against vimentin (H84), whereas in Figure 3-8 I used a custom made rabbit antibody against the VP1u of MVM, containing the PLA2 domain, and a mouse antibody against MTs (DM1A). This VP1u region has been shown to be essential for MVM viral infectivity, specifically for triggering the endosomal release of virions from endosomes to the cytoplasm in the low pH environment (Farr *et al.*, 2005; Mani *et al.*, 2006; Zadori *et al.*, 2001). This viral release process into the cytoplasm has been shown to be inefficient for parvoviruses, including MVM and canine parvovirus, with many virions remaining in endosomal compartments up to 8 h after the virus has entered endosomes (Mani *et al.*, 2006; Ros *et al.*, 2002; Suikkanen *et al.*, 2002; Vihinen-Ranta *et al.*, 2000). Thus, at 24 h P.I., the staining of infected cells with the antibody against the VP1u region identifies virus that has exposed VP1 and presumably remained trapped in endosomes, rather than progeny virion.

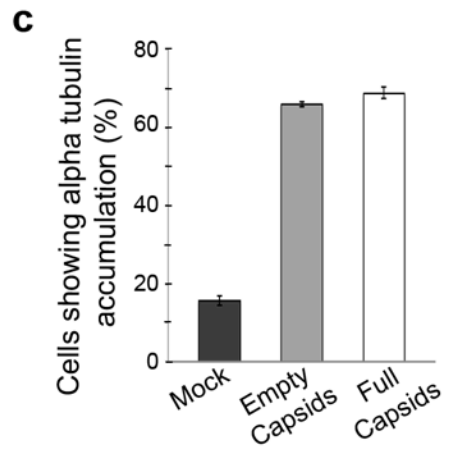
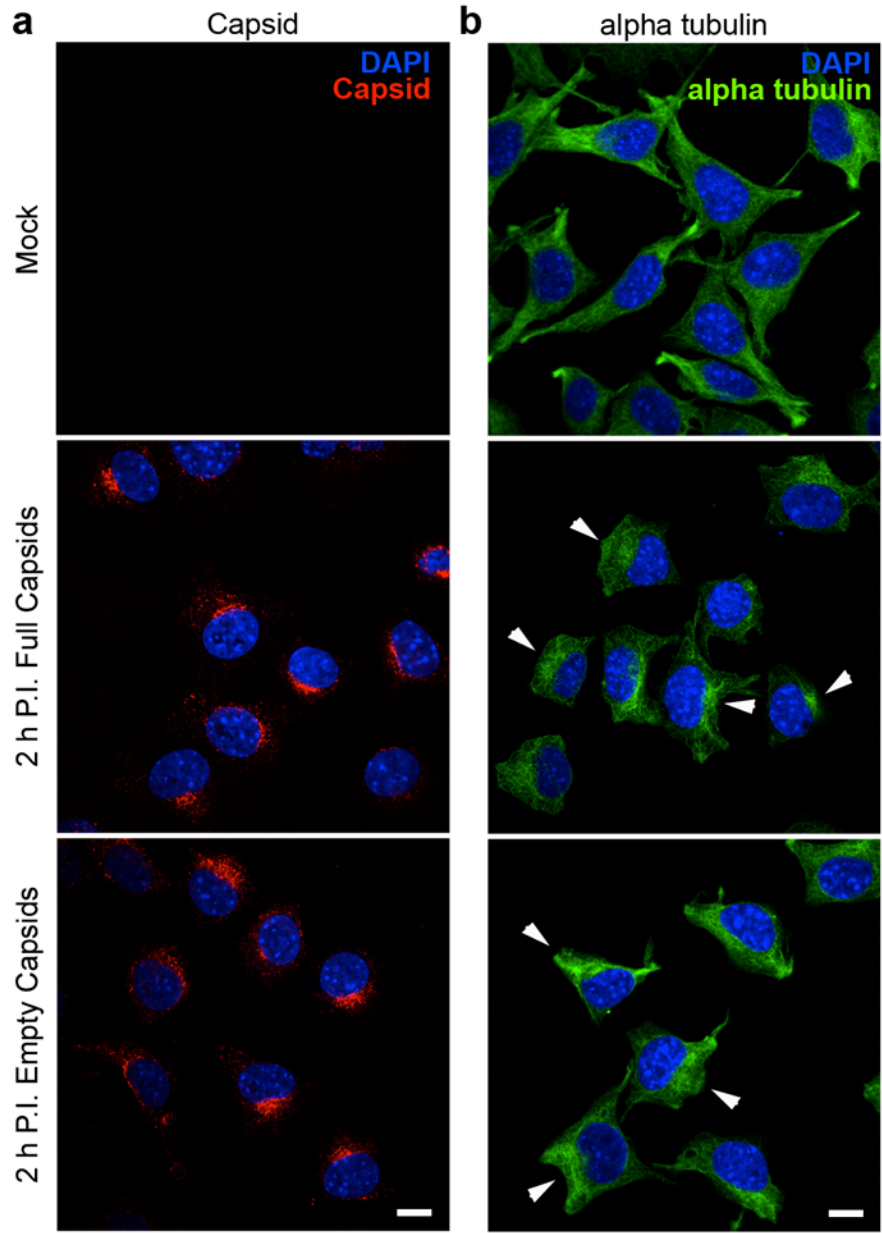


Figure 3-9: The rearrangements to the microtubule network are due to trafficking of MVM-containing vesicles. LA9 cells were mock infected, infected with MVM (MOI of 4), or incubated with empty viral capsids in two sets of parallel replicates and prepared for indirect immunofluorescence microscopy 2 h P.I. Cells were fixed with 3% PFA and permeabilized with 0.2% Triton. (a) Representative confocal microscopy images of cells labeled with an anti-capsid antibody (MAb B7; red), and with DAPI to detect DNA (blue). (b) Representative confocal microscopy images of cells labeled with an anti-alpha tubulin antibody (DM1A; green) and with DAPI to detect DNA (blue). Arrowheads point to cells that show accumulation of the alpha tubulin immunostaining at the perinuclear region. Scale bars, 10 μ m. (c) Bar graph of the proportion of cells showing accumulation of the alpha tubulin immunostaining at the perinuclear region as a percentage of total cells. Shown are the mean values and standard error measured for 3 independent experiments (100 cells were counted for each condition).

3.2.7 The rearrangements to the microtubule network are due to trafficking of MVM-containing vesicles

Since endosomal release of MVM into the cytoplasm is inefficient with only few virions leaving this compartment and entering the cytosol (Mani *et al.*, 2006), it is possible that the rearrangement of the MT network detected 2 h P.I. may be due to an interaction between the MVM-containing vesicles with the MT network, rather than with the few free virions in the cytoplasm. To test this, I visualized by indirect fluorescence microscopy whether there are any changes in the distribution of the MT network in cells incubated with empty capsids (devoid of DNA) 2 h P.I. Cells were immunostained in parallel for MVM capsids and MTs (Fig. 3-9, a and b, respectively). The presence of MVM capsid immunostaining confirms successful infection in MVM-infected cells and cells incubated with empty capsids (Fig. 3-9a). Yet, cells incubated with empty capsids have the same pattern of MT immunostaining on one side of the nucleus as seen in MVM-infected cells (Fig. 3-9b) and similar quantification of the percentage of cells that show accumulation of MT immunostaining on one side of the nucleus (Fig. 3-9c). Thus, this suggests that the rearrangements to the MT network are due to trafficking of MVM-containing vesicles.

3.2.8 The actin network is unaltered during early MVM infection, however exhibits patchiness 24 h P.I.

There is crosstalk among all three cytoskeleton components in the cell, with IFs coordinating cytoskeletal activities and relaying information between the cell surface and other cellular compartments (Chang & Goldman, 2004). To investigate whether the

IF network changes that I observed also have an effect on the actin network, I performed immunofluorescence microscopy of MVM-infected and mock infected mouse fibroblast cells labeled with an antibody against intact MVM capsids along with phalloidin-FITC to detect F-actin at 2, 4, 6, and 24 hours P.I. I found that the actin network remains largely unaltered (Fig. 3-10). At 24 h P.I., the actin network gains a patchy appearance as the AFs begin to break down. These results are consistent with the findings of Nüesch *et al.* (2005), which showed that during late infection with MVM (24-48 h P.I.), during the process of cellular egress, the AF network is disrupted.

3.2.9 Lamin B network is disrupted during early infection with MVM

It has been previously shown that MVM infection causes small transient nuclear envelope disruptions, disruption of the immunostaining of the nuclear lamina, and changes to nuclear shape (Cohen & Pante, 2005; Cohen *et al.*, 2006). Furthermore, it has been shown that B-type lamins, but not A/C-type lamins, are cleaved in a caspase dependent manner in MVM-infected cells (Cohen *et al.*, 2011). However, this disruption has yet to be observed by immunofluorescence microscopy. In addition, studies using *in situ* hybridization to label MVM DNA during the process of nuclear entry are limited. Here I have created biotin-probes against two regions of the MVM-genome (Fig. 3-11a) and used them in conjunction with lamin-B and MVM capsid immunostaining in order to visualize the disruptions to the nuclear lamina network during MVM infection, and the location of MVM DNA and MVM capsids in relation to the nuclear lamina disruptions. I performed *in situ* hybridization along with immunostaining protocols 2 h P.I. The lamin-B

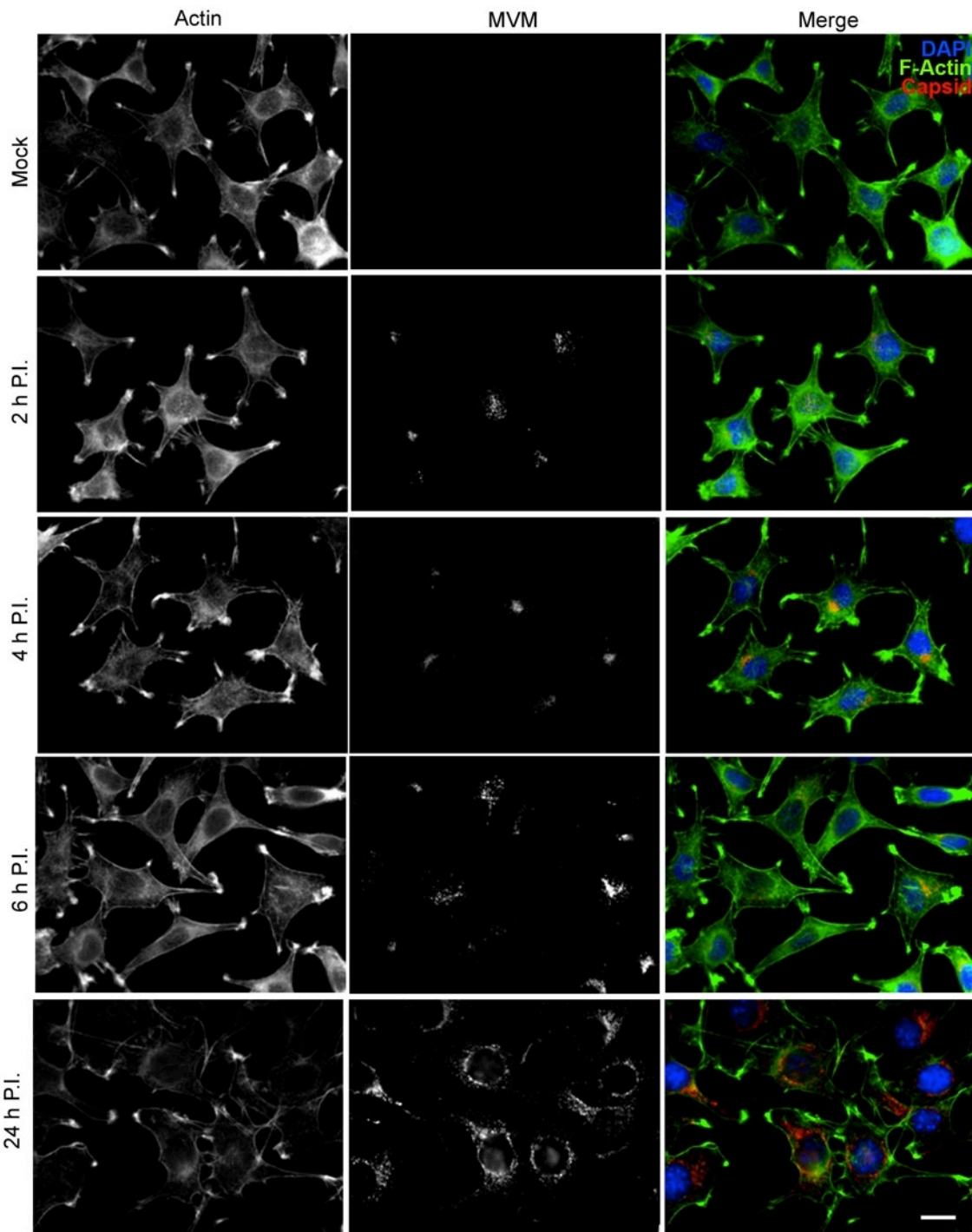


Figure 3-10: The actin filament network is unaltered during early MVM infection, however exhibits patchiness 24 h P.I. LA9 cells were mock infected or infected with MVM (MOI of 4) and prepared for indirect immunofluorescence microscopy 2, 4, 6, and 24 h P.I. Cells were fixed with 3% PFA and permeabilized with 0.2% Triton and labeled with phalloidin-FITC for F-actin (green), an anti-capsid antibody (MAb B7; red), and with DAPI to detect. Shown are representative epifluorescence microscopy images of cells mock infected or infected with MVM. Scale bar, 10 μ m.

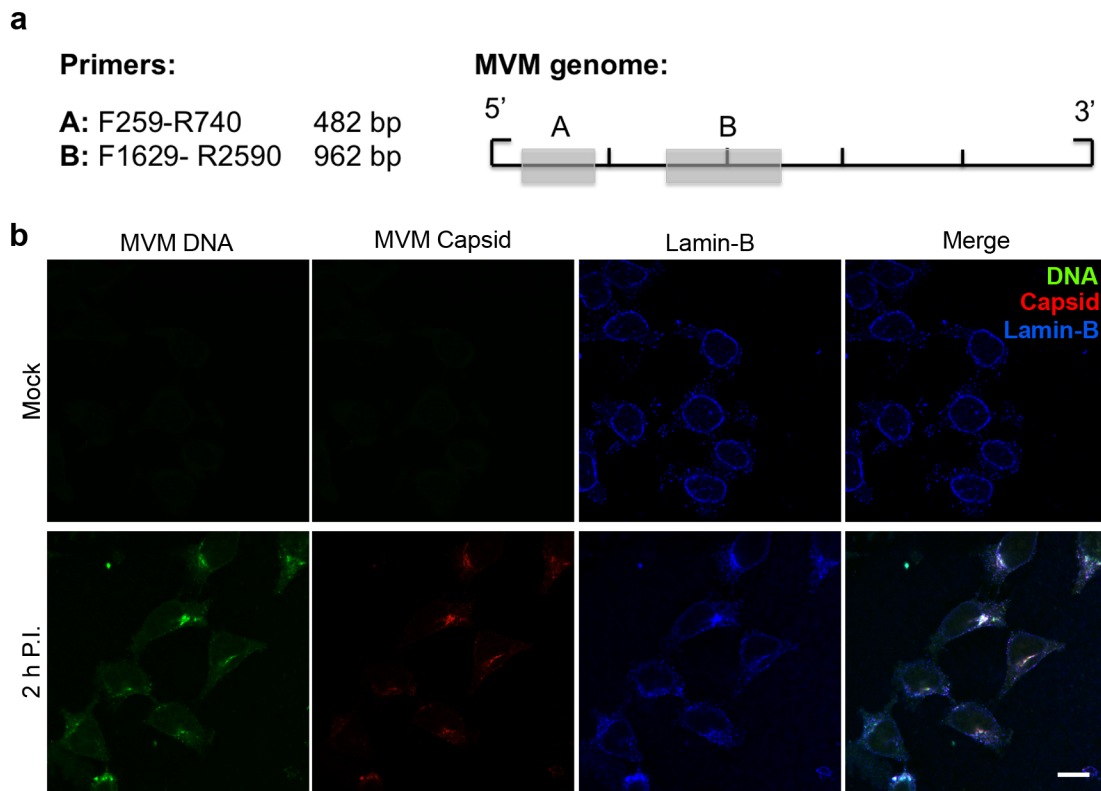


Figure 3-11: Lamin B immunostaining is disrupted during early infection with MVM. LA9 cells were mock infected or infected with MVM (MOI of 4) and prepared for *in situ* hybridization in combination with indirect immunofluorescence confocal microscopy 2 h P.I. (a) Biotinylated probes created against MVM genome. MVM genomic regions covered by the probes are shadowed and labeled A and B and made using primers A and B respectively. (b) Representative confocal microscopy images of cells mock infected or infected with MVM were examined by *in situ* hybridization with biotinylated probes and Streptavidin-FITC to detect MVM DNA (green), an anti-capsid antibody (MAb B7); red), and an anti-lamin-B antibody (blue). Scale bar, 10 μ m.

immunostaining was shown in mock-infected cells as a distinct rim surrounding the nucleus (Fig. 3-11b). In contrast, cells infected with MVM showed disrupted lamin-B immunostaining at 2 h P.I., which coincided with the location of MVM DNA, as well as MVM capsids. Thus, MVM causes disruption to the lamin-B immunostaining during early infection, which correlated with the proteolytic cleavage of lamin-B (Cohen *et al.*, 2011).

3.2.10 MVM decreases stiffness of fibroblast cells during early infection

The significant changes in the cytoskeleton, nuclear shape, and nuclear lamina during MVM infection that I have observed could impact the mechanical properties of cells. I wanted to use a technique that could determine the mechanical properties of the cell during MVM infection, as an independent measure of the changes that I observed to the cytoskeleton. There have been many techniques developed to measure mechanical properties of cells, one of which is AFM. This technique was first used in biological fields for its two advantages: it provides nanometer-scale resolution imaging and the samples can be in aqueous solution, meaning a biological sample can be imaged in its physiological environment (Alexander *et al.*, 1989; Bustamante *et al.*, 1997). AFM has provided structural and architectural insights for countless biological systems. Some examples include: the surface architecture of viruses (reviewed by Kuznetsov & McPherson, 2011; Kuznetsov *et al.*, 2001), the surface topography of biological membranes (reviewed by Frederix *et al.*, 2009; Muller & Dufrene, 2011), the structure and topology of nucleic acids (reviewed by Hansma *et al.*, 2004; Lyubchenko *et al.*, 2011), the structure and conformational changes of the nuclear pore complex (Mooren *et al.*, 2004; Stoffler *et al.*, 1999), and the assembly and structure of the IF network (Mucke *et al.*, 2004; Strelkov *et al.*, 2003).

However, due to its highly sensitive probe, AFM has gained many new applications beyond simply providing structure and topology information of biological samples. One of these applications is to provide measurements of the mechanical properties of cells and biological systems under various conditions. As an example, using the AFM probe to apply force, studies have examined the assembly dynamics of the IF network in cells when exposed to stress (Kreplak *et al.*, 2005). Furthermore, studies have begun to record force distance (FD) curves (Dufrene *et al.*, 2013), which could measure changes in mechanical properties of cells under specific conditions. For example, FD curves have been used in studies to show the effects on the mechanical properties of cells after modulation of the vimentin IF network in rat fibroblasts (Plodinec *et al.*, 2011).

Thus, I have performed AFM and recorded FD curves of mock- and MVM-infected cells in order to determine the mechanical properties of the cell, as an independent measure of the changes I observed to the cytoskeleton. The mechanical properties of cells can be determined by calculating the elastic modulus from FD curves (Fig 3-12). Here, LA9 cells were mock- and MVM-infected and prepared for AFM 2 to 3 h P.I. The AFM tip was visualized and positioned at defined regions of the cell between the nucleus and cellular periphery (Fig. 3-13a), producing a FD curve (Fig. 3-13b), from which the slope of the curve gave the elastic modulus as a measure for the membrane tension or mechanical property of the cell (Fig. 3-13c). I found that at 2 to 3 h P.I. with MVM, the elastic modulus of cells decreased from 34.9 ± 4.4 kPa to 10.6 ± 4.0 kPa in mock-infected cells (Fig. 3-13c). This suggests that upon MVM infection the cell is less stiff overall, and thus, the change in the mechanical property of cells provides a confirmation for the observed cytoskeletal, nuclear, and lamina changes during MVM infection.

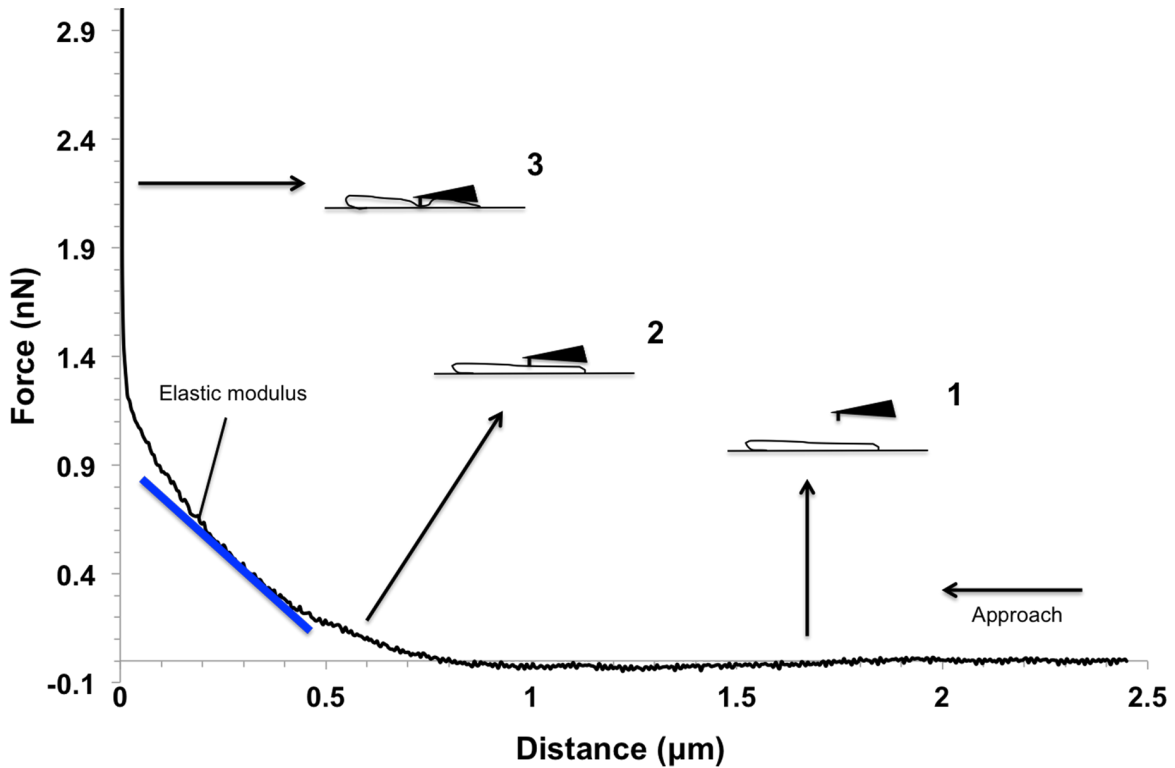


Figure 3-12: Atomic force microscopy can record FD curves and provide the elastic modulus of a cell. The AFM cantilever approaches the sample (measured as distance) making rapid pokes at a fixed point, and measures the mechanical deformation or resistance of the sample (measured as force) as it does so. (1) Before the cantilever has approached the sample, the force is measured as near 0. (2) A curve begins to form as the cantilever approaches the sample and the cell begins to deflect back on the cantilever. (3) At last, when the cantilever has made contact with the dish that holds the cells, the curve reaches a vertical line. The elastic modulus is then calculated as the slope of the curve (blue line), from a point after the cantilever has made contact with the sample.

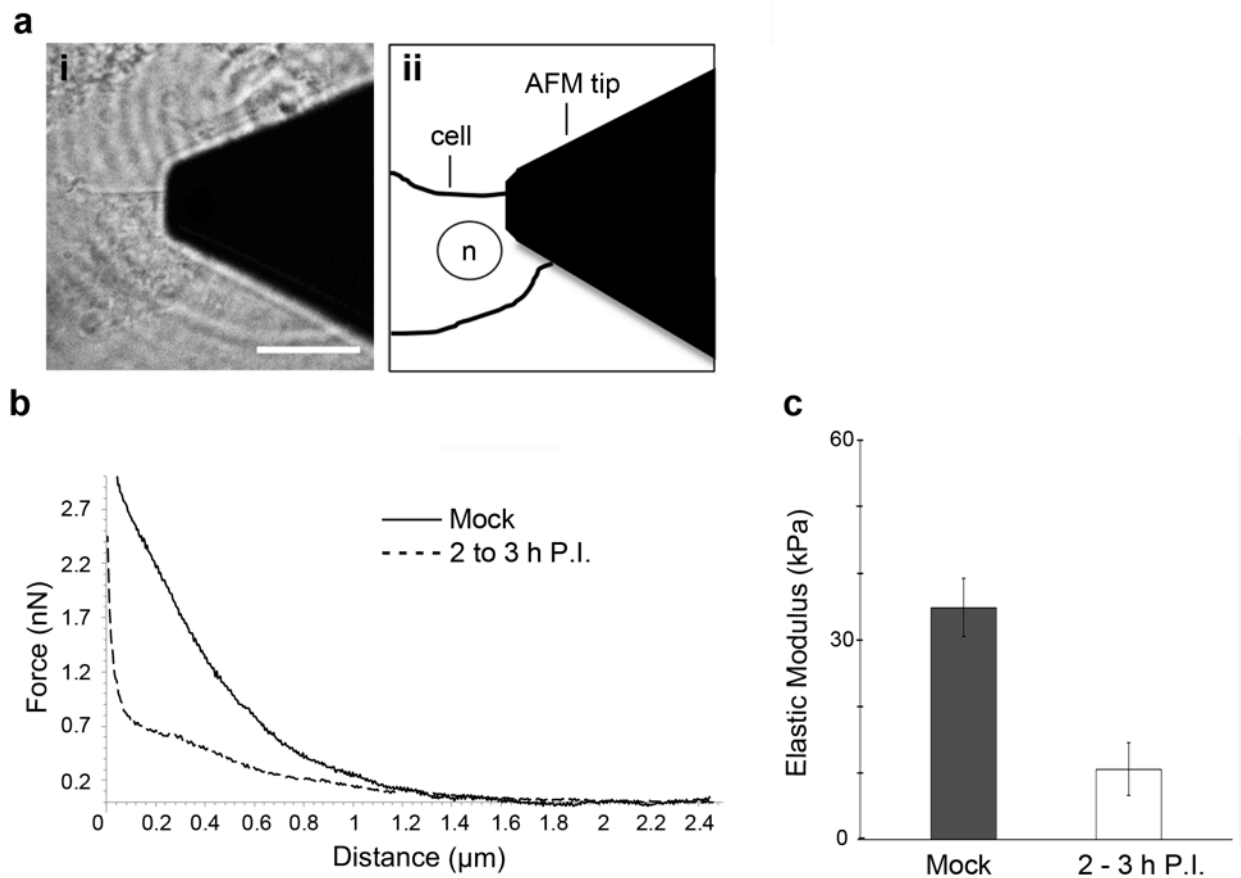


Figure 3-13: Atomic force microscopy shows decrease in stiffness of MVM-infected mouse fibroblast cells. LA9 cells were mock infected or infected with MVM (MOI of 4) and prepared for AFM 2 h P.I. (a) Representative bright field image (i) and schematic drawing (ii) of an AFM tip at a defined region of a cell between the nucleus (n) and cellular periphery 2 to 3 h P.I. with MVM. Scale bar, 10 μm . (b) Representative FD curves for a mock-infected cell and a MVM-infected cell. (c) The elastic modulus for every cell was calculated using average values of the slope of the FD curves from a distance of 0.1-0.5 μm . Shown are the mean values and standard deviation. Mean values were calculated from n=4 independent measurements for mock-infected cells and n=12 for MVM-infected cells.

3.3 Discussion

Our data indicate that in mouse fibroblast cells, the vimentin IF network is rearranged, accumulating at the nuclear periphery at 2 h P.I. with MVM (Fig. 3-1). These rearrangements only occur during infection with virus containing DNA (full capsids) and not for cells incubated with empty capsids (devoid of DNA), which were produced and extensively purified by the same protocol as the full capsids (Fig. 3-1). The empty capsids are non-infectious and are unable to escape from endosomes (Farr *et al.*, 2005). Thus, incubating cells with empty capsids offers insight into whether the observed changes in the vimentin immunostaining occur due to endosomal trafficking of the virus or upon its exit from endosomes. The results indicate that the rearrangements most likely occur upon MVM endosomal escape and release into the cytoplasm, as the number of cells showing rearrangement of vimentin for experiments with empty capsids is similar to mock-infected cells. Furthermore, the vimentin IF network is rearranged to accumulate on one side of the nucleus, in an asymmetric manner, likely because MVM traffics toward the MTOC and is released from endosomes near one side of the nucleus (Fig. 3-2) where it can then cause rearrangement to the vimentin network. In addition, I found that these vimentin rearrangements occurred during both early and late infection (Figs. 3-3 and 3-4), and were cell type specific – being dependent on the pre-existing distribution of the vimentin network in the cell (Figs. 3-5 and 3-6).

There have been several other viruses reported to also cause rearrangements and collapse of the vimentin network during viral infection. Among these are rotavirus (Weclawicz *et al.*, 1994), dengue virus (Chen *et al.*, 2008), African swine fever virus

(Stefanovic *et al.*, 2005), and HIV-1 (Honer *et al.*, 1991). Although for African swine fever virus the role of the vimentin network rearrangement has been established (it forms a protective cage around viral factories during viral replication) (Heath *et al.*, 2001), the specific role of vimentin rearrangement during infection with other viruses, including MVM, remains to be elucidated.

Both cleavage and phosphorylation of vimentin could lead to rearrangements of the vimentin IF network and its eventual collapse that I observed in MVM-infected cells. For HIV-1 and adenovirus, which induce vimentin rearrangement during infection, it is a result of proteolytic cleavage of vimentin (Belin & Boulanger, 1987; Defer *et al.*, 1990; Shoeman *et al.*, 1990), which then results in the collapse or rearrangements of the vimentin IF network (Honer *et al.*, 1991). In the case of HIV-1, it has been demonstrated that a viral protease cleaves vimentin (Honer *et al.*, 1991; Shoeman *et al.*, 1990). For adenovirus, however, the data suggest that a cellular protease, rather than a viral protease may lead to the proteolytic processing of vimentin. MVM proteins have no known proteolytic activities, thus similar to adenovirus, a cellular protease may also be responsible for the cleavage of vimentin during MVM infection. Recently, it has been shown that during early MVM infection, caspase-3 cleaves lamin-B (Cohen *et al.*, 2011). Similar to lamin-B, vimentin may also be cleaved by caspase-3 during MVM infection, causing the rearrangement and further collapse of the vimentin IF network that I observed around the nucleus. However, here I have found that vimentin was not cleaved at 2 h P.I. (Fig. 3-7).

A virus that has been shown to rearrange vimentin by means of phosphorylation is African swine fever virus (Stefanovic *et al.*, 2005). These authors reported that phosphorylation of vimentin may be necessary for the rearrangement of vimentin and may be due to the activation of CaMK-II. MVM is known to be dependent on the activation of cellular kinases such as those in the PKC family for nuclear envelope breakdown and lamina disruptions (Porwal *et al.*, 2013) as well as the phosphorylation of NS1 (Lachmann *et al.*, 2003; Nuesch & Rommelaere, 2006; Nuesch *et al.*, 2003). It is possible that these activated kinases could be responsible for the phosphorylation and rearrangement of the vimentin network, once the virus has been released from the endosomes and entered the cytoplasm.

In addition to examining the vimentin IF network, I have also investigated the overall distribution of the MT and actin networks in mouse fibroblast cells. The MT network was altered at 2 h P.I. showing accumulated immunostaining of alpha tubulin at the nuclear periphery (Fig. 3-8). However, these rearrangements most likely occur due to trafficking of MVM-containing vesicles, as the number of cells showing rearrangement of MT for experiments with empty capsids is similar to MVM-infected cells (Fig. 3-9). The AF network remained largely unaltered during early infection; however, in agreement with previous published results (Nuesch *et al.*, 2005) the network became patchy at 24 h P.I., probably due to virus egress (Fig. 3-10).

Previous findings have already shown that MVM infection disrupts the nuclear envelope and the lamin A/C immunostaining pattern, cleaves lamin B, and changes nuclear

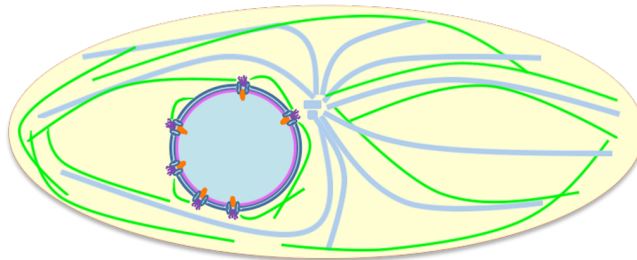
morphology (Cohen & Pante, 2005; Cohen *et al.*, 2006; Cohen *et al.*, 2011). I found here that MVM also causes disruption to the lamin B network immunostaining at 2 h P.I., which coincides with the location of MVM DNA, and MVM capsids (Fig. 3-11).

Last, I sought a method to independently support the changes that I observed during MVM infection to the cytoskeleton, nucleus, and nuclear lamina. By AFM I showed that cells were less stiff overall 2 to 3 h P.I. with MVM (Fig. 3-13). This observed change in the mechanical properties of cells could indicate significant changes in the cytoskeleton, nuclear shape, and nuclear lamina (Fletcher & Mullins, 2010; Gardel *et al.*, 2008). Thus, this result independently supports the changes to the cytoskeleton that I observed during MVM infection.

In summary (as illustrated in Fig. 3-14), the data in this chapter suggest that, at 2 h P.I., MVM causes:

- Morphological changes to the cell
- Rearrangements of the MT network
- Rearrangements of the vimentin IF network to the perinuclear region
- Disruption of the nuclear lamina
- A decrease in the elastic modulus of the cell, rendering the cell less stiff overall

A. Un-infected cell:



Legend

- MVM capsid
- Intermediate Filaments
- Microtubules
- Nuclear lamina

B. MVM-infected cell:

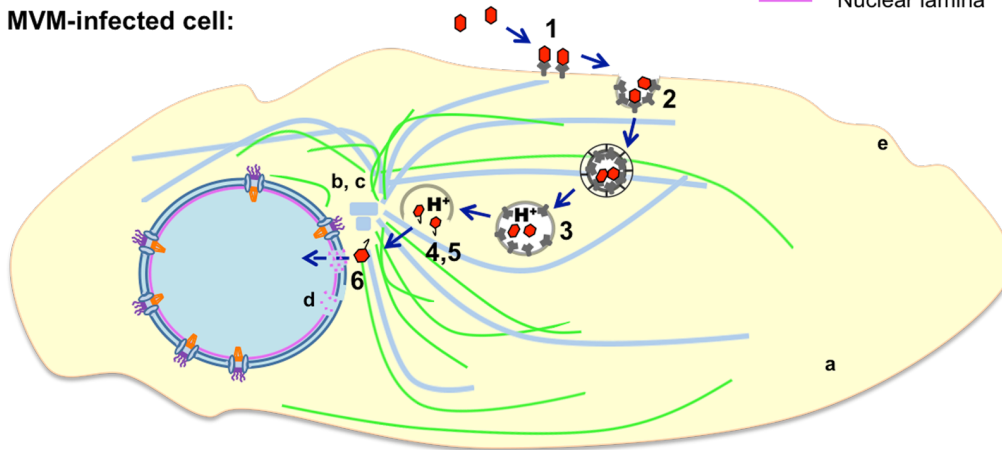


Figure 3-14: MVM induces morphological changes to the host cell 2 h P.I. (A) A representation of an un-infected cell with intact and evenly distributed cytoskeletal networks. (B) A representation of the earlier steps of MVM infection. [1]: virus attachment to cellular receptor (unknown for MVM). [2]: cellular entry through clathrin mediated endocytosis. [3]: Acidification of endosomes, leading to [4]: conformational changes in the MVM capsid, exposure of the unique VP1 region containing the PLA2 motif, and endosomal release of the MVM. [5]: MVM trafficking toward the perinuclear region either while still in vesicles or once virions have lysed out of the endosomes. [6]: MVM enters the nucleus through breaks in the nuclear envelope. The data in this chapter suggest that, at 2 h P.I., MVM causes (a) morphological changes to the cell; (b) rearrangements to the MT network; (c) rearrangement to the vimentin IF network to the perinuclear region; (d) disruption to the nuclear lamina; and (e) a decrease in the elastic modulus of the cell, rendering the cell less stiff overall.

Chapter 4 – Vimentin Facilitates a Productive MVM Infection²

4.1 Introduction

IFs have long been known to serve structural functions within the cell. More recently we are beginning to understand that they are more than just structural proteins (reviewed by Goldman *et al.*, 2012; Herrmann *et al.*, 2007; Styers *et al.*, 2005). Interestingly, in recent years we have begun to understand that IFs may also play important roles during viral infection. There are now several viruses that have been shown to require the IF protein vimentin for a successful infection (reviewed by Spripada & Dayaraj, 2010). Viruses that replicate in the cytoplasm, such as African swine fever virus, rearrange and accumulate vimentin in the perinuclear region to form vimentin cages where replication of the virus can then occur (Stefanovic *et al.*, 2005). Others such as HIV-1 cause cleavage and rearrangement of vimentin, although the function of this cleavage is unclear (Honer *et al.*, 1991; Shoeman *et al.*, 2001). And yet other viruses such as CMV require an intact vimentin network for the onset of replication (Hertel, 2011; Miller & Hertel, 2009). However, the role of the vimentin network during parvovirus infection remains undetermined.

In Chapter 3 I have documented that during early infection with MVM at 2 h P.I. the vimentin immunostaining is dramatically altered, ultimately collapsing around the

² Parts of this chapter have been published:

Nikta Fay and Panté N. (2013). The intermediate filament network protein, vimentin, is required for parvoviral infection. *Virology* **444**: 181-90, doi: 10.1016/j.virol.2013.06.009
<http://www.sciencedirect.com/science/article/pii/S0042682213003589>

nucleus by 24 h P.I. In this chapter, I determine whether the vimentin network has an effect on productive MVM infection.

4.2 Results

4.2.1 The vimentin network of LA9 mouse fibroblasts collapses and forms aggregates after acrylamide treatment

There are currently no commercially available inhibitors of IF polymerization. ACR has instead been widely used to selectively and reversibly disrupt the IF network, without disrupting the MT network (Aggeler & Seely, 1990; Durham *et al.*, 1983; Miller & Hertel, 2009). In these studies it has been documented using indirect immunofluorescence microscopy that after treatment of cells with ACR, the IF network forms aggregates and eventually collapses. ACR has also been widely used to disrupt vimentin prior to viral infection in order to study the role of vimentin during infection with CMV, junin virus, bluetongue virus, foot-and-mouth disease virus and dengue virus (Bhattacharya *et al.*, 2007; Cordo & Candurra, 2003; Gladue *et al.*, 2013; Kanlaya *et al.*, 2010; Miller & Hertel, 2009). Thus, I also used ACR to investigate whether a vimentin network is involved in the MVM infection cycle. For these experiments, our first step was to characterize the effect of ACR on LA9 cells. Cells were treated with 5 mM of ACR for 2, 4, 6, and 8 h, fixed, immunostained with an antibody against vimentin and examined by fluorescence microscopy. As documented before for other cell lines treated with 2-5 mM ACR (Aggeler & Seely, 1990; Durham *et al.*, 1983; Miller & Hertel, 2009), the vimentin immunostaining of LA9 cells collapsed around the nucleus (Fig. 4-1), instead of filaments throughout the cells as seen in control cells. This effect increased with increasing incubation time with ACR (Fig. 4-1).

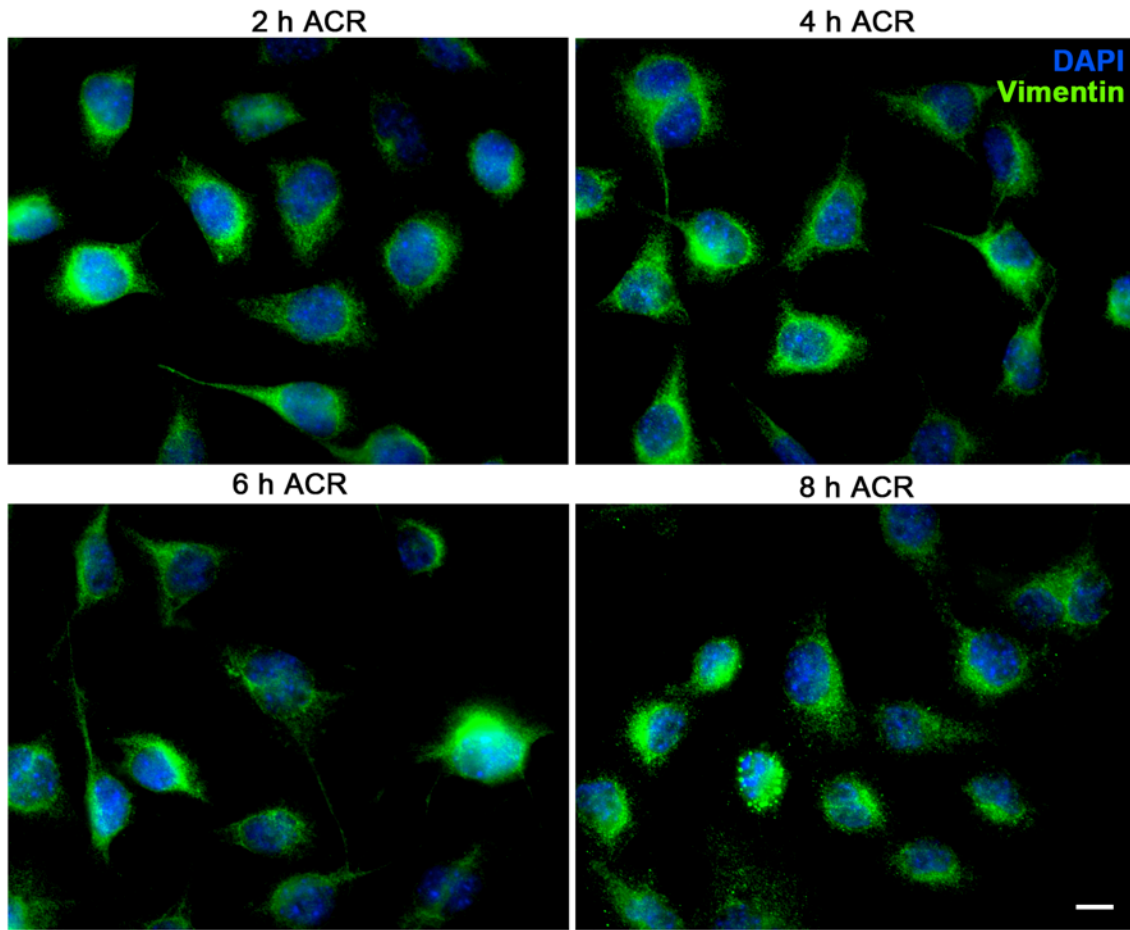


Figure 4-1: The vimentin network of LA9 mouse fibroblasts collapses and forms perinuclear aggregates after acrylamide treatment. LA9 cells were treated with 5 mM ACR solution for 2, 4, 6 or 8 h and then prepared for indirect immunofluorescence microscopy. Cells were fixed with 3% PFA, permeabilized with 0.003% digitonin and were labeled with an anti-vimentin antibody (H84; green), and with DAPI to detect DNA (blue). Scale bar, 10 μ m. (Figure reproduced with permission from Fay and Pante, 2013)

4.2.2 ACR treatment is reversible after 12 hours

To determine whether the effect of ACR treatment on the vimentin network in LA9 cells is reversible, cells were treated with 5 mM of ACR for 8 h, then washed with medium and further incubated with medium for 12 h. As a control, cells were incubated with medium for the entire duration of the experiment. The vimentin immunostaining of control LA9 cells showed filaments throughout the cells, whereas cells treated with ACR for 8 h showed collapsed vimentin around the nucleus (Fig. 4-2). When cells were washed and incubated with medium after the 8 h ACR treatment, the vimentin immunostaining resembled control cells, showing a filamentous network throughout the cell. This is consistent with other findings showing that treatment of PtK1 cells with 5 mM ACR for 4 h is reversible within 18 h (Eckert & Yeagle, 1988). Thus similarly, in LA9 cells the effects of 5 mM ACR treatment for 8 h is reversible.

4.2.3 An intact vimentin cytoskeleton facilitates MVM replication

To investigate whether MVM replication occurs in LA9 cells after ACR treatment, ACR-treated cells were infected and the viral nonstructural protein NS1, was immunostained 12 h P.I. NS1 is the first non-structural protein to be expressed during MVM infection and is essential for viral DNA replication. Thus, similar to Fig. 3-6, NS1 was used again here as a readout for MVM replication. The number of cells expressing NS1 was significantly reduced in an ACR-incubation time dependent manner (Fig. 4-3). The control cells showed $51 \pm 3\%$ cells expressing NS1, whereas the cells treated for 8 h with 5 mM showed only $13 \pm 5\%$ of cells expressing NS1 (Fig. 4-3).

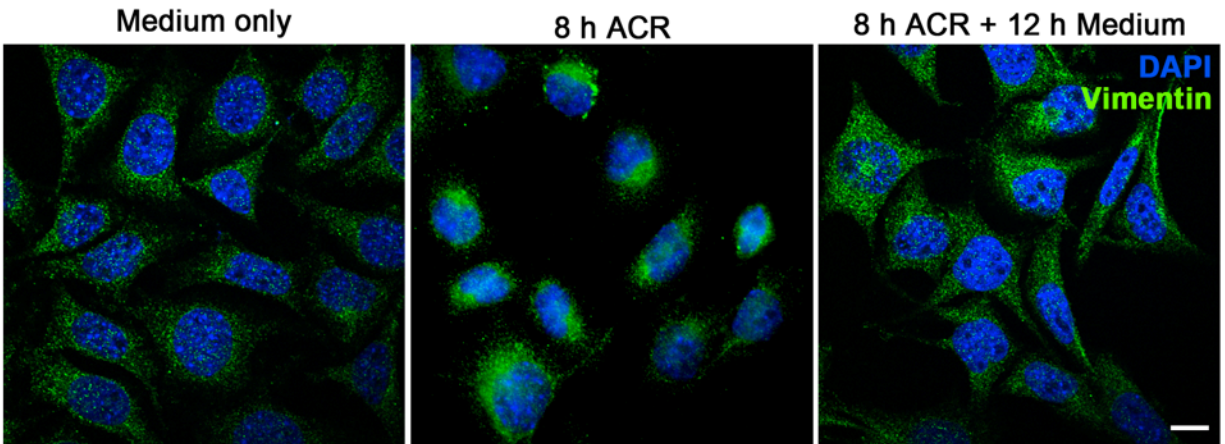


Figure 4-2: ACR treatment is reversible after 12 hours. LA9 cells were treated with 5 mM of ACR or medium for 8 h, then washed with medium and further incubated with medium for 12 h and prepared for indirect immunofluorescence microscopy. Cells were fixed with 3% PFA, permeabilized with 0.003% digitonin and were labeled with an anti-vimentin antibody (H84; green), and with DAPI to detect DNA (blue). Shown are representative confocal microscopy images. Scale bar, 10 μ m.

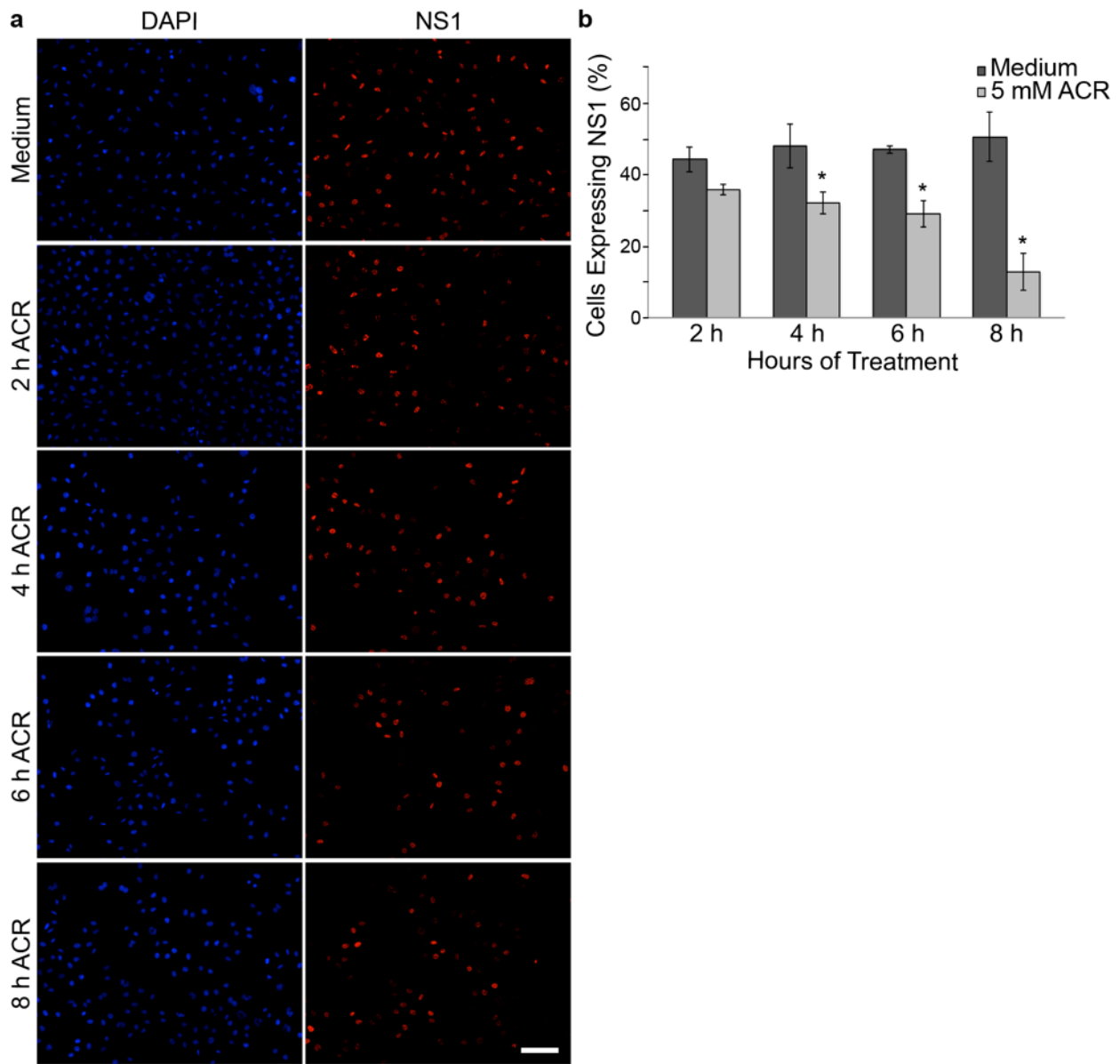


Figure 4-3: An intact vimentin cytoskeleton facilitates MVM replication. LA9 cells were treated with medium (as a control) or 5 mM ACR solution for 2, 4, 6 or 8 h, infected with MVM (MOI of 4) and prepared for indirect immunofluorescence microscopy 12 h P.I. Cells were fixed with 3% PFA, permeabilized with 0.2% Triton X-100 and labeled with an anti-NS1 antibody (red) and with DAPI to detect DNA (blue). (a) Representative field of cells infected with MVM. Scale bar, 50 μ m. (b) Bar graph of the proportion of cells expressing NS1 for the conditions indicated above (a). Shown are the mean values and standard error measured for 3 independent experiments (approximately 1000 cells were counted for each condition). *, $P < 0.05$ compared to mock infection (unpaired Student t test). (Figure reproduced with permission from Fay and Pante, 2013)

4.2.4 Endosomal uptake of MVM is not inhibited by pre-treatment with acrylamide

To rule out whether this reduction in MVM replication was a result of ACR initially inhibiting the cellular entry of the virus into endosomes, cells pretreated with medium (as control) or 5 mM ACR for 2, 4, 6, and 8 h were infected with MVM, and the virus capsid was detected by immunofluorescence microscopy 2 h P.I. As described above, this ACR treatment caused collapse of the vimentin network and the formation of vimentin immunostaining aggregates, a defect that is more pronounced with time of ACR treatment (Fig. 4-4, vimentin panels). The immunostaining of MVM capsid of the ACR-treated cells (Fig. 4-4, MVM 2h P.I. panels) is comparable to that of cells incubated with medium as a control. Thus, endosomal uptake of MVM appears to be normal at all ACR treatment levels (Fig. 4-4).

4.2.5 LA9 cells incubated for 8 h with 5 mM ACR exhibit no effect on cell growth

Parvoviruses replicate only during S phase. Therefore, to determine whether ACR treatment induced defects in the cell cycle, I measured the growth rate for LA9 cells treated with 5 or 10 mM ACR over a 24 h period (Fig. 4-5). I found that at higher concentrations of ACR (10 mM), the growth rate of LA9 cells decreased; however, treatment with 5 mM ACR did not alter the growth rate of the cells, as compared with untreated cells (Fig. 4-5). Therefore, the decrease in NS1 expression, and ultimately MVM replication, was not due to defects in the cell cycle in the ACR-treated cells. Taken together, these results indicate that ACR treatment, and subsequently the artificial disruption of the vimentin network before MVM infection, can reduce MVM replication. Thus, the vimentin network facilitates efficient infection by MVM.

4.2.6 MVM replication is significantly reduced in vimentin-null cells

To investigate further the requirement of the vimentin network during infection by MVM, I next used immortalized $\text{vim}^{+/+}$ and $\text{vim}^{-/-}$ MEF cells derived from wild type and vimentin knockout mice. These cells have been previously characterized, and are viable, although they lack a vimentin network (Colucci-Guyon *et al.*, 1994; Holwell *et al.*, 1997). The MEFs and LA9 cells were infected with MVM, and immunostained with an antibody against NS1 12 h P.I. (Fig. 4-6). In comparison with the control LA9 cells and the wild type $\text{vim}^{+/+}$ cells, the proportion of cells expressing NS1 significantly decreased in the $\text{vim}^{-/-}$ cells (Fig. 4-6a), with only $8.3 \pm 0.8\%$ of $\text{vim}^{-/-}$ cells, $30 \pm 4\%$ of $\text{vim}^{+/+}$ cells, and $44 \pm 3\%$ of LA9 cells expressing NS1 (Fig. 4-6b).

In addition, I have performed *in situ* hybridization experiments in order to visualize DNA replication 16 h P.I. with MVM (Fig. 4-7). The number of cells showing DNA replication was significantly reduced in the $\text{vim}^{-/-}$ cells (Fig. 4-7a) with only $13.9 \pm 1.6\%$ of $\text{vim}^{-/-}$ cells, $26.9 \pm 2.3\%$ of $\text{vim}^{+/+}$ cells, and $41.2 \pm 4\%$ of LA9 cells expressing DNA positive nuclei (Fig. 4-7b). Thus, these results indicate that a vimentin network facilitates MVM infection.

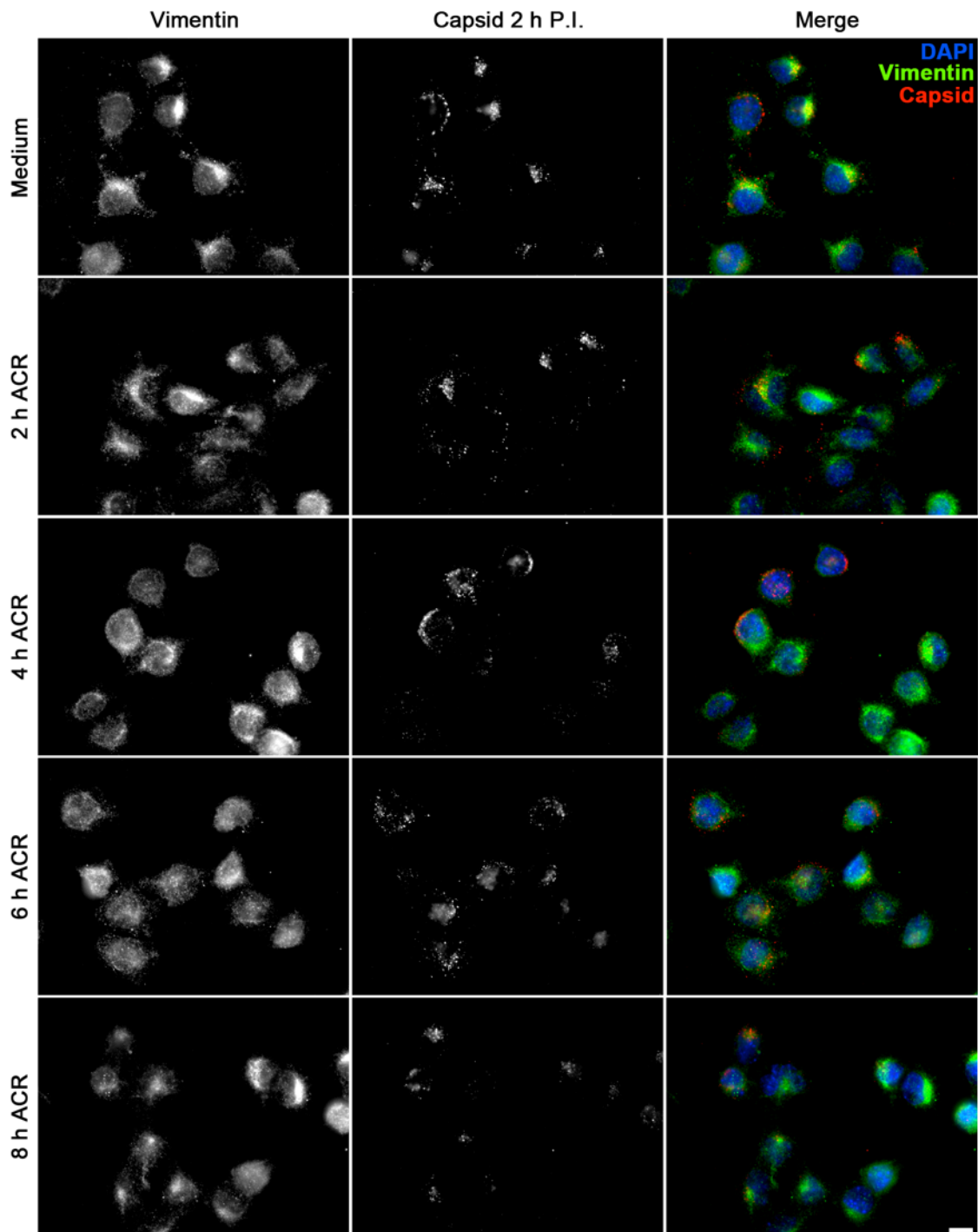


Figure 4-4: Endosomal uptake of MVM is not inhibited by pre-treatment with acrylamide. LA9 cells were treated with medium or 5 mM ACR solution for 2, 4, 6 or 8 h, infected with MVM (MOI of 4) and prepared for indirect immunofluorescence microscopy 2 h P.I. Cells were fixed with 3% PFA, permeabilized with 0.003% digitonin and labeled with an anti-vimentin antibody (H84; green), an anti-capsid antibody (MAb B7; red) and with DAPI to detect DNA (blue). Scale bar, 10 μ m. (Figure reproduced with permission from Fay and Pante, 2013)

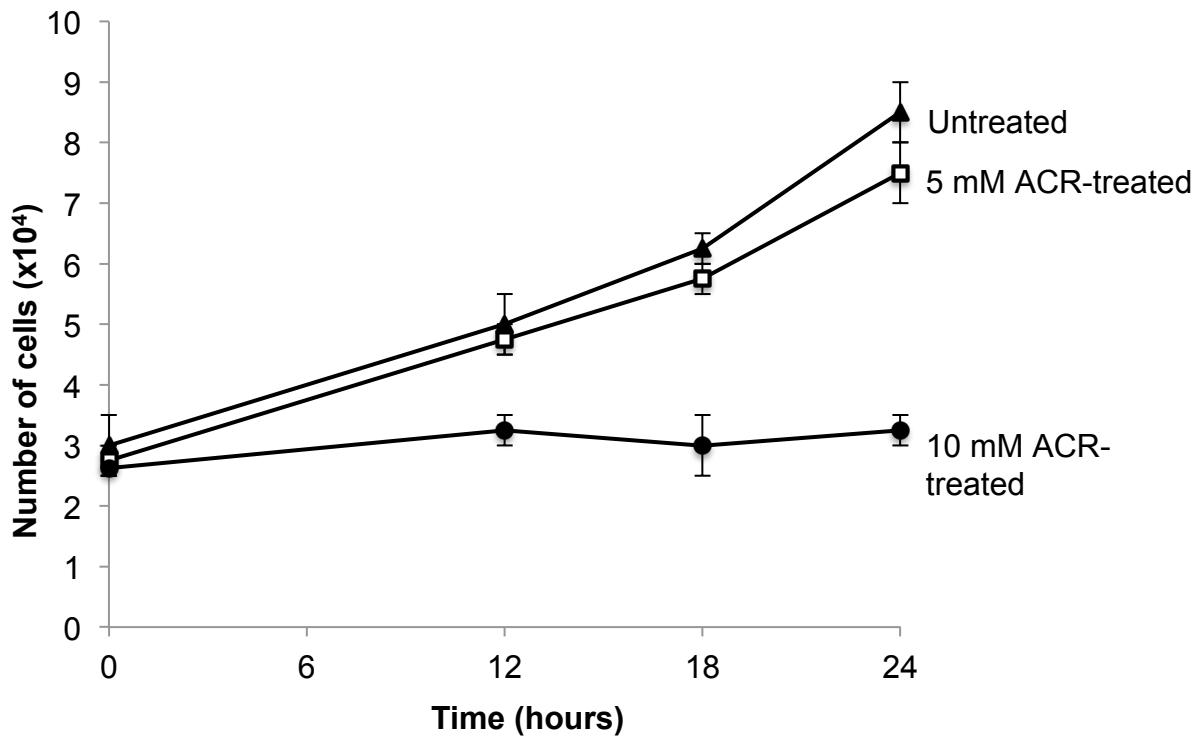


Figure 4-5: Growth curve of LA9 cells untreated or treated with 5 mM and 10 mM acrylamide. Cells were seeded on 12 well dishes. After 24 hours (to allow time for attachment), cells were incubated with medium (as a control), 5 mM or 10 mM ACR for 8 h, washed twice, and incubated with fresh culture medium. Cell numbers were counted at determined time points of 0, 12, 18 and 24 hours. Cells were trypsinized, stained with trypan blue solution, and counted by light microscopy using a hemocytometer. Shown are the mean values and standard error measured for 2 independent experiments.

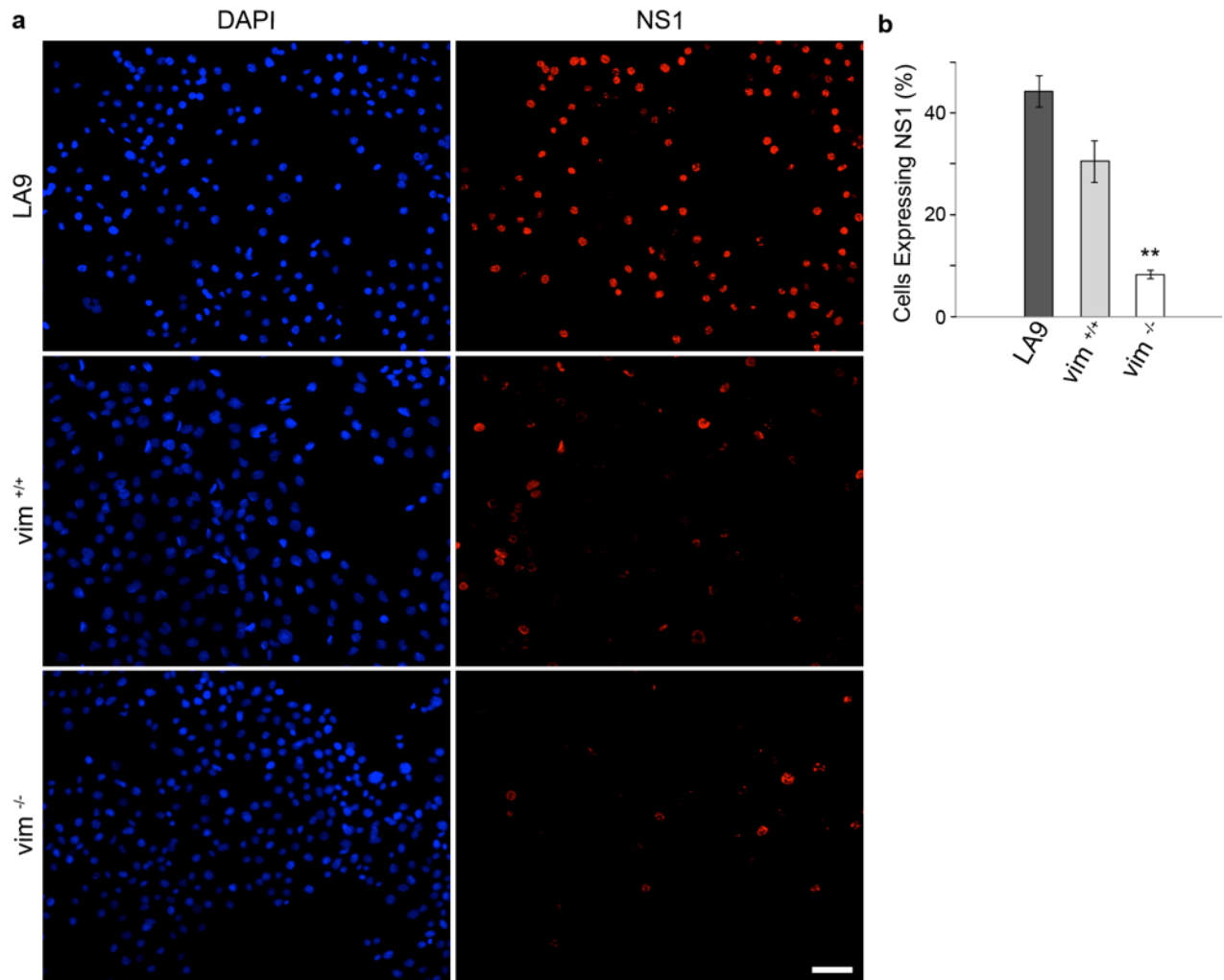


Figure 4-6: MVM replication is significantly reduced in vimentin-null cells. LA9 cells, wild type vim^{+/+} and vim^{-/-} MEF cells were infected with MVM at a MOI of 4 PFU per cell, and infected cells were examined by immunofluorescence microscopy 12 h P.I. Cells were fixed with 3% PFA, permeabilized with 0.2% Triton X-100 and labeled with an anti-NS1 antibody (red) and DAPI to detect DNA (blue). (a) Representative field of cells infected with MVM. Scale bar, 50 μ m. (b) Bar graph of the proportion of cells expressing NS1. Shown are the mean values and standard error measured for 3 independent experiments (approximately 2000 cells were counted for each condition). **, $P < 0.01$ compared to MVM infection in vim^{+/+} cells (unpaired Student *t* test). (Figure reproduced with permission from Fay and Pante, 2013)

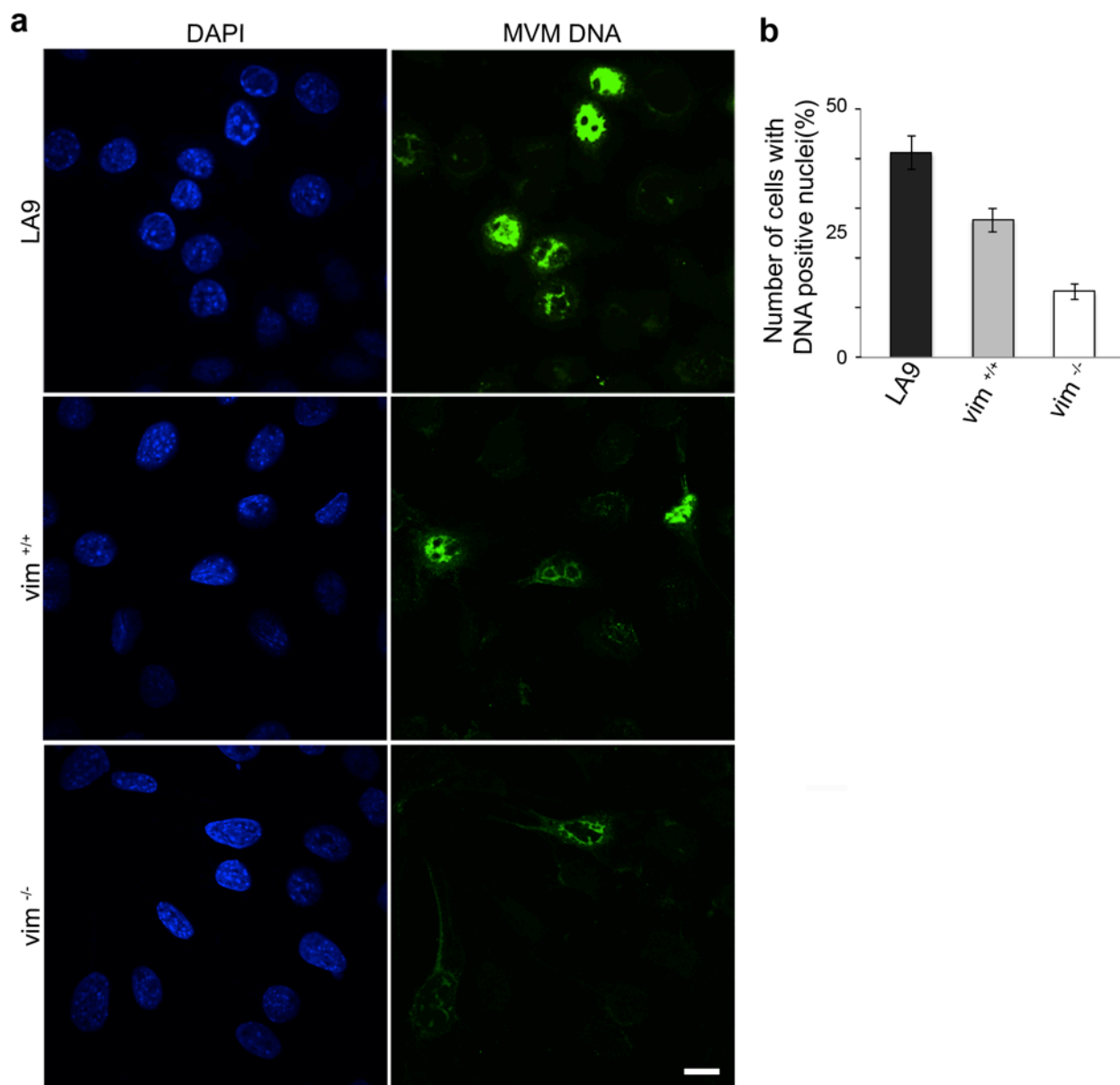


Figure 4-7: MVM DNA replication is significantly reduced in vimentin-null cells. LA9 cells, vim^{+/+} and vim^{-/-} MEF cells were infected with MVM at a MOI of 4 PFU per cell, and prepared for *in situ* hybridization in combination with indirect immunofluorescence microscopy 12 h P.I. (a) Representative confocal microscopy images of cells infected with MVM were examined by *in situ* hybridization with biotinylated probes and Streptavidin-FITC to detect MVM DNA (green), and with DAPI to detect cellular DNA (blue). Scale bar, 10 μ m. (b) Bar graph of the proportion of cells with DNA positive nuclei. Shown are the mean values and standard error measured for 3 independent experiments (approximately 150 cells were counted for each condition).

4.2.7 Vimentin null cells seem to progress through the S-phase similar to the vimentin wild type cells

Because parvoviruses replicate only during S phase, the reduced NS1 expression and DNA replication observed in the $\text{vim}^{-/-}$ cells (Figs. 4-6 and 4-7) may be due to slower cell cycle in these cells. To test this, I measured the growth rate for the $\text{vim}^{+/+}$ and $\text{vim}^{-/-}$ MEF cells, and for the LA9 cells, as a control (Fig. 4-8). The MEF cells have roughly similar growth rates, with $\text{vim}^{-/-}$ cells slightly faster than wild type cells. Both MEF cells grow at even a faster rate than the control LA9 cells. At 12 h P.I. (time when the NS1 assay was performed; see Fig. 4-6) the $\text{vim}^{-/-}$ MEF cells have already duplicated (in an average of three experiments increased from 3×10^4 cells to 6×10^4 cells at 12 hours). Thus, the reduced MVM replication observed in the $\text{vim}^{-/-}$ MEF cells is not due to defects on the cell cycle, and can be attributed to the absence of vimentin in these cells.

4.2.8 Cell growth is unaltered in MVM-infected vimentin-null cells as compared to MVM-infected control cells

It is well known that MVM infection causes cell lysis and induces cell cycle arrest (reviewed by Chen & Qiu, 2010), which then leads to the lack of cell growth over infection time. Thus, a measurement of cell growth during MVM infection is a way to determine whether cells have been infected. To investigate further the requirement of the vimentin network during infection by MVM, I next measured cell growth of MVM-infected $\text{vim}^{-/-}$ MEF cells. Control experiments were performed with wild type $\text{vim}^{+/+}$ MEF and LA9 cells. The MEFs and LA9 cells were mock infected or infected with MVM, and their growth rates were measured over a period of three days. As expected, the mock-infected MEF and LA9 cells showed the same growth pattern as previously

measured (Fig. 4-8). However, with MVM infection, the LA9 and wild type $\text{vim}^{+/+}$ cells both showed a decrease in cell growth over the 3-day period, as compared to mock infection (Fig. 4-9). This is likely either due to MVM induced cell lysis or cell cycle arrest. In contrast, the MVM-infected $\text{vim}^{-/-}$ MEF cells did not show an altered growth pattern as compared to mock-infection (Fig. 4-9). Thus, cell growth is unaltered with MVM infection in vimentin-null cells, likely due to reduced cell lysis or lack of cell cycle arrest.

4.2.9 Absence of vimentin does not affect endosomal uptake, but leads to reduced accumulation of MVM capsid immunostaining on one side of the nucleus

Finally, to begin to understand why MVM replication decreased in cells lacking vimentin, I compared MVM capsid immunostaining among the wild type $\text{vim}^{+/+}$ and $\text{vim}^{-/-}$ MEF cells at different 1 and 2 h P.I. The MVM capsid immunostaining was present in both types of cells (Fig. 4-10). Thus, MVM is able to enter the endosomes of these cells, even in the absence of vimentin. However, the distribution of the MVM capsid immunostaining at 2 h P.I. most likely from MVM still in endosomes, is distinctly different in the $\text{vim}^{-/-}$ cells compared with the $\text{vim}^{+/+}$ cells. While the wild type $\text{vim}^{+/+}$ cells have most of their MVM-containing vesicles accumulated at the perinuclear region in one side of the nucleus, these MVM-compartments have a more disperse cytoplasmic location in the $\text{vim}^{-/-}$ cells (Fig. 4.10a). Indeed, quantification of the number of cells showing perinuclear accumulation of MVM on only one side of the nucleus was $26 \pm 3\%$ in $\text{vim}^{-/-}$ cells as compared to $48 \pm 7\%$ in wild type $\text{vim}^{+/+}$ cells at 2 h P.I. (Fig. 4-10b). Thus, the endocytic trafficking of MVM-containing vesicles toward the perinuclear region seems to be different in the $\text{vim}^{-/-}$ cells compared with wild type $\text{vim}^{+/+}$ cells.

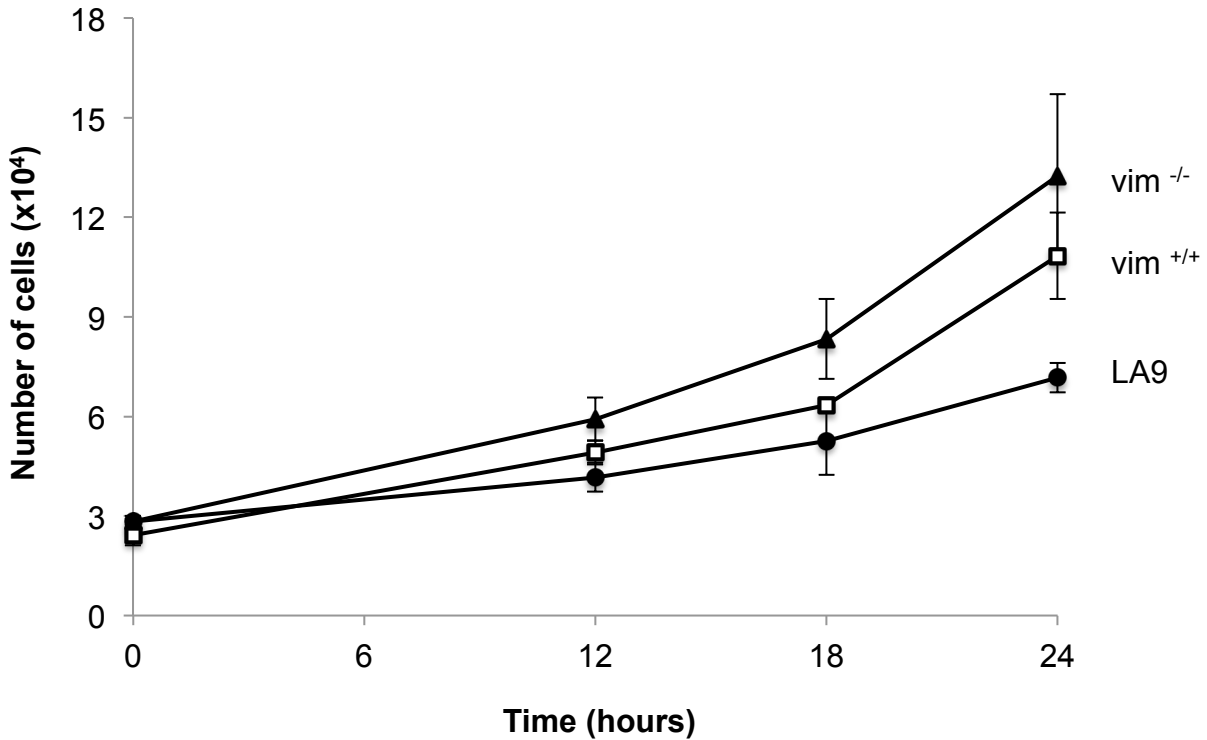


Figure 4-8: Growth curve for LA9, vim^{+/+} and vim^{-/-} MEF cells. Cells were seeded on 12 well dishes. After 24 hours (to allow time for attachment), cell numbers were counted at determined time points of 0, 12, 18 and 24 hours. Cells were trypsinized, stained with trypan blue solution, and counted by light microscopy using a hemocytometer. Shown are the mean values and standard error measured for 3 independent experiments.

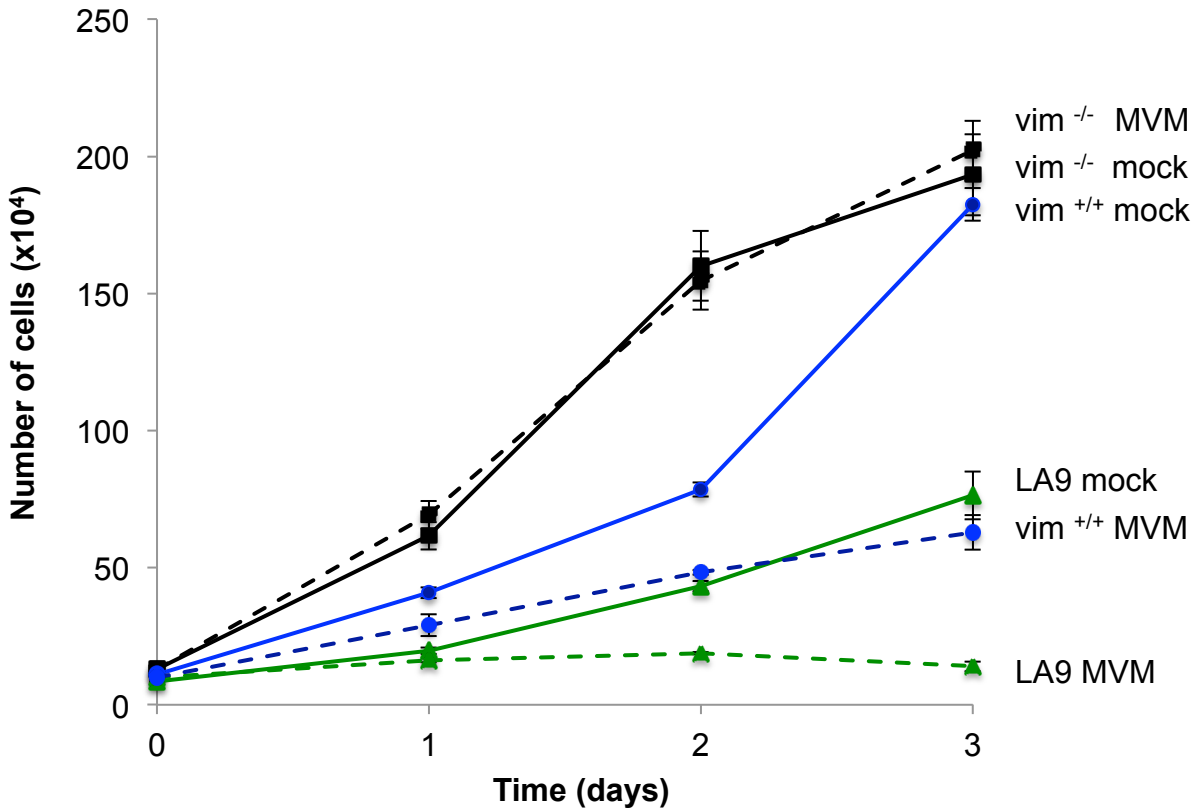


Figure 4-9: Cell growth is unaltered in MVM-infected vimentin-null cells as compared to MVM-infected control cells. LA9 cells, vim^{+/+} and vim^{-/-} MEF cells were seeded on 12 well dishes. After 24 hours (to allow time for attachment), cells were mock infected or infected with MVM at a MOI of 4 PFU per cell, and cell numbers were counted at determined time points of 0, 1, 2 and 3 days P.I. Cells were trypsinized, stained with trypan blue solution, and counted by light microscopy using a hemocytometer. Shown are the mean values and standard error measured for 3 independent experiments.

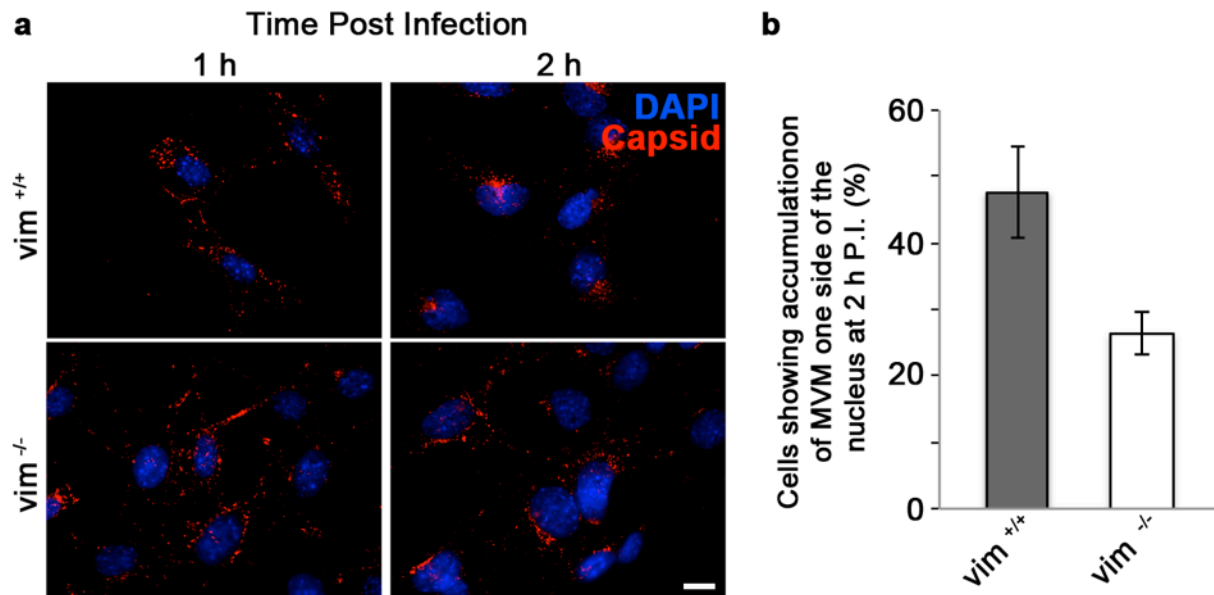


Figure 4-10: The absence of vimentin does not affect endosomal uptake, but leads to the reduction of perinuclear accumulation of MVM capsid immunostaining on one side of the nucleus.

vim^{+/+} and *vim*^{-/-} MEF cells were infected with MVM at a MOI of 4 PFU per cell, labeled with an anti-capsid antibody (MAb B7; red) and DAPI to detect DNA (blue) at 1 or 2 h P.I., and examined by immunofluorescence microscopy. Cells were fixed with 3% PFA and permeabilized with 0.2% Triton X-100. (a) Representative field of cells infected with MVM are shown; Scale bar, 10 μ m. (b) Bar graph of the proportion of cells showing perinuclear accumulation of MVM capsid immunostaining on one side of the nucleus 2 h P.I. Shown are the mean values and standard error measured for 3 independent experiments (85 cells were counted for each condition). (Figure reproduced with permission from Fay and Pante, 2013)

4.3 Discussion

Our results in the previous chapter documented that during early infection with MVM the vimentin immunostaining is dramatically altered, ultimately collapsing around the nucleus by 24 h P.I. In this chapter I have determined that the IF network has an effect on productive MVM infection by using cells that have an artificially disrupted vimentin filament network due to ACR treatment, and *vim*^{-/-} MEFs derived from vimentin knockout mice.

There are currently no commercially available inhibitors of IF polymerization. Instead, to selectively and reversibly disrupt the vimentin IF network, ACR has been extensively used (Aggeler & Seely, 1990; Durham *et al.*, 1983). Other studies have examined the role of vimentin during viral infection by disrupting the IF network using ACR. For example, for dengue virus, disruption of vimentin with ACR reduced dengue NS1 expression, as well as viral replication and release (Kanlaya *et al.*, 2010). A second example is CMV; ACR treatment of cells prior to infection inhibits the onset of infection of two distinct strains of CMV (Miller & Hertel, 2009). Similar to these two studies, I have first characterized the effect of ACR treatment, and showed that it selectively and reversibly disrupts the vimentin IF network in mouse fibroblast cells (Fig. 4-1, Fig. 4-2), and demonstrated that the vimentin IF network facilitates MVM replication (Fig. 4-3). However, the decrease in MVM replication observed in ACR-treated cells was not a result of ACR initially inhibiting the cellular entry of the virus into endosomes (Fig. 4-4). Furthermore, this decrease in MVM replication is not due to defects in the cell cycle. Assessment of cell viability in LA9 cells incubated for 8 h with 5 mM ACR exhibited no effect on cell growth over a 24 h period (Fig.4-5).

Additionally, evidence for the role of vimentin during CMV infection was provided using $\text{vim}^{-/-}$ cells (Miller & Hertel, 2009). It was found that an intact vimentin network is required for CMV infection, and that in $\text{vim}^{-/-}$ cells the virus remained in the cytoplasm longer than in $\text{vim}^{+/+}$ cells. Thus, it was concluded that viral trafficking toward the nucleus was delayed in the $\text{vim}^{-/-}$ cells, likely involving vimentin for progression within endosomes or direct binding to vimentin for trafficking on the MT network (Miller & Hertel, 2009). I have also found that in cells lacking vimentin MVM replication is reduced (Figs. 4-6 and 4-7), leading to unaltered cell growth upon MVM infection, likely due to reduced cell lysis or lack of cell cycle arrest (Fig. 4-9). Similar to ACR-treated cells, the reduction in MVM replication in $\text{vim}^{-/-}$ MEF cells is not due to a slower growth rate, since I have shown that $\text{vim}^{-/-}$ MEF cells did not have a slower growth rate than $\text{vim}^{+/+}$ MEF cells (Fig. 4-8). Similar to the studies with CMV (Miller & Hertel, 2009), for MVM I have also found that there was a reduction in perinuclear accumulation of MVM-containing vesicles on one side of the nucleus in cells lacking vimentin (Fig. 4-10). This result is intriguing as it points at the fact that vimentin is required during early steps of viral infection.

In summary (as illustrated in Fig. 4-11), the data in this chapter indicate that the absence of an IF network in cells affects MVM infection by reducing:

- 1) Accumulation of MVM capsid immunostaining on one side of the nucleus
- 2) MVM DNA replication
- 3) NS1 expression
- 4) Cell lysis or cell cycle arrest

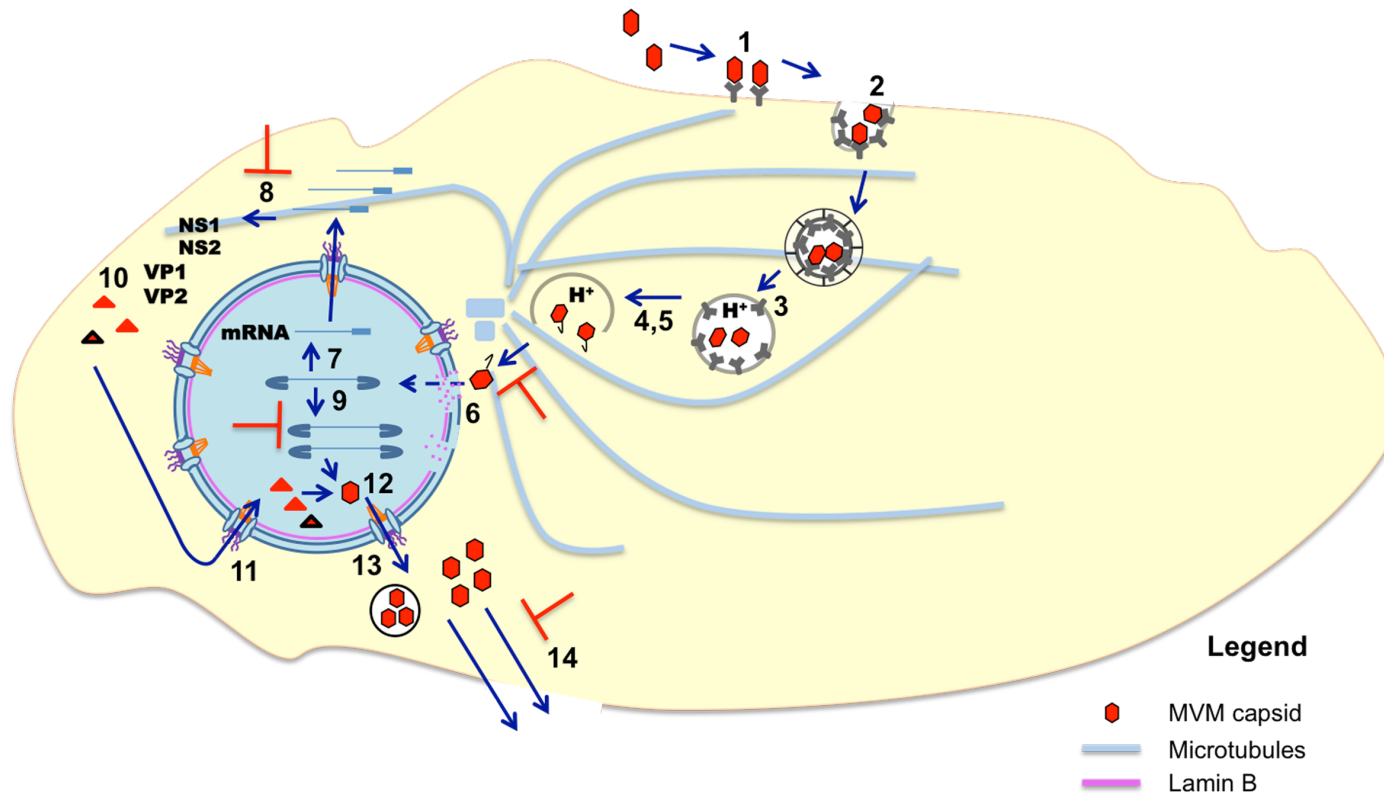


Figure 4-11: Vimentin facilitates productive MVM infection. A representation of the MVM infection cycle in vimentin null cells that lack the IF network protein vimentin. [1]: virus attachment to cellular receptor [2]: cellular entry through clathrin mediated endocytosis. [3]: acidification of endosomes, leading to [4]: conformational changes in the MVM capsid, exposure of the unique VP1 region containing the PLA2 motif and endosomal release of MVM. [5]: MVM trafficking toward the perinuclear region either while still in vesicles or virions have lysed out of the endosomes. [6]: MVM enters the nucleus through breaks in the nuclear envelope. [7]: DNA transcription. [8]: protein translation. [9]: DNA replication. [10]: capsid protein assembly into trimers. [11]: nuclear import of capsid proteins. [12]: assembly of viral progeny. [13]: nuclear export of viral progeny through the NPCs. [14]: cellular exit either by cell lysis or transport in vesicles and fusion. The data in this chapter suggest that steps 5, 8, 9, and 14 of the MVM infection cycle are reduced in MVM-infected vimentin null cells.

Chapter 5 – Vimentin Plays a Role in the Progression of MVM Through the Endocytic Pathway

5.1 Introduction

In Chapters 3 and 4 I found that during early infection with MVM at 2 h P.I. the vimentin immunostaining is dramatically altered and that vimentin facilitates MVM infection. In addition, I found that there was a reduction in perinuclear accumulation of MVM-containing vesicles on one side of the nucleus in cells lacking vimentin. To follow up, I next wanted to determine the specific role of the vimentin IF network during a productive MVM infection. Although the traffic and cellular position of organelles of the endocytic pathway have long been known to require MTs, AFs, and their motor proteins (Caviston & Holzbaur, 2006; Vale, 2003), there is now increasing evidence for the involvement of the vimentin network in membrane bound organelle transport and cellular distribution (Chang *et al.*, 2009; Nekrasova *et al.*, 2011; Styers *et al.*, 2004). It has already been shown that cells lacking vimentin have mislocalized late endosomes/lysosomes and a decreased capacity to acidify their lysosomes (Styers *et al.*, 2004). Infection by all parvoviruses depends on progression through the endocytic pathway, and escape of virions from endosomes into the cytoplasm is pH-dependent (Harbison *et al.*, 2009; Quattrocchi *et al.*, 2012; Ros *et al.*, 2002; Suikkanen *et al.*, 2002; Vihinen-Ranta & Parrish, 2006). It is likely then that the decrease in the cell's ability to acidify its lysosomes would lead to the inability of the virus to escape from endosomes in the $\text{vim}^{-/-}$ cells. The reduced MVM replication I have observed in $\text{vim}^{-/-}$ MEF cells may then be explained, at least in part, to the previously reported misdistribution of late-

endosomes/lysosomes in $\text{vim}^{-/-}$ cells, since MVM depends on the endocytic pathway. Thus, in this chapter I examined the role of vimentin in the progression of MVM through the endocytic pathway toward the nucleus.

5.2 Results

5.2.1 Late endosome/lysosome immunostaining is altered in $\text{vim}^{-/-}$ cells compared to $\text{vim}^{+/+}$ cells

Previous studies have shown that cells lacking vimentin have mislocalized late endosomes/lysosomes and a decreased capacity to acidify their lysosomes (Styers *et al.*, 2004). In order to investigate whether this factor contributes to the lack of productive MVM infection in $\text{vim}^{-/-}$ MEF cells, I first confirmed that the distribution of the endocytic pathway in $\text{vim}^{-/-}$ MEF cells is indeed altered as compared to wild type cells. $\text{Vim}^{-/-}$ and $\text{vim}^{+/+}$ MEF cells were immunostained for three markers of different stages of the endocytic pathway: early endosomes (EEA1: early endosome antigen-1), late endosomes (M6PR: Mannose-6-phosphate receptor), and late endosomes/lysosomes (LAMP1: lysosomal associated membrane protein-1) (Fig. 5-1). Similar to previous findings by Styers *et al.* (2004), I found that the most notable change was in the distribution of late endosomes/lysosomes. The EEA1 staining showed the characteristic cytoplasmic staining in both $\text{vim}^{-/-}$ and $\text{vim}^{+/+}$ cells. However, in $\text{vim}^{-/-}$ cells, the M6PR and LAMP1 staining are more juxtannuclear as compared to the wild type $\text{vim}^{+/+}$ cells, where the staining is more cytoplasmic. Thus, in cells lacking vimentin, late endosomes/lysosomes are mislocalized as compared to wild type cells.

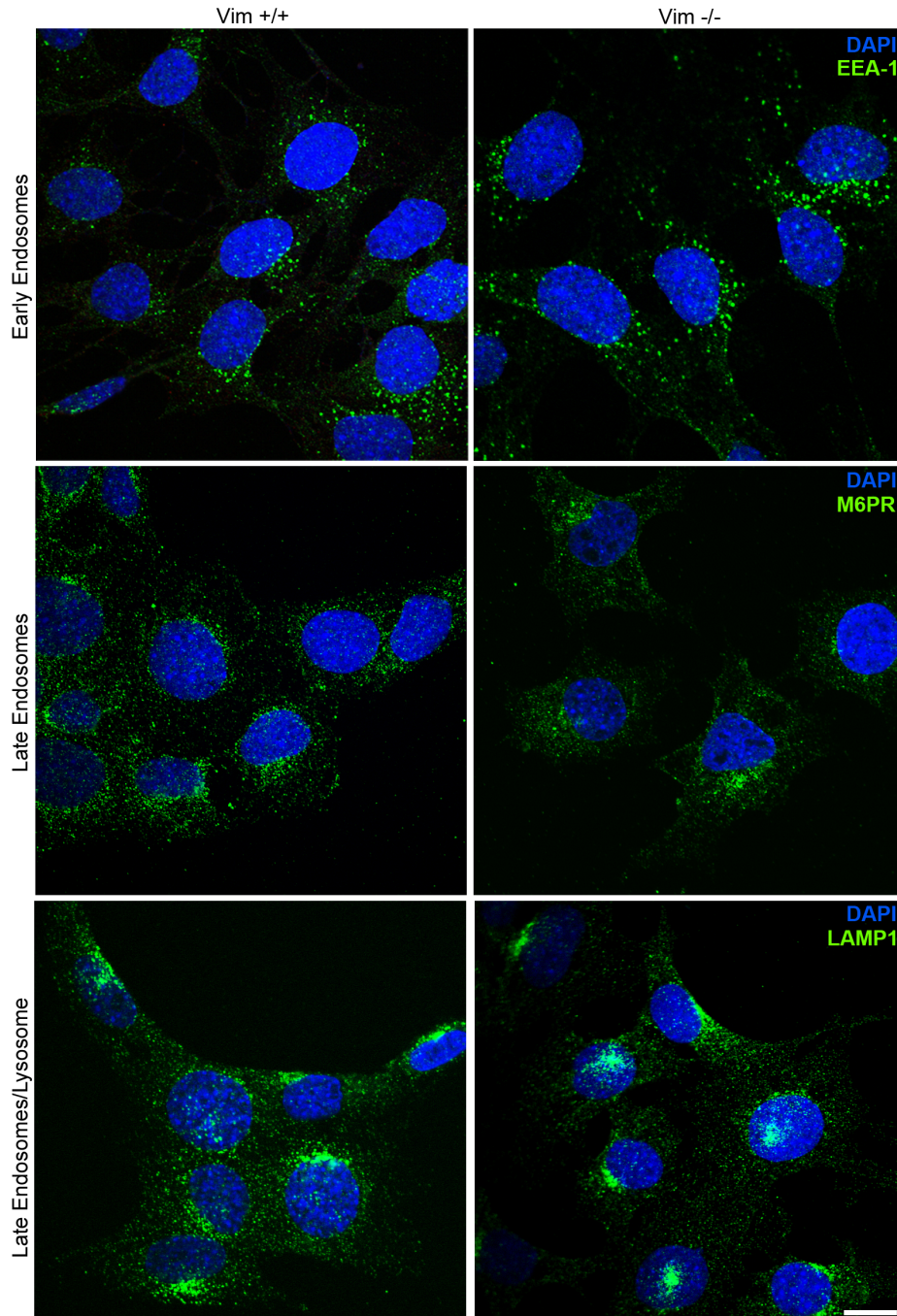


Figure 5-1: Late endosome/Lysosome immunostaining is altered in $\text{vim}^{-/-}$ cells compared to $\text{vim}^{+/+}$ cells. $\text{Vim}^{+/+}$ and $\text{vim}^{-/-}$ MEF cells were prepared for indirect immunofluorescence microscopy. Cells were fixed with 3% PFA, permeabilized with 0.2% Triton X-100, and labeled with either an antibody against early endosomes (anti-EEA1; green), late endosomes (anti-M6PR; green), or late endosomes/lysosomes (anti-LAMP1; green), and DAPI to detect DNA (blue). Shown are representative confocal microscopy images. Scale bar, 10 μm .

5.2.2 Cells lacking vimentin show an increased amount of MVM in early endosomes at 1 and 2 h P.I. compared to $\text{vim}^{+/+}$ cells

Next, I determined whether the progression of MVM through the endocytic pathway is altered in these $\text{vim}^{-/-}$ MEF cells by co-immunolabeling MVM and several markers of the endocytic pathway at different time points after virus entry. Since early endosomes serve as the first target of endocytic vesicles (Jovic *et al.*, 2010), I first began by observing the progression of MVM capsid immunostaining with early endosomes. I performed immunofluorescence microscopy of MVM-infected $\text{vim}^{-/-}$ and wild type $\text{vim}^{+/+}$ MEF cells labeled with an antibody against intact MVM capsids and an early endosome marker (EEA1) at 5 min, 30 min, 1 h, and 2 h P.I. (Fig. 5-2). The wild type $\text{vim}^{+/+}$ MEF cells (as a control), showed the expected progression of MVM through the endocytic pathway. The MVM capsid immunostaining had the greatest overlap with EEA1 immunostaining immediately after internalization at 5 and 30 min P.I. (Fig. 5-2a, $\text{vim}^{+/+}$ panel). This overlap with EEA1 immunostaining decreased after 30 min P.I. (Fig. 5.2a, $\text{vim}^{+/+}$ panel), presumably as MVM progressed through the endocytic pathway to late endosomes. However, the MVM immunostaining pattern was altered in $\text{vim}^{-/-}$ cells. Similar to $\text{vim}^{+/+}$ cells, the greatest overlap with EEA1 immunostaining was the highest at 30 min P.I.; however, unlike $\text{vim}^{+/+}$ MEF cells, this overlap did not decrease after 30 min P.I. and remained present up to 2 h P.I. in early endosomes (Fig, 5-2a, $\text{vim}^{-/-}$ panel). Quantification analysis of the percent of MVM-capsid staining pixels that co-localize with EEA1 staining pixels confirmed this observation (Fig 5-2b). The percent of co-localization of MVM and EEA1 in $\text{vim}^{+/+}$ cells decreased from 18% at 5 min to 4% by 2 h P.I. On the other hand, in $\text{vim}^{-/-}$ cells the percent of co-localization stayed relatively

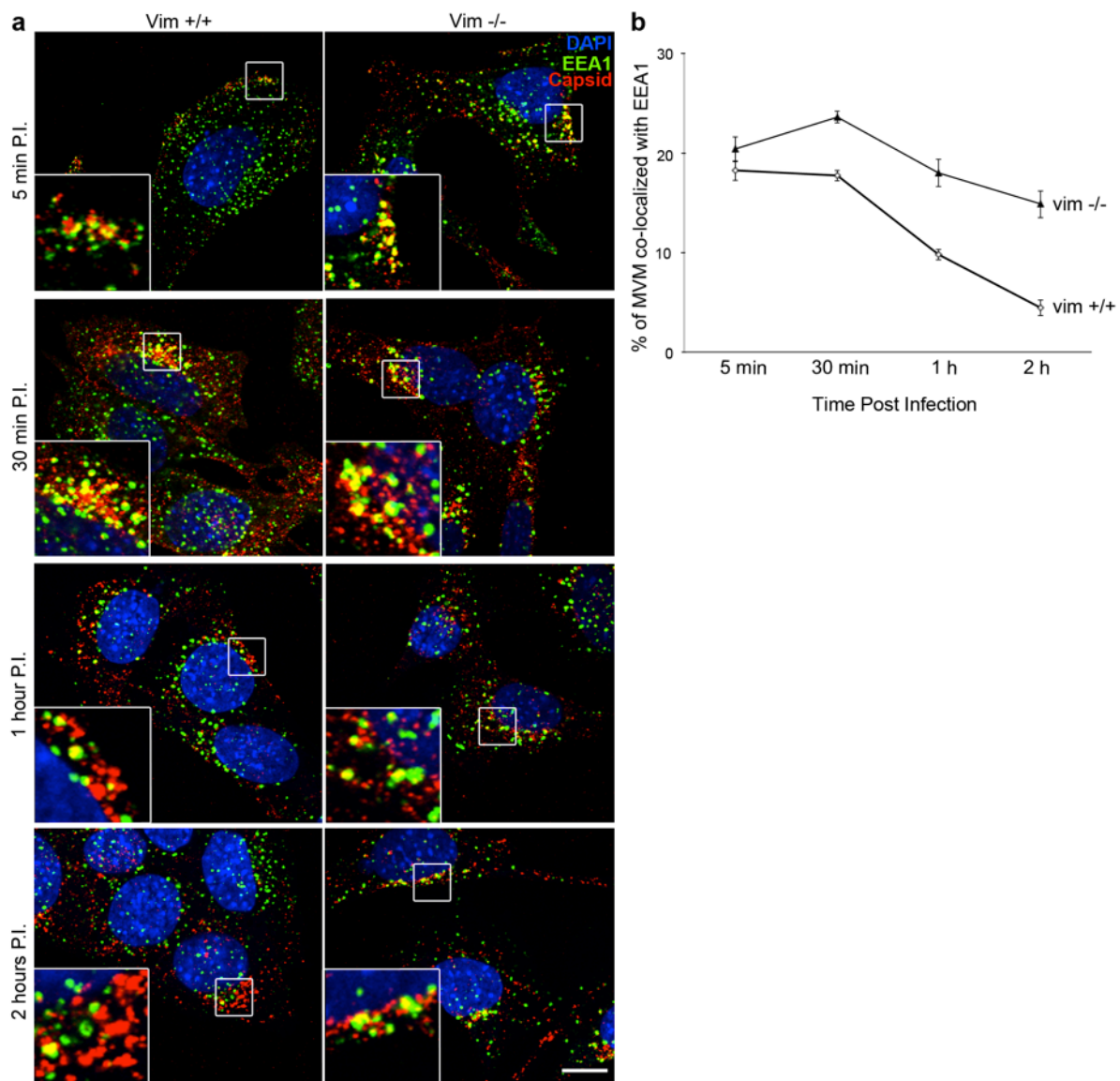


Figure 5-2: Vim^{-/-} cells show an increased amount of MVM remaining in early endosomes at 1 and 2 h P.I. as compared to MVM-infected vim^{+/+} cells. Vim^{+/+} and vim^{-/-} MEF cells were infected with MVM at a m.o.i. of 4 p.f.u. per cell, and prepared for indirect immunofluorescence microscopy 5 min, 30 min, 1 h and 2 h P.I. Cells were fixed with 3% PFA, permeabilized with 0.2% Triton X-100 and labeled with an anti-capsid antibody (MAb B7; red), anti-EEA1 antibody (C45B10; green) and DAPI to detect DNA (blue). (a) Shown are representative confocal microscopy images of cells infected with MVM. Small boxes in each image point to regions of overlap between EEA1 and MVM-capsid immunostaining. Zoom in the bottom left show high magnification of these regions. Scale bar, 10 μ m. (b) Quantification analysis was performed using BioImageXD. The co-localization percentage shown represents the percent of MVM-capsid staining pixels co-localizing with EEA1 staining pixels. Shown are the mean values and standard error measured for 3 independent experiments (25 cells were counted for each condition).

consistent with 20% at 5 min and 15% at 2 h P.I. Thus, this result provides preliminary evidence for MVM being less able to progress through the endocytic pathway in $\text{vim}^{-/-}$ cells, and possibly remaining trapped in early endosomes.

5.2.3 MVM capsid immunostaining is reduced in late endosomes and lysosomes in $\text{vim}^{-/-}$ MEF cells

To further examine the finding that MVM is less able to progress from early endosomes to late endosomes in $\text{vim}^{-/-}$ cells, I next performed immunofluorescence microscopy of MVM-infected cells with endocytic markers downstream of early endosomes. Thus, MVM-infected $\text{vim}^{-/-}$ and $\text{vim}^{+/+}$ MEF cells were labeled with an antibody against intact MVM capsids and either late endosomes (M6PR) or late endosomes/lysosomes (LAMP1) markers at 5 min, 30 min, 1 h, and 2 h P.I. (Fig. 5-3). As expected, for the wild type $\text{vim}^{+/+}$ cells, the greatest overlap with M6PR immunostaining was observed at 1 h P.I. (Fig. 5.3a, $\text{vim}^{+/+}$ panel) and similarly, the greatest overlap with LAMP1 immunostaining was also observed at 1 h P.I. (Fig. 5.3b, $\text{vim}^{+/+}$ panels). Since endosomal escape of MVM is inefficient, for both M6PR and LAMP1 immunostaining some overlap was still seen at 2 h P.I., but this was a low amount compared to the amount observed at 1 h P.I. (Fig. 5.3, a and b, $\text{vim}^{+/+}$ panels). This result indicates that in $\text{vim}^{+/+}$ MEF cells, MVM is in late endosomes/lysosomes by 1 h P.I., where it likely manages to escape into the cytosol.

For $\text{vim}^{-/-}$ cells the overlap with M6PR and LAMP1 immunostaining remained relatively constant over infection time with a minimal amount of overlap (Fig. 5-3, a and b, $\text{vim}^{-/-}$

panels). Similar to $\text{vim}^{+/+}$ cells, the greatest overlap with M6PR immunostaining, although very minimal, was observed at 1 h (Fig. 5-3a, $\text{vim}^{-/-}$ panel). Furthermore, unlike $\text{vim}^{+/+}$ cells, the overlap with LAMP1 immunostaining remained low from 5 min to 30 min P.I. and was the highest at 2 h P.I. (although still minimal) (Fig. 5-3b, $\text{vim}^{-/-}$ panel). Quantification of the percent of MVM-capsid staining pixels that co-localize with M6PR or LAMP1 for all conditions confirms the above observations (Fig. 5.3c). Therefore, these results together with the results of early endosome immunostaining (Fig. 5.2), indicate that in $\text{vim}^{-/-}$ cells MVM virions are less able to move from early endosomes to late endosomes/lysosomes.

To verify that MVM is less able to progress to late endosomes/lysosomes in $\text{vim}^{-/-}$ cells, I treated $\text{vim}^{-/-}$ and $\text{vim}^{+/+}$ MEF cells with Bafilomycin A1 (BafA1), an inhibitor of vacuolar-ATPase, prior to infection with MVM, and labeled cells with an antibody against MVM intact capsids and late endosomes/lysosomes (LAMP1) at 5 h P.I. BafA1 treatment would lead to an increase in pH of endosomal/lysosomal compartments; therefore, MVM would not be able to escape from late endosomes and would remain associated with lysosomes over time. As expected, at 5 h P.I., in untreated wild type $\text{vim}^{+/+}$ cells MVM showed overlap with late endosomes/lysosomes. This is due to the inefficiency of endosomal release of MVM into the cytoplasm. Therefore, only few virions leave these compartments; most virions follow the endocytic pathway into lysosomes, where they can remain for up to 8 h P.I. (Mani *et al.*, 2006). In BafA1-treated wild type $\text{vim}^{+/+}$ cells, MVM remained even more co-localized with late endosomes/lysosomes (Fig. 5-4). However, in $\text{vim}^{-/-}$ cells, both untreated and BafA1

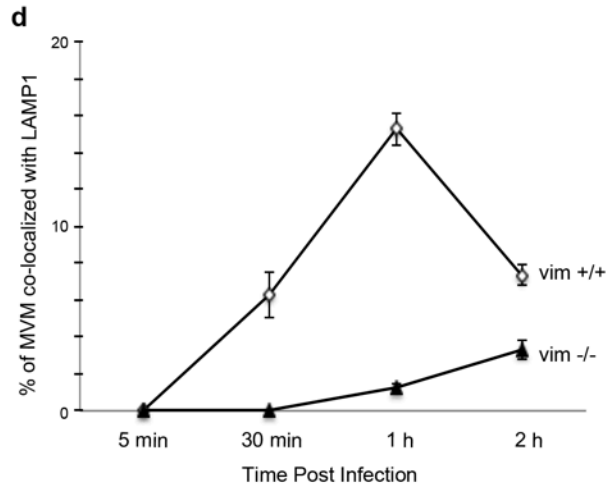
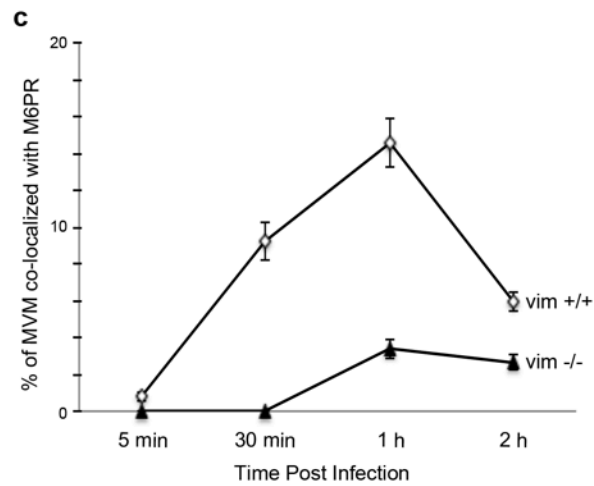
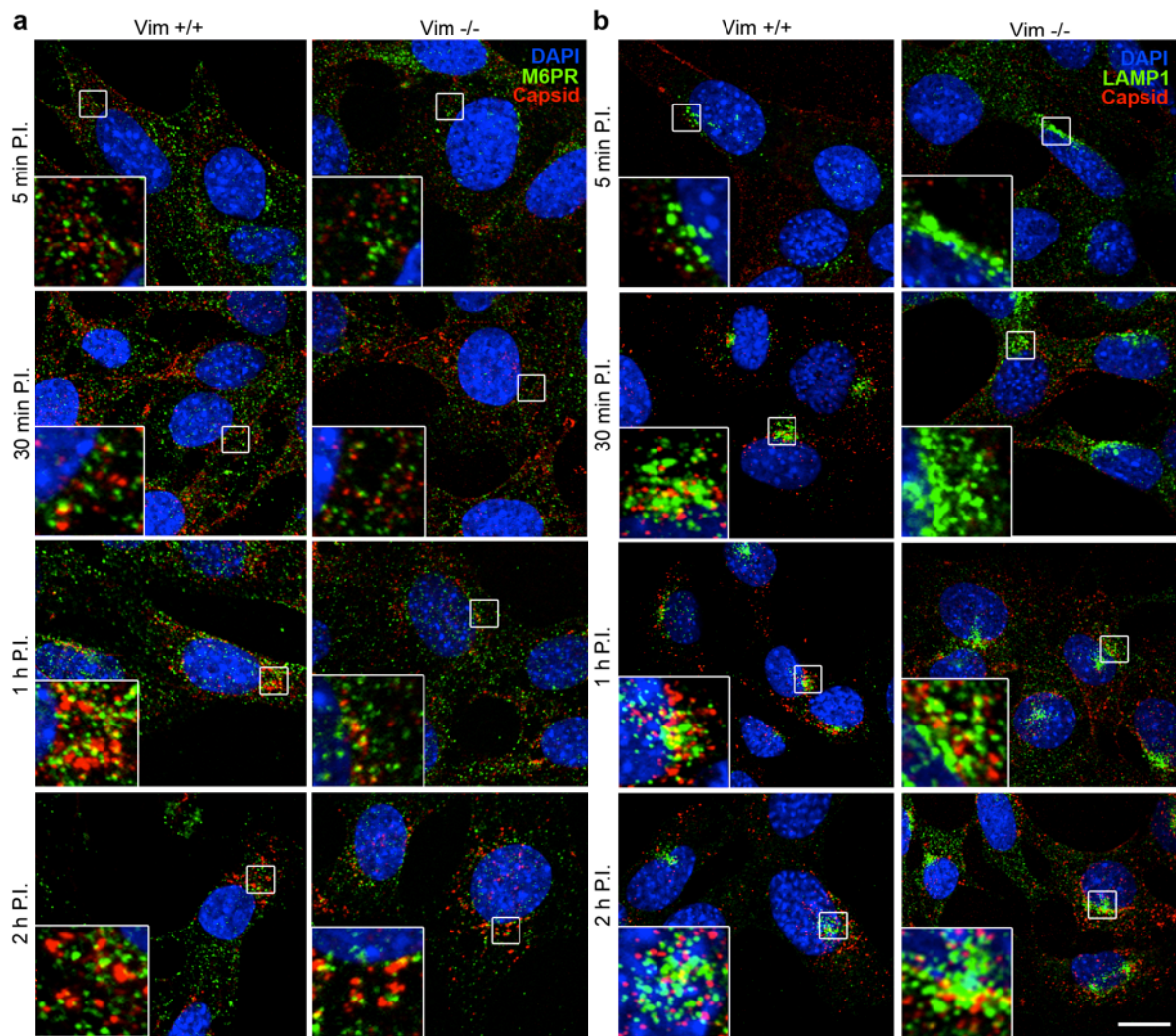


Figure 5-3: MVM capsid immunostaining in late endosomes/lysosomes appears reduced in $\text{vim}^{-/-}$ cells at 1 h and 2 h P.I. as compared to MVM-infected $\text{vim}^{+/+}$ cells. $\text{Vim}^{+/+}$ and $\text{vim}^{-/-}$ MEF cells were infected with MVM at a m.o.i. of 4 p.f.u. per cell, and prepared for indirect immunofluorescence microscopy 5 min, 30 min, 1 h, and 2 h P.I. Cells were fixed with 3% PFA, permeabilized with 0.2% Triton X-100 and labeled with an anti-capsid antibody (MAb B7; red) and either anti-M6PR antibody (C45B10; green) or anti-LAMP1 antibody (green). DAPI was used to detect DNA (blue). (a) Shown are representative confocal microscopy images of cells infected with MVM. Small boxes in each image point to regions of overlap between M6PR or LAMP1 and MVM-capsid immunostaining. Zoom in the bottom left show high magnification of these regions. Scale bar, 10 μm . (b) Quantification analysis was performed using BioImageXD. The co-localization percentage shown represents the percent of MVM-capsid staining pixels co-localizing with either M6PR or LAMP1 staining pixels in $\text{vim}^{+/+}$ and $\text{vim}^{-/-}$ cells. Shown are the mean values and standard error measured for 3 independent experiments (25 cells were counted for each condition).

treated cells showed minimal overlap between MVM and late endosomes/lysosomes (Fig 5-4). Additionally, similar to Fig. 4-10, the distribution of the MVM capsid immunostaining at 5 h P.I. is distinctly different in the $\text{vim}^{-/-}$ cells compared with the $\text{vim}^{+/+}$ cells. While the $\text{vim}^{-/-}$ cells have most of their MVM-containing vesicles accumulated at the perinuclear region in one side of the nucleus, these MVM-compartments have a more disperse cytoplasmic location in the $\text{vim}^{+/+}$ cells. Therefore, these results together indicate that in cells lacking vimentin, MVM is less able to reach late endosomes/lysosomes than in cells with an intact vimentin network.

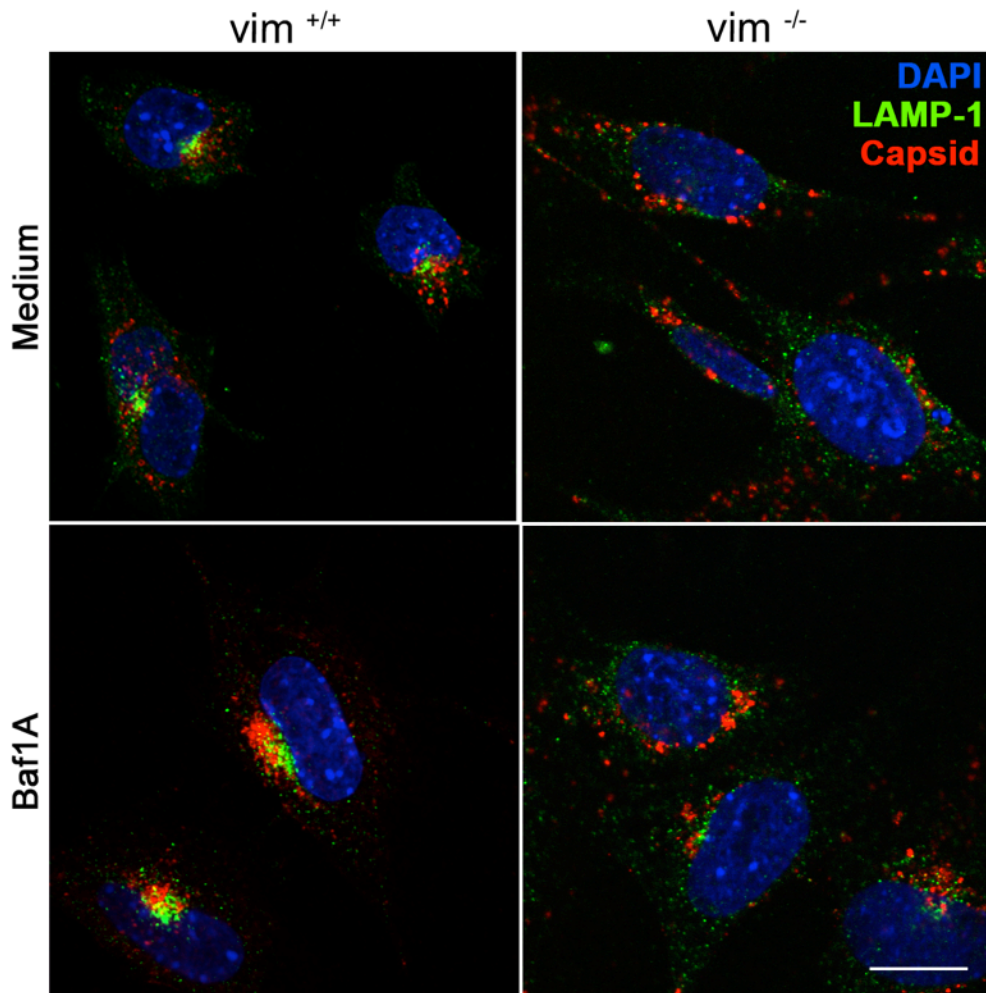


Figure 5-4: MVM does not reach late endosomes/lysosomes in *vim*^{-/-} cells treated with BafilomycinA as compared to *vim*^{+/+} cells. *Vim*^{+/+} and *vim*^{-/-} MEF cells were incubated with BafA1 or medium for 1 h, infected with MVM at a m.o.i. of 4 p.f.u. per cell (in the presence or absence of BafA1) and prepared for indirect immunofluorescence microscopy 5 h P.I. Cells were fixed with 3% PFA, permeabilized with 0.2% Triton X-100, and labeled with an anti-capsid antibody (MAb B7; red), LAMP1 (green), and DAPI to detect DNA (blue). Shown are representative confocal microscopy images. Scale bar, 10 μ m.

5.3 Discussion

Here I have examined the role of the misdistribution of late endosomes/lysosomes as a result of the lack of vimentin during MVM infection. I examined the progression of MVM through the endocytic pathway by co-immunolabeling MVM capsids with each of EEA1, M6PR, and LAMP1 at 5 min, 30 min, 1 h, and 2 h P.I. (Figs. 5-2 and 5-3). The wild type $\text{vim}^{+/+}$ MEF cells showed the expected progression of MVM from early endosomes to late endosomes, where virions are then able to escape from these acidic compartments into the cytosol (Figs. 5-2 and 5-3, $\text{vim}^{+/+}$ panels). However, it is important to note that endosomal release of MVM into the cytoplasm is inefficient. Therefore, only few virions leave these compartments; most virions follow the endocytic pathway into lysosomes, where they can remain for up to 8 h P.I. (Mani *et al.*, 2006). However, the progression of MVM through the endocytic pathway was altered in $\text{vim}^{-/-}$ MEF cells. In $\text{vim}^{-/-}$ cells, as compared to wild type $\text{vim}^{+/+}$ cells, MVM capsid immunostaining was accumulated in early endosomes and was reduced in late endosomes/lysosomes (Figs. 5-2 and 5-3, $\text{vim}^{-/-}$ panels). Additionally, preventing release of MVM from late endosomal/lysosomal compartments by the addition of BafA1 caused accumulation of capsid immunostaining at the nuclear periphery of $\text{vim}^{+/+}$ cells, but not in $\text{vim}^{-/-}$ cells (Fig. 5-4). This further indicates that MVM is less able to progress from early endosomes to late endosomes.

I propose that the effect I observed in Chapter 4 on MVM infection in $\text{vim}^{-/-}$ MEF cells, including the absence of perinuclear accumulation of MVM-containing vesicles and a decrease in NS1 and DNA expression may be explained by alterations to the endocytic pathway in $\text{vim}^{-/-}$ cells. Previous research may offer an explanation for my findings.

Cells lacking vimentin have mislocalized late endosomes/lysosomes, and have a decreased capacity to acidify their late endosomes/lysosomes (Styers *et al.*, 2004). MVM infection depends on the endocytic pathway and MVM escape from endosomes is pH-dependent. Therefore, I propose that the previously reported misdistribution of late endosomes/lysosomes in $\text{vim}^{-/-}$ cells, and the decrease in the ability of $\text{vim}^{-/-}$ cells to acidify late endosomes/lysosomes (Styers *et al.* 2004), leads to the observed alterations to MVM infection in $\text{vim}^{-/-}$ cells. In cells lacking vimentin, MVM is less able to progress from early endosomes to late endosomes/lysosomes. Furthermore, those virions that do manage to move through the endocytic pathway are possibly less able to exit into the cytosol from the endosome/lysosomes.

In summary (as illustrated in Fig. 5-5), the data in this chapter indicate that the absence of a vimentin IF network in cells causes:

- Retention of MVM in early endosomes at 1 and 2 h P.I.
- Reduction of MVM in late endosome/lysosomes

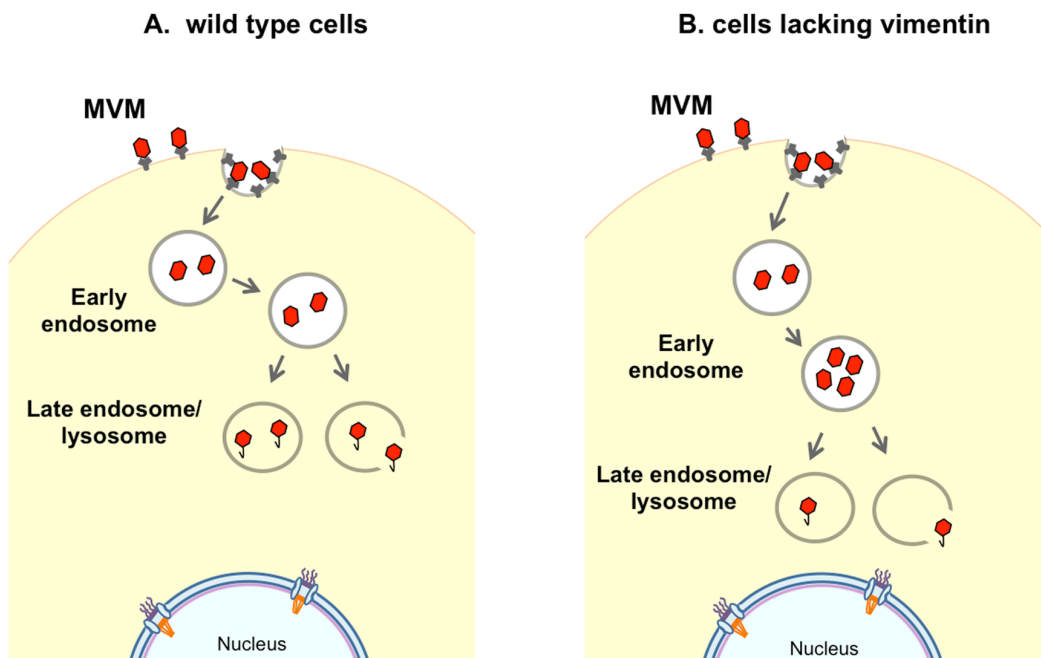


Figure 5-5: Lack of vimentin in cells leads to alteration of the progression of MVM through the endocytic pathway. (A) A representation of the progression of MVM through the endocytic pathway in MVM-infected wild type ($\text{vim}^{+/+}$) cells. Shown is the progression of MVM from early endosomes to late endosomes, where virions are then able to escape from these acidic compartments into the cytosol. The endosomal release of MVM into the cytoplasm is inefficient; therefore, most virions follow the endocytic pathway into lysosomes. (B) A representation of the progression of MVM through the endocytic pathway of MVM-infected cells lacking vimentin ($\text{vim}^{-/-}$ cells). MVM is seen accumulated in early endosomes, with fewer entering late endosomes and lysosomes.

Chapter 6 – General Discussion and Future Directions

For decades the role of AFs and MTs during the entry and intracellular trafficking of viruses has been extensively studied. However, there is a lack of information about the role of the third cytoskeleton component, IFs, during viral infection. In general, among the cytoskeleton components within the cell, IFs are heavily understudied; they have no commercially available inhibitors and their unique properties, such as lack of polarity and associated motor proteins, make them especially difficult to study. My thesis has established the foundation to answer several pertinent questions regarding the use of the IF network by parvovirus during infection. First, I have determined that after MVM infection, the vimentin network is rearranged, accumulating at the nuclear periphery after virions have escaped from endosomes. Second, I found that vimentin plays an important role in the infection cycle of MVM. The number of cells that successfully replicated MVM was reduced in infected cells in which the vimentin network was pharmacologically modified and in cells lacking a vimentin network, even though viral endocytosis remained unaltered. Third, perinuclear accumulation of MVM-containing vesicles and progression of virions through the endocytic pathway was reduced in cells lacking vimentin. Thus, I propose a dual role for vimentin during the MVM infection cycle, whereby vimentin facilitates the progression of MVM through the endocytic pathway and also plays a yet undetermined role immediately following MVM escape from endosomes, leading to rearrangement of the vimentin network (Fig. 6-1).

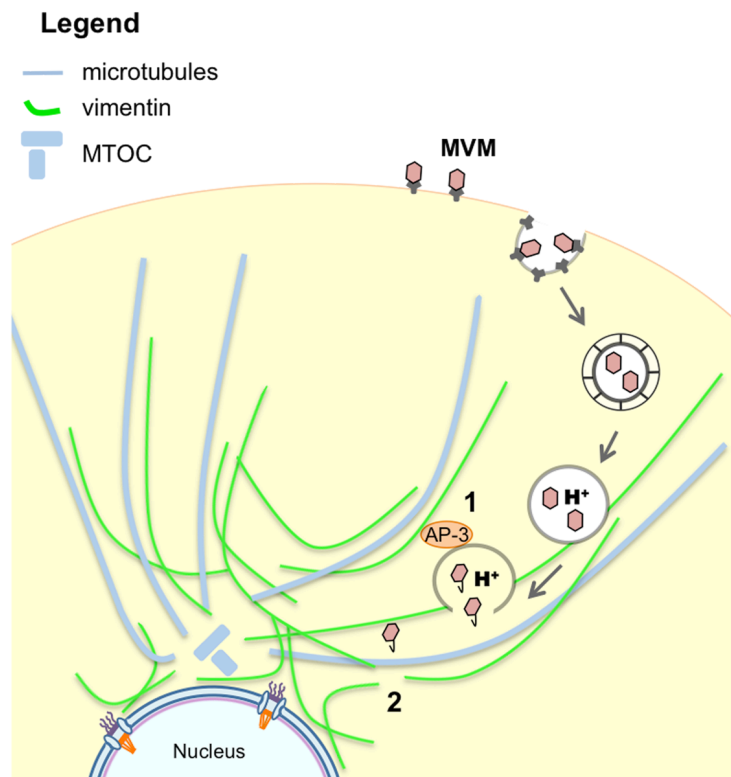


Figure 6-1: The dual role of vimentin during MVM infection cycle. (1) Vimentin facilitates progression of MVM through the endocytic pathway from early endosomes to late endosomes where MVM escapes into the cytoplasm, and (2) also plays a yet undetermined role immediately following MVM escape from endosomes, leading to rearrangement of the vimentin network.

6.1 The role of the vimentin network in the progression of MVM through the endocytic pathway

There is now increasing evidence for the involvement of the vimentin network in membrane bound organelle transport and cellular distribution (Chang *et al.*, 2009; Nekrasova *et al.*, 2011; Styers *et al.*, 2004). For example, vimentin has been shown to be involved in the cellular positioning of the Golgi network and late endosomal/lysosomal complexes (reviewed by Styers *et al.*, 2005; Toivola *et al.*, 2005). Vimentin interactions with a peripherally associated Golgi protein, formiminotransferase cyclodeaminase, is involved in the distribution of the Golgi network (Gao & Sztul, 2001). On the other hand, distribution and acidification of the endosomal-lysosomal compartments involves vimentin binding to the adapter protein AP-3, a heterotetrameric adaptor complex that carries vesicles between endosomal-lysosomal compartments and regulates sorting of lysosomes (Styers *et al.*, 2004). It has already been shown that cells lacking vimentin have mislocalized late endosomes/lysosomes and a decreased capacity to acidify their lysosomes (Styers *et al.*, 2004). Infection by all parvoviruses depends on progression through the endocytic pathway, and escape of virions from endosomes into the cytoplasm is pH-dependent (Harbison *et al.*, 2009; Quattrocchi *et al.*, 2012; Ros *et al.*, 2002; Suikkanen *et al.*, 2002; Vihinen-Ranta & Parrish, 2006). Therefore, the reduced MVM replication I have observed in $\text{vim}^{-/-}$ MEF cells may be explained, at least in part, to the misdistribution of late-endosomes/lysosomes in $\text{vim}^{-/-}$ cells, since MVM depends on the endocytic pathway. Furthermore, although this requires further investigation, it is likely that the decrease in the cell's ability to acidify its

lysosomes would lead to the inability of the virus to escape from endosomes in the $\text{vim}^{-/-}$ cells.

Overall I found that vimentin facilitates productive MVM infection and that there was a reduction in perinuclear accumulation of MVM-containing vesicles on one side of the nucleus in cells lacking vimentin. I found that this is likely due to an alteration of the endocytic pathway in cells lacking vimentin. Similar results were seen with CMV (Miller & Hertel, 2009). Treatment of cells with ACR prior to infection with CMV leads to lack of viral protein production and protein expression. Furthermore, with CMV infection, the virus remained in the cytoplasm longer in cells lacking vimentin as compared to wild type cells. Thus, it was concluded that viral trafficking toward the nucleus was delayed in cells lacking an intact vimentin network (Miller & Hertel, 2009). This may be due to the virus using vimentin to interact with dynein and traffic toward the nucleus using the MT network, after fusion of the viral envelope with the plasma membrane for cell entry. CMV has also been shown to enter cells via endocytosis, therefore, possibly requiring vimentin for progression through the endocytic pathway. This is similar to what my data indicate for MVM infection. However, in contrast to MVM infection, with CMV infection no rearrangements of the vimentin network were observed (Miller & Hertel, 2009). Thus, there may be a second role for vimentin during MVM infection that is different than in CMV infection.

6.2 Possible roles for vimentin rearrangements after MVM escape from endosomes

6.2.1 Vimentin rearrangements may be involved in MVM utilizing the aggresome/proteasome pathway

In Chapter 3, I found that MVM causes rearrangements to the vimentin network 2 h P.I., ultimately leading to the collapse of the network at 24 h P.I. There have been several other viruses reported to cause rearrangements and collapse of the vimentin network during viral infection, such as African swine fever virus (Stefanovic *et al.*, 2005), rotavirus (Weclawicz *et al.*, 1994), dengue virus (Chen *et al.*, 2008), and HIV-1 (Honer *et al.*, 1991). Among these, the only virus for which the role of the vimentin network rearrangements has been well established is African swine fever virus. For this virus, and those like it that replicate in the cytoplasm, vimentin and tubulin rearrange during infection to provide a mechanical scaffold for viral proteins as a part of the viral replication factory (Heath *et al.*, 2001). These structures often resemble cellular aggresomes, which are located close to centrosomes and are enclosed in a characteristic vimentin cage (Heath *et al.*, 2001). The ability of aggresomes to concentrate proteins and cellular chaperones (Kopito, 2000) make them highly suitable for facilitating virus assembly (reviewed by Wileman, 2006, 2007). Viruses probably use the aggresome pathway to avoid being recognized as foreign while replicating in the cytoplasm, and to instead be mistaken for a misfolded protein by the cell. It is unlikely that parvoviruses would use these aggresome-like structures to replicate in the cytoplasm, since it is well known that MVM replication occurs in the nucleus (reviewed by Cotmore & Tattersall, 2006b). However, it has been shown that viruses that replicate

in the nucleus, such as adenovirus, also can use aggresome formation. For viruses like adenovirus, this is to protect the viral DNA from cellular proteins that inhibit viral replication. Host cellular proteins that normally inhibit viral replication are sequestered in the cytoplasm so that their degradation can be greatly accelerated by proteasomes (Liu *et al.* 2005, reviewed by Schreiner *et al.*, 2012). It has already been described that proteasomes may play a role during MVM infection after endosomal escape, likely in partial capsid disassembly or nuclear entry (Ros & Kempf, 2004; Ros *et al.*, 2002). Thus, it is possible that MVM could use a similar aggresome and proteasome pathway that would lead to vimentin rearrangement at the perinuclear region of cells near the MTOC.

6.2.2 Vimentin rearrangements could facilitate nuclear entry of MVM

Interestingly, vimentin is highly active, binds with high affinity to ssDNA, and enters the nucleus (Hartig *et al.*, 1998; Perides *et al.*, 1987; Traub *et al.*, 1992). Therefore, it is possible that vimentin could increase the movement of MVM to the nucleus. Other viruses, such as HIV-1, provide an example of a virus using vimentin cleavage products in order to enter the nucleus. Although there is some evidence that nuclear entry of HIV-1 preintegration complex (PIC) is an active process requiring the help of importin 7 (Bukrinsky *et al.*, 1992; Fassati *et al.*, 2003), it has also been proposed that vimentin may play a role in fostering the uptake of PIC into the nucleus (Thomas *et al.*, 1996). It has been observed that overexpression of the HIV-1 protein Vpr causes nuclear envelope disruptions and decreases integrity of the nuclear envelope (de Noronha *et al.*, 2001), leading to the entry of the HIV-1 PIC into the nucleus (Segura-Totten &

Wilson, 2001). MVM also causes small nuclear envelope disruptions and decreases lamina integrity, which facilitates the nuclear entry of MVM through the resulting membrane brakes (Cohen & Pante, 2005; Cohen *et al.*, 2006; Cohen *et al.*, 2011). Furthermore, since PKC has been shown to be required for nuclear envelope breakdown and lamina disruptions (Porwal *et al.*, 2013), it is likely that this kinase could also phosphorylate vimentin, leading to a subsequent role of vimentin in speeding up nuclear entry of MVM. However, to come up with a definitive model further examination needs to be conducted.

6.2.3 Vimentin may be involved in the trafficking of MVM toward the nucleus

As described in Section 1.3, in general there are several roles shown for vimentin during viral infection, ranging from viral cell entry, to viral replication, and finally cellular trafficking and viral egress. Of these roles, since MVM was able to enter both *vim*^{+/+} and *vim*^{-/-} cells in the same proportions, then the role for vimentin as a ligand for MVM cell attachment and entry is unlikely.

Parvoviruses such as CPV and AAV both exploit MTs and dynein for the process of trafficking toward the nucleus (Kelkar *et al.*, 2006; Suikkanen *et al.*, 2003; Xiao & Samulski, 2012). Vimentin traffics and assembles on the MT network using dynein (Helfand *et al.* 2002). Thus, it is possible that MVM could bind directly to vimentin and subsequently dynein and the MT network, in order to traffic toward the nucleus after endosomal escape. A similar vimentin role has been proposed for CMV (Miller & Hertel, 2009). The binding of viral capsids to vimentin, as the virus traffics with it toward the

nucleus, could then lead to the observed rearrangement of the vimentin network. For several other viruses, interactions between a viral protein and vimentin have already been observed to mediate the rearrangement of the network and proposed to mediate trafficking within the cytoplasm (Gladue et al., 2013; Haolong et al., 2013; Kanlaya et al., 2010; Teo & Chu, 2014).

6.3 Possible mechanisms for vimentin rearrangement during MVM infection

The vimentin rearrangements that I observed during MVM infection could either involve cleavage of vimentin or the phosphorylation of the vimentin N-terminal domain. For HIV-1 and adenovirus, which induce vimentin rearrangement during infection, it is a result of proteolytic cleavage of vimentin (Belin & Boulanger, 1987; Defer *et al.*, 1990; Shoeman *et al.*, 1990), which then results in the collapse or rearrangements of the vimentin IF network (Honer *et al.*, 1991). In the case of HIV-1, it has been demonstrated that a viral protease cleaves vimentin (Honer *et al.*, 1991; Shoeman *et al.*, 1990). For adenovirus, however, the data indicate that a cellular protease, rather than a viral protease may lead to the proteolytic processing of vimentin. MVM proteins have no known proteolytic activities, thus similar to adenovirus a cellular protease may also be responsible for the cleavage of vimentin during MVM infection. However, in Chapter 3 I have found that vimentin is not cleaved at 2 h P.I., therefore an alternate mechanism may be involved in vimentin rearrangement.

Several viruses have been shown to phosphorylate vimentin leading to its rearrangement. The vimentin network rearrangement observed during African swine

fever virus and enterovirus 71 infection involves phosphorylation of vimentin at serine 38 or serine 82 by CaMK-II (Haolong *et al.*, 2013; Stefanovic *et al.*, 2005), while dengue virus infection involves activation of ROCK in addition to phosphorylation of vimentin at serine 38 by CaMK-II (Lei *et al.*, 2013; Teo & Chu, 2014). MVM is known to be dependent on the activation of cellular kinases such as those in the PKC family for the phosphorylation of NS1 (Lachmann *et al.*, 2003; Nuesch & Rommelaere, 2006; Nuesch *et al.*, 2003). In addition, activated PKC has also been found to be involved in nuclear envelope breakdown (Porwal *et al.*, 2013). It is possible that these activated kinases could be responsible for the phosphorylation and rearrangement of the vimentin network, once the virus has been released from the endosomes and entered the cytoplasm.

6.4 Future directions

In this thesis I sought to address the effects on the cytoskeleton after infection with MVM and the role of the vimentin IF network during MVM infection. However, there still remain many interesting questions about the role of endocytic trafficking and vimentin during MVM infection. For example, how and at which stage of infection MVM releases its genome, and the precise mechanism of MVM cytoplasmic trafficking remain to be determined. Here I present the following interesting questions regarding the role of vimentin during MVM infection that need to be explored further to better understand the role of vimentin in MVM infection:

- 1) Is acidification of endosomes affected in MVM-infected cells lacking vimentin?

(Section 6.4.1).

- 2) Do cells lacking vimentin become susceptible to MVM infection when transfected with vimentin? (Section 6.4.2).
- 3) Does vimentin facilitate partial uncoating of MVM DNA progressing toward the nucleus? (Section 6.4.3).
- 4) What is the mechanism for vimentin rearrangement during MVM infection? (Section 6.4.4).
- 5) Is the MVM-induced vimentin rearrangement involved in forming aggresomes? (Section 6.4.5).

6.4.1 Is acidification of endosomes affected in MVM-infected cells lacking vimentin?

As explained in Section 6.1, the reduced MVM replication I have observed in $\text{vim}^{-/-}$ MEF cells may be explained, at least in part, to the misdistribution of late endosomes/lysosomes in $\text{vim}^{-/-}$ cells, since MVM depends on the endocytic pathway. However, although I show that MVM is less able to progress through the endocytic pathway, I have not directly shown that the release of MVM from endosomes is reduced. As previously stated, this viral release process into the cytoplasm has been shown to be inefficient for parvoviruses, including MVM. Thus, although many virions remain within early endosomes, in order to come up with a definitive model, we need to determine if in MVM-infected cells lacking vimentin, the amount of MVM released from endosomes is indeed reduced due to a reduction in acidification of endosomes. My hypothesis is that the decrease in the $\text{vim}^{-/-}$ cell's ability to acidify its endosomes would lead to the inability of MVM to escape from endosomes in the $\text{vim}^{-/-}$ cells. *Styers et al.*

2004, have already determined that endosomal acidification is reduced in $\text{vim}^{-/-}$ cells. This was demonstrated using Lysosensor probes, which possess a pH-dependent emission shift to longer wavelengths in acidic environments. With these probes, they showed that Lysosensor green-positive organelles were decreased in $\text{vim}^{-/-}$ cells as compared to wild type cells (Styers *et al.*, 2004). Instead of using Lysosensor, I propose to instead use pHRodo Red indicators (Invitrogen). In contrast to Lysosensor, which also requires a separate MVM-fluorophore conjugate in order to detect both MVM and the environment simultaneously, using pHRodo will enable us to generate an MVM-pHrodo red conjugate. $\text{Vim}^{-/-}$ and $\text{vim}^{+/+}$ infected-cells would be incubated with MVM conjugated with pHrodo Red and using live fluorescence microscopy, we could determine the pH of the environment in which the virions reside as they progress through the endocytic pathway. I predict that in $\text{vim}^{-/-}$ cells there will be a reduction in red fluorescence, as MVM will be less able to progress through the endocytic pathway and the pHrodo red dye will therefore not emit fluorescence.

6.4.2 Do cells lacking vimentin become susceptible to MVM infection when transfected with vimentin?

By using $\text{vim}^{-/-}$ MEF cells that lack a vimentin network I have shown that vimentin facilitates MVM infection. I propose to use vimentin constructs in a gain of function experiment to investigate the role of full-length vimentin during MVM infection. Vimentin constructs would be transfected into $\text{vim}^{+/+}$ and $\text{vim}^{-/-}$ MEF cells, prior to MVM infection and prepared for immunofluorescence microscopy using an antibody against MVM NS1 protein at 15 h P.I to detect the onset of MVM replication. My prediction is that, with

transfection of vimentin, $\text{vim}^{-/-}$ cells will once again become susceptible to MVM infection, confirming the requirement of vimentin during MVM infection.

6.4.3 Does vimentin facilitate the partial uncoating of MVM DNA progressing toward the nucleus?

I have shown that in $\text{vim}^{-/-}$ cells, perinuclear accumulation of MVM-containing vesicles, and progression of virions through the endocytic pathway was reduced in cells lacking vimentin. However, the approaches used only detected MVM capsids and not MVM DNA. Since low pH is required for the MVM DNA to be partially exposed in the endocytic pathway (Mani *et al.*, 2006), I hypothesize that in cells lacking vimentin, MVM DNA is unable to partially uncoat in endosomes. I would use *in situ* hybridization in combination with immunofluorescence microscopy, for simultaneous visualization of the viral capsid and viral DNA at increasing time points of infection, 5 min, 15 min, 30 min, 45 min, 1 h, and 2 h. I would predict that in $\text{vim}^{+/+}$ cells, the usual progression of MVM DNA would be seen as the viral DNA becomes exposed at 30 min P.I., whereas in $\text{vim}^{-/-}$ cells it will remain unexposed. Furthermore, the progression of MVM could once again be studied, but observing MVM DNA instead. At 1 and 2 P.I., I would expect MVM DNA to be more perinuclear in $\text{vim}^{+/+}$ cells, as compared to $\text{vim}^{-/-}$ cells.

6.4.4 What is the mechanism for vimentin rearrangement during MVM infection?

As discussed in Section 6.3, MVM is known to be dependent on the activation of cellular kinases such as those in the PKC family for the phosphorylation of NS1 (Lachmann *et al.*, 2003; Nuesch & Rommelaere, 2006; Nuesch *et al.*, 2003). In addition, activated

PKC has also been found to be involved in parvoviral-induced nuclear envelope breakdown (Porwal *et al.*, 2013). Vimentin is a substrate for a number of kinases and several PKC sites have previously been identified (Ku *et al.*, 1998; Takai *et al.*, 1996; Yasui *et al.*, 2001). Thus, I hypothesize that these activated kinases could be responsible for the phosphorylation of vimentin and subsequent rearrangement of the vimentin network, once MVM has been released from the endosomes and entered the cytoplasm. In order to test this hypothesis, I propose to first use western blot analysis using antibodies that detect specific phosphorylated amino acid sites of vimentin, such as serine 33 and serine 55, which are the amino acids targets of PKC on vimentin (Takai *et al.*, 1996). I would expect that MVM-infected cells would have increased levels of phosphorylated serine 33 and serine 55 as compared to mock-infected cells. Second, I would use PKC inhibitors such as bisindolylmaleimide-I (BIM-I), prior to mock- or MVM-infection and prepare cells for immunofluorescence microscopy labeling of vimentin at 2 h P.I. I would expect that with the addition of PKC inhibitors, vimentin would no longer rearrange to one side of the nucleus, as its phosphorylation would not be occurring.

6.4.5 Is the MVM-induced vimentin rearrangement involved in forming aggresomes?

As described in Section 6.2.1, it has been shown that viruses that replicate in the nucleus, such as adenovirus, can use aggresome formation to protect the viral DNA from cellular proteins that inhibit viral replication (Liu *et al.*, 2005). It has already been described that proteasomes may play a role during MVM infection after endosomal

escape, likely in capsid disassembly or nuclear entry (Ros & Kempf, 2004; Ros *et al.*, 2002). Thus, it is possible that MVM could use a similar aggresome and proteasome pathway that would lead to vimentin rearrangement at the perinuclear region of cells near the MTOC.

In early MVM infection, I have found vimentin to rearrange and accumulate at the perinuclear region, suggesting the involvement of aggresomes during early infection as a vimentin cage often surrounds them. Thus, I hypothesize that aggresomes form during early MVM infection, virions are localized to these areas, and that they are involved in partial capsid disassembly and nuclear entry mechanisms of MVM. This hypothesis could be tested by first immunolabeling MVM infected and mock infected cells for the following several common markers of aggresomes: two cellular chaperone proteins, Hsp40 and Hsp70, and mitochondria, using MitoTracker (Invitrogen). I would expect that these cellular components would increase greatly at the perinuclear region in MVM infected cells as compared to mock infected cells, because they will be recruited to aggresomes. Furthermore, *in situ* hybridization of MVM DNA and the indicators of aggresomes, as stated above, may elucidate further the role of aggresomes in MVM infection. I would expect that MVM DNA would be found in these aggresome-like structures during infection.

6.5 Concluding remarks

I have found that vimentin plays an important role in the infection cycle of MVM. The vimentin IF network is rearranged post endosomal escape during early infection with the parvovirus MVM (summarized in Fig. 3-14). MVM is less able to replicate in cells that

have an artificially disrupted vimentin IF network and in cells lacking vimentin, even though endosomal uptake remains unaltered. Additionally, there is a reduction in perinuclear accumulation of MVM-containing vesicles on one side of the nucleus in cells lacking vimentin (summarized in Fig. 4-11), which may be due to the altered endosomal pathway in these cells, whereby MVM remains in early endosomes less able to progress through the endocytic pathway (summarized in Fig. 5-5). This work has provided the foundation for studying many more aspects of the MVM infection cycle related to the cytoskeleton. Future studies will help further uncover the mysteries of the IF network in cells and elucidate the many roles it plays during viral infection.

By studying the mechanisms employed by parvoviruses during early infection we will increase our understanding of the extent to which viruses take advantage of host mechanisms in order to replicate and spread. This increase in knowledge will guide us toward thinking of new approaches for drug therapies targeting other human pathogenic viruses as well as the creation of more effective vectors for gene therapy and cancer therapy. In general, studies on the role of the IF network during viral infection have opened the doors to potential novel therapeutics, and continue to broaden our understanding of the role of the cytoskeleton within the cell.

Bibliography

- Adeyemi, R. O. & Pintel, D. J. (2012).** Replication of minute virus of mice in murine cells is facilitated by virally induced depletion of p21. *J Virol* **86**, 8328-8332.
- Adeyemi, R. O. & Pintel, D. J. (2014).** Parvovirus-induced depletion of cyclin B1 prevents mitotic entry of infected cells. *PLoS Pathog* **10**, e1003891.
- Adeyemi, R. O., Landry, S., Davis, M. E., Weitzman, M. D. & Pintel, D. J. (2010).** Parvovirus minute virus of mice induces a DNA damage response that facilitates viral replication. *PLoS Pathog* **6**, e1001141.
- Aggeler, J. & Seely, K. (1990).** Cytoskeletal dynamics in rabbit synovial fibroblasts: I. Effects of acrylamide on intermediate filaments and microfilaments. *Cell Motil Cytoskel* **16**, 110-120.
- Alexander, S., Hellemans, L., Marti, O., Schneir, J., Elings, V., Hansma, P. K., Longmire, M. & J., G. (1989).** An atomic-resolution atomic-force microscope implemented using an optical lever. *Journal of Applied Physics* **65**, 164-167.
- Allan, V. J. (2011).** Cytoplasmic dynein. *Biochem Soc Trans* **39**, 1169-1178.
- Allander, T., Tammi, M. T., Eriksson, M., Bjerkner, A., Tiveljung-Lindell, A. & Andersson, B. (2005).** Cloning of a human parvovirus by molecular screening of respiratory tract samples. *Proc Natl Acad Sci USA* **102**, 12891-12896.
- Angelova, A. L., Aprahamian, M., Grekova, S. P., Hajri, A., Leuchs, B., Giese, N. A., Dinsart, C., Herrmann, A., Balboni, G. & other authors (2009a).** Improvement of gemcitabine-based therapy of pancreatic carcinoma by means of oncolytic parvovirus H-1PV. *Clin Cancer Res* **15**, 511-519.
- Angelova, A. L., Aprahamian, M., Balboni, G., Delecluse, H. J., Feederle, R., Kiprianova, I., Grekova, S. P., Galabov, A. S., Witzens-Harig, M. & other authors (2009b).** Oncolytic rat parvovirus H-1PV, a candidate for the treatment of human lymphoma: In vitro and in vivo studies. *Mol Ther* **17**, 1164-1172.
- Armer, H., Moffat, K., Wileman, T., Belsham, G. J., Jackson, T., Duprex, W. P., Ryan, M. & Monaghan, P. (2008).** Foot-and-mouth disease virus, but not bovine enterovirus, targets the host cell cytoskeleton via the nonstructural protein 3Cpro. *J Virol* **82**, 10556-10566.
- Asokan, A., Schaffer, D. V. & Samulski, R. J. (2012).** The AAV vector toolkit: poised at the clinical crossroads. *Mol Ther* **20**, 699-708.
- Asokan, A., Hamra, J. B., Govindasamy, L., Agbandje-McKenna, M. & Samulski, R. J. (2006).** Adeno-associated virus type 2 contains an integrin alpha5beta1 binding domain essential for viral cell entry. *J Virol* **80**, 8961-8969.
- Astell, C. R., Gardiner, E. M. & Tattersall, P. (1986).** DNA sequence of the lymphotropic variant of minute virus of mice, MVM(i), and comparison with the DNA sequence of the fibrotropic prototype strain. *J Virol* **57**, 656-669.
- Au, S., Cohen, S. & Pante, N. (2010).** Microinjection of *Xenopus laevis* oocytes as a system for studying nuclear transport of viruses. *Methods* **51**, 114-120.
- Bantel-Schaal, U., Braspenning-Wesch, I. & Kartenbeck, J. (2009).** Adeno-associated virus type 5 exploits two different entry pathways in human embryo fibroblasts. *J Gen Virol* **90**, 317-322.

- Bar, S., Rommelaere, J. & Nuesch, J. P. (2013).** Vesicular transport of progeny parvovirus particles through ER and Golgi regulates maturation and cytolysis. *PLoS Pathog* **9**, e1003605.
- Bar, S., Daeffler, L., Rommelaere, J. & Nuesch, J. P. (2008).** Vesicular egress of non-enveloped lytic parvoviruses depends on gelsolin functioning. *PLoS Pathog* **4**, e1000126.
- Bashir, T., Rommelaere, J. & Cziepluch, C. (2001).** In vivo accumulation of cyclin A and cellular replication factors in autonomous parvovirus minute virus of mice-associated replication bodies. *J Virol* **75**, 4394-4398.
- Belin, M. T. & Boulanger, P. (1987).** Processing of vimentin occurs during the early stages of adenovirus infection. *J Virol* **61**, 2559-2566.
- Berns, K. I. & Parrish, C.R. (2013).** Parvoviridae. In *Fields Virology*, 6th edn, pp. 1768-1791. Philadelphia, PA: Lippincott Williams & Wilkins.
- Bhattacharya, B., Noad, R. J. & Roy, P. (2007).** Interaction between Bluetongue virus outer capsid protein VP2 and vimentin is necessary for virus egress. *Virology* **4**, 7.
- Bhattacharya, R., Gonzalez, A. M., Debiase, P. J., Trejo, H. E., Goldman, R. D., Flitney, F. W. & Jones, J. C. (2009).** Recruitment of vimentin to the cell surface by beta3 integrin and plectin mediates adhesion strength. *J Cell Sci* **122**, 1390-1400.
- Bisi, S., Disanza, A., Malinverno, C., Frittoli, E., Palamidessi, A. & Scita, G. (2013).** Membrane and actin dynamics interplay at lamellipodia leading edge. *Curr Opin Cell Biol* **25**, 565-573.
- Blanchoin, L., Boujemaa-Paterski, R., Sykes, C. & Plastino, J. (2014).** Actin dynamics, architecture, and mechanics in cell motility. *Physiol Rev* **94**, 235-263.
- Boisvert, M., Fernandes, S. & Tijssen, P. (2010).** Multiple pathways involved in porcine parvovirus cellular entry and trafficking toward the nucleus. *J Virol* **84**, 7782-7792.
- Bouard, D., Alazard-Dany, D. & Cosset, F. L. (2009).** Viral vectors: from virology to transgene expression. *Br J Pharmacol* **157**, 153-165.
- Bremner, K. H., Scherer, J., Yi, J., Vershinin, M., Gross, S. P. & Vallee, R. B. (2009).** Adenovirus transport via direct interaction of cytoplasmic dynein with the viral capsid hexon subunit. *Cell Host Microbe* **6**, 523-535.
- Broliden, K., Tolfvenstam, T. & Norbeck, O. (2006).** Clinical aspects of parvovirus B19 infection. *J Intern Med* **260**, 285-304.
- Brownstein, D. G., Smith, A. L., Jacoby, R. O., Johnson, E. A., Hansen, G. & Tattersall, P. (1991).** Pathogenesis of infection with a virulent allotropic variant of minute virus of mice and regulation by host genotype. *Lab Invest* **65**, 357-364.
- Brownstein, D. G., Smith, A. L., Johnson, E. A., Pintel, D. J., Naeger, L. K. & Tattersall, P. (1992).** The pathogenesis of infection with minute virus of mice depends on expression of the small nonstructural protein NS2 and on the genotype of the allotropic determinants VP1 and VP2. *J Virol* **66**, 3118-3124.
- Bukrinsky, M. I., Sharova, N., Dempsey, M. P., Stanwick, T. L., Bukrinskaya, A. G., Haggerty, S. & Stevenson, M. (1992).** Active nuclear import of human immunodeficiency virus type 1 preintegration complexes. *Proc Natl Acad Sci USA* **89**, 6580-6584.

- Burkhardt, J. K., Echeverri, C. J., Nilsson, T. & Vallee, R. B. (1997).** Overexpression of the dynamitin (p50) subunit of the dynactin complex disrupts dynein-dependent maintenance of membrane organelle distribution. *J Cell Biol* **139**, 469-484.
- Bustamante, C., Rivetti, C. & Keller, D. J. (1997).** Scanning force microscopy under aqueous solutions. *Curr Opin Struct Biol* **7**, 709-716.
- Cai, Y., Singh, B. B., Aslanukov, A., Zhao, H. & Ferreira, P. A. (2001).** The docking of kinesins, KIF5B and KIF5C, to Ran-binding protein 2 (RanBP2) is mediated via a novel RanBP2 domain. *J Biol Chem* **276**, 41594-41602.
- Caviston, J. P. & Holzbaur, E. L. (2006).** Microtubule motors at the intersection of trafficking and transport. *Trends Cell Biol* **16**, 530-537.
- Chang, L. & Goldman, R. D. (2004).** Intermediate filaments mediate cytoskeletal crosstalk. *Nat Rev Mol Cell Biol* **5**, 601-613.
- Chang, L., Barlan, K., Chou, Y. H., Grin, B., Lakonishok, M., Serpinskaya, A. S., Shumaker, D. K., Herrmann, H., Gelfand, V. I. & other authors (2009).** The dynamic properties of intermediate filaments during organelle transport. *J Cell Sci* **122**, 2914-2923.
- Charlton, C. A. & Volkman, L. E. (1991).** Sequential rearrangement and nuclear polymerization of actin in baculovirus-infected *Spodoptera frugiperda* cells. *J Virol* **65**, 1219-1227.
- Charlton, C. A. & Volkman, L. E. (1993).** Penetration of *Autographa californica* nuclear polyhedrosis virus nucleocapsids into IPLB Sf 21 cells induces actin cable formation. *Virology* **197**, 245-254.
- Chen, A. Y. & Qiu, J. (2010).** Parvovirus infection-induced cell death and cell cycle arrest. *Future Virol* **5**, 731-743.
- Chen, L. K., Lin, Y. L., Liao, C. L., Lin, C. G., Huang, Y. L., Yeh, C. T., Lai, S. C., Jan, J. T. & Chin, C. (1996).** Generation and characterization of organ-tropism mutants of Japanese encephalitis virus in vivo and in vitro. *Virology* **223**, 79-88.
- Chen, W., Gao, N., Wang, J. L., Tian, Y. P., Chen, Z. T. & An, J. (2008).** Vimentin is required for dengue virus serotype 2 infection but microtubules are not necessary for this process. *Arch Virol* **153**, 1777-1781.
- Chhabra, E. S. & Higgs, H. N. (2007).** The many faces of actin: matching assembly factors with cellular structures. *Nat Cell Biol* **9**, 1110-1121.
- Chiramel, A. I., Brady, N. R. & Bartenschlager, R. (2013).** Divergent roles of autophagy in virus infection. *Cells* **2**, 83-104.
- Christensen, J. & Tattersall, P. (2002).** Parvovirus initiator protein NS1 and RPA coordinate replication fork progression in a reconstituted DNA replication system. *J Virol* **76**, 6518-6531.
- Christensen, J., Cotmore, S. F. & Tattersall, P. (1997).** A novel cellular site-specific DNA-binding protein cooperates with the viral NS1 polypeptide to initiate parvovirus DNA replication. *J Virol* **71**, 1405-1416.
- Clemens, K. E. & Pintel, D. J. (1988).** The two transcription units of the autonomous parvovirus minute virus of mice are transcribed in a temporal order. *J Virol* **62**, 1448-1451.

- Clement, C., Tiwari, V., Scanlan, P. M., Valyi-Nagy, T., Yue, B. Y. & Shukla, D. (2006).** A novel role for phagocytosis-like uptake in herpes simplex virus entry. *J Cell Biol* **174**, 1009-1021.
- Cohen, S. & Pante, N. (2005).** Pushing the envelope: microinjection of Minute virus of mice into *Xenopus* oocytes causes damage to the nuclear envelope. *J Gen Virol* **86**, 3243-3252.
- Cohen, S., Behzad, A. R., Carroll, J. B. & Pante, N. (2006).** Parvoviral nuclear import: bypassing the host nuclear-transport machinery. *J Gen Virol* **87**, 3209-3213.
- Cohen, S., Marr, A. K., Garcin, P. & Pante, N. (2011).** Nuclear envelope disruption involving host caspases plays a role in the parvovirus replication cycle. *J Virol* **85**, 4863-4874.
- Colucci-Guyon, E., Portier, M. M., Dunia, I., Paulin, D., Pournin, S. & Babinet, C. (1994).** Mice lacking vimentin develop and reproduce without an obvious phenotype. *Cell* **79**, 679-694.
- Cordo, S. M. & Candurra, N. A. (2003).** Intermediate filament integrity is required for Junin virus replication. *Virus Res* **97**, 47-55.
- Cotmore, S. F. & Tattersall, P. (2006a).** Structure and Organization of the viral genome. In *Parvoviruses*, pp. 73-94. Edited by J. R. Kerr, S. F. Cotmore, M. E. Bloom, R. M. Linden & C. R. Parrish. London, UK: Hodder Arnold.
- Cotmore, S. F. & Tattersall, P. (2006b).** A rolling-hairpin strategy: basic mechanisms of DNA replication in the parvoviruses. In *Parvoviruses*, pp. 171-188. Edited by J. R. Kerr, S. F. Cotmore, M. E. Bloom, R. M. Linden & C. R. Parrish. London, UK: Hodder Arnold.
- Cotmore, S. F. & Tattersall, P. (2007).** Parvoviral host range and cell entry mechanisms. *Adv Virus Res* **70**, 183-232.
- Cotmore, S. F. & Tattersall, P. (2013).** Parvovirus diversity and DNA damage responses. *Cold Spring Harb Perspect Biol* **5**, pii: a012989
- Cotmore, S. F., D'Abramo, A. M., Jr., Carbonell, L. F., Bratton, J. & Tattersall, P. (1997).** The NS2 polypeptide of parvovirus MVM is required for capsid assembly in murine cells. *Virology* **231**, 267-280.
- Cotmore, S. F., Agbandje-McKenna, M., Chiorini, J. A., Mukha, D. V., Pintel, D. J., Qiu, J., Soderlund-Venermo, M., Tattersall, P., Tijssen, P. & other authors (2014).** The family Parvoviridae. *Arch Virol* **159**, 1239-1247.
- Cureton, D. K., Harbison, C. E., Cocucci, E., Parrish, C. R. & Kirchhausen, T. (2012).** Limited transferrin receptor clustering allows rapid diffusion of canine parvovirus into clathrin endocytic structures. *J Virol* **86**, 5330-5340.
- Das, S., Ravi, V. & Desai, A. (2011).** Japanese encephalitis virus interacts with vimentin to facilitate its entry into porcine kidney cell line. *Virus Res* **160**, 404-408.
- Dave, J. M. & Bayless, K. J. (2014).** Vimentin as an integral regulator of cell adhesion and endothelial sprouting. *Microcirculation* **21**, 333-344.
- de Noronha, C. M., Sherman, M. P., Lin, H. W., Cavois, M. V., Moir, R. D., Goldman, R. D. & Greene, W. C. (2001).** Dynamic disruptions in nuclear envelope architecture and integrity induced by HIV-1 Vpr. *Science* **294**, 1105-1108.

- Defer, C., Belin, M. T., Caillet-Boudin, M. L. & Boulanger, P. (1990).** Human adenovirus-host cell interactions: comparative study with members of subgroups B and C. *J Virol* **64**, 3661-3673.
- Desai, A. & Mitchison, T. J. (1997).** Microtubule polymerization dynamics. *Annu Rev Cell Dev Biol* **13**, 83-117.
- Dodding, M. P. & Way, M. (2011).** Coupling viruses to dynein and kinesin-1. *EMBO J* **30**, 3527-3539.
- Dohner, K., Nagel, C. H. & Sodeik, B. (2005).** Viral stop-and-go along microtubules: taking a ride with dynein and kinesins. *Trends Microbiol* **13**, 320-327.
- Dohner, K., Wolfstein, A., Prank, U., Echeverri, C., Dujardin, D., Vallee, R. & Sodeik, B. (2002).** Function of dynein and dynactin in herpes simplex virus capsid transport. *Mol Biol Cell* **13**, 2795-2809.
- Dominguez, R. & Holmes, K. C. (2011).** Actin structure and function. *Annu Rev Biophys* **40**, 169-186.
- Douglas, M. W., Diefenbach, R. J., Homa, F. L., Miranda-Saksena, M., Rixon, F. J., Vittone, V., Byth, K. & Cunningham, A. L. (2004).** Herpes simplex virus type 1 capsid protein VP26 interacts with dynein light chains RP3 and Tctex1 and plays a role in retrograde cellular transport. *J Biol Chem* **279**, 28522-28530.
- Doxsey, S. J., Stein, P., Evans, L., Calarco, P. D. & Kirschner, M. (1994).** Pericentrin, a highly conserved centrosome protein involved in microtubule organization. *Cell* **76**, 639-650.
- Du, N., Cong, H., Tian, H., Zhang, H., Zhang, W., Song, L. & Tien, P. (2014).** Cell surface vimentin is an attachment receptor for enterovirus 71. *J Virol* **88**, 5816-5833.
- Dufrene, Y. F., Martinez-Martin, D., Medalsy, I., Alsteens, D. & Muller, D. J. (2013).** Multiparametric imaging of biological systems by force-distance curve-based AFM. *Nat Methods* **10**, 847-854.
- Durham, H. D., Pena, S. D. & Carpenter, S. (1983).** The neurotoxins 2,5-hexanedione and acrylamide promote aggregation of intermediate filaments in cultured fibroblasts. *Muscle Nerve* **6**, 631-637.
- Eckert, B. S. & Yeagle, P. L. (1988).** Acrylamide treatment of PtK1 cells causes dephosphorylation of keratin polypeptides. *Cell Motil Cytoskel* **11**, 24-30.
- Eichwald, V., Daeffler, L., Klein, M., Rommelaere, J. & Salome, N. (2002).** The NS2 proteins of parvovirus minute virus of mice are required for efficient nuclear egress of progeny virions in mouse cells. *J Virol* **76**, 10307-10319.
- Engelke, M. F., Burckhardt, C. J., Morf, M. K. & Greber, U. F. (2011).** The dynactin complex enhances the speed of microtubule-dependent motions of adenovirus both towards and away from the nucleus. *Viruses* **3**, 233-253.
- Engelsma, D., Valle, N., Fish, A., Salome, N., Almendral, J. M. & Fornerod, M. (2008).** A supraphysiological nuclear export signal is required for parvovirus nuclear export. *Mol Biol Cell* **19**, 2544-2552.
- Faisst, S., Guittard, D., Benner, A., Cesbron, J. Y., Schlehofer, J. R., Rommelaere, J. & Dupressoir, T. (1998).** Dose-dependent regression of HeLa cell-derived tumours in SCID mice after parvovirus H-1 infection. *Int J Cancer* **75**, 584-589.

- Farr, G. A., Zhang, L. G. & Tattersall, P. (2005).** Parvoviral virions deploy a capsid-tethered lipolytic enzyme to breach the endosomal membrane during cell entry. *Proc Natl Acad Sci USA* **102**, 17148-17153.
- Fassati, A., Gorlich, D., Harrison, I., Zaytseva, L. & Mingot, J. M. (2003).** Nuclear import of HIV-1 intracellular reverse transcription complexes is mediated by importin 7. *EMBO J* **22**, 3675-3685.
- Fletcher, D. A. & Mullins, R. D. (2010).** Cell mechanics and the cytoskeleton. *Nature* **463**, 485-492.
- Frederix, P. L., Bosshart, P. D. & Engel, A. (2009).** Atomic force microscopy of biological membranes. *Biophys J* **96**, 329-338.
- Frischknecht, F., Moreau, V., Rottger, S., Gonfloni, S., Reckmann, I., Superti-Furga, G. & Way, M. (1999).** Actin-based motility of vaccinia virus mimics receptor tyrosine kinase signalling. *Nature* **401**, 926-929.
- Gao, Y. & Sztul, E. (2001).** A novel interaction of the Golgi complex with the vimentin intermediate filament cytoskeleton. *J Cell Biol* **152**, 877-894.
- Gardel, M. L., Kasza, K. E., Brangwynne, C. P., Liu, J. & Weitz, D. A. (2008).** Chapter 19: Mechanical response of cytoskeletal networks. *Methods Cell Biol* **89**, 487-519.
- Geletneky, K., Huesing, J., Rommelaere, J., Schlehofer, J. R., Leuchs, B., Dahm, M., Krebs, O., von Knebel Doeberitz, M., Huber, B. & other authors (2012).** Phase I/IIa study of intratumoral/intracerebral or intravenous/intracerebral administration of Parvovirus H-1 (ParvOryx) in patients with progressive primary or recurrent glioblastoma multiforme: ParvOryx01 protocol. *BMC Cancer* **12**, 99.
- Ghosh, S., Ahrens, W. A., Phatak, S. U., Hwang, S., Schrum, L. W. & Bonkovsky, H. L. (2011).** Association of filamin A and vimentin with hepatitis C virus proteins in infected human hepatocytes. *J Viral Hepat* **18**, e568-577.
- Gladue, D. P., O'Donnell, V., Baker-Branstetter, R., Holinka, L. G., Pacheco, J. M., Sainz, I. F., Lu, Z., Ambroggio, X., Rodriguez, L. & other authors (2013).** Foot-and-mouth disease virus modulates cellular vimentin for virus survival. *J Virol*.
- Goldberg, M. B. (2001).** Actin-based motility of intracellular microbial pathogens. *Microbiol Mol Biol Rev* **65**, 595-626, table of contents.
- Goldman, R. D., Cleland, M. M., Murthy, S. N., Mahammad, S. & Kuczmarski, E. R. (2012).** Inroads into the structure and function of intermediate filament networks. *J Struct Biol* **177**, 14-23.
- Goley, E. D. & Welch, M. D. (2006).** The ARP2/3 complex: an actin nucleator comes of age. *Nat Rev Mol Cell Biol* **7**, 713-726.
- Goley, E. D., Ohkawa, T., Mancuso, J., Woodruff, J. B., D'Alessio, J. A., Cande, W. Z., Volkman, L. E. & Welch, M. D. (2006).** Dynamic nuclear actin assembly by Arp2/3 complex and a baculovirus WASP-like protein. *Science* **314**, 464-467.
- Greber, U. F. & Way, M. (2006).** A superhighway to virus infection. *Cell* **124**, 741-754.
- Grekova, S., Zawatzky, R., Horlein, R., Cziepluch, C., Mincberg, M., Davis, C., Rommelaere, J. & Daeffler, L. (2010a).** Activation of an antiviral response in normal but not transformed mouse cells: a new determinant of minute virus of mice oncotropism. *J Virol* **84**, 516-531.

- Grekova, S., Aprahamian, M., Giese, N., Schmitt, S., Giese, T., Falk, C. S., Daeffler, L., Cziepluch, C., Rommelaere, J. & other authors (2010b).** Immune cells participate in the oncosuppressive activity of parvovirus H-1PV and are activated as a result of their abortive infection with this agent. *Cancer Biol Ther* **10**, 1280-1289.
- Grekova, S. P., Raykov, Z., Zawatzky, R., Rommelaere, J. & Koch, U. (2012).** Activation of a glioma-specific immune response by oncolytic parvovirus Minute Virus of Mice infection. *Cancer Gene Ther* **19**, 468-475.
- Grove, J. & Marsh, M. (2011).** The cell biology of receptor-mediated virus entry. *J Cell Biol* **195**, 1071-1082.
- Halder, S., Cotmore, S., Heimbürg-Molinari, J., Smith, D. F., Cummings, R. D., Chen, X., Trollope, A. J., North, S. J., Haslam, S. M. & other authors (2014).** Profiling of glycan receptors for minute virus of mice in permissive cell lines towards understanding the mechanism of cell recognition. *PLoS One* **9**, e86909.
- Hansma, H. G., Kasuya, K. & Oroudjev, E. (2004).** Atomic force microscopy imaging and pulling of nucleic acids. *Curr Opin Struct Biol* **14**, 380-385.
- Haolong, C., Du, N., Hongchao, T., Yang, Y., Wei, Z., Hua, Z., Wenliang, Z., Lei, S. & Po, T. (2013).** Enterovirus 71 VP1 activates calmodulin-dependent protein kinase II and results in the rearrangement of vimentin in human astrocyte cells. *PLoS One* **8**, e73900.
- Harbison, C. E., Lyi, S. M., Weichert, W. S. & Parrish, C. R. (2009).** Early steps in cell infection by parvoviruses: host-specific differences in cell receptor binding but similar endosomal trafficking. *J Virol* **83**, 10504-10514.
- Hartig, R., Shoeman, R. L., Janetzko, A., Tolstonog, G. & Traub, P. (1998).** DNA-mediated transport of the intermediate filament protein vimentin into the nucleus of cultured cells. *J Cell Sci* **111 (Pt 24)**, 3573-3584.
- Heald, R. & Nogales, E. (2002).** Microtubule dynamics. *J Cell Sci* **115**, 3-4.
- Heath, C. M., Windsor, M. & Wileman, T. (2001).** Aggresomes resemble sites specialized for virus assembly. *J Cell Biol* **153**, 449-455.
- Helfand, B. T., Mikami, A., Vallee, R.B., & Goldman, R.D. (2002).** A requirement for cytoplasmic dynein and dynactin in intermediate filament network assembly and organization. *J Cell Biol* **157 (5)**: 795-806.
- Helfand, B. T., Chang, L. & Goldman, R. D. (2004).** Intermediate filaments are dynamic and motile elements of cellular architecture. *J Cell Sci* **117**, 133-141.
- Herrmann, H., Bar, H., Kreplak, L., Strelkov, S. V. & Aebi, U. (2007).** Intermediate filaments: from cell architecture to nanomechanics. *Nat Rev Mol Cell Biol* **8**, 562-573.
- Hertel, L. (2011).** Herpesviruses and intermediate filaments: close encounters with the third type. *Viruses* **3**, 1015-1040.
- Hirokawa, N., Noda, Y., Tanaka, Y. & Niwa, S. (2009).** Kinesin superfamily motor proteins and intracellular transport. *Nat Rev Mol Cell Biol* **10**, 682-696.
- Hirosue, S., Senn, K., Clement, N., Nonnenmacher, M., Gigout, L., Linden, R. M. & Weber, T. (2007).** Effect of inhibition of dynein function and microtubule-altering drugs on AAV2 transduction. *Virology* **367**, 10-18.

- Holwell, T. A., Schweitzer, S. C. & Evans, R. M. (1997).** Tetracycline regulated expression of vimentin in fibroblasts derived from vimentin null mice. *J Cell Sci* **110 (Pt 16)**, 1947-1956.
- Honer, B., Shoeman, R. L. & Traub, P. (1991).** Human immunodeficiency virus type 1 protease microinjected into cultured human skin fibroblasts cleaves vimentin and affects cytoskeletal and nuclear architecture. *J Cell Sci* **100 (Pt 4)**, 799-807.
- Hristov, G., Kramer, M., Li, J., El-Andaloussi, N., Mora, R., Daeffler, L., Zentgraf, H., Rommelaere, J. & Marchini, A. (2010).** Through its nonstructural protein NS1, parvovirus H-1 induces apoptosis via accumulation of reactive oxygen species. *J Virol* **84**, 5909-5922.
- Hsieh, M. J., White, P. J. & Pouton, C. W. (2010).** Interaction of viruses with host cell molecular motors. *Curr Opin Biotechnol* **21**, 633-639.
- Huang, C. Y., Lu, T. Y., Bair, C. H., Chang, Y. S., Jwo, J. K. & Chang, W. (2008).** A novel cellular protein, VPEF, facilitates vaccinia virus penetration into HeLa cells through fluid phase endocytosis. *J Virol* **82**, 7988-7999.
- Ivaska, J., Pallari, H. M., Nevo, J. & Eriksson, J. E. (2007).** Novel functions of vimentin in cell adhesion, migration, and signaling. *Exp Cell Res* **313**, 2050-2062.
- Izmailyan, R., Hsao, J. C., Chung, C. S., Chen, C. H., Hsu, P. W., Liao, C. L. & Chang, W. (2012).** Integrin beta1 mediates vaccinia virus entry through activation of PI3K/Akt signaling. *J Virol* **86**, 6677-6687.
- Jacquot, G., Maidou-Peindara, P. & Benichou, S. (2010).** Molecular and functional basis for the scaffolding role of the p50/dynamitin subunit of the microtubule-associated dynactin complex. *J Biol Chem* **285**, 23019-23031.
- Janus, L. M. & Bleich, A. (2012).** Coping with parvovirus infections in mice: health surveillance and control. *Lab Anim* **46**, 14-23.
- Jartti, T., Hedman, K., Jartti, L., Ruuskanen, O., Allander, T. & Soderlund-Venermo, M. (2012).** Human bocavirus-the first 5 years. *Rev Med Virol* **22**, 46-64.
- Jovic, M., Sharma, M., Rahajeng, J. & Caplan, S. (2010).** The early endosome: a busy sorting station for proteins at the crossroads. *Histol Histopathol* **25**, 99-112.
- Kanlaya, R., Pattanakitsakul, S. N., Sinchaikul, S., Chen, S. T. & Thongboonkerd, V. (2010).** Vimentin interacts with heterogeneous nuclear ribonucleoproteins and dengue nonstructural protein 1 and is important for viral replication and release. *Mol Biosyst* **6**, 795-806.
- Katz, E., Ward, B. M., Weisberg, A. S. & Moss, B. (2003).** Mutations in the vaccinia virus A33R and B5R envelope proteins that enhance release of extracellular virions and eliminate formation of actin-containing microvilli without preventing tyrosine phosphorylation of the A36R protein. *J Virol* **77**, 12266-12275.
- Kaufmann, B., Lopez-Bueno, A., Mateu, M. G., Chipman, P. R., Nelson, C. D., Parrish, C. R., Almendral, J. M. & Rossmann, M. G. (2007).** Minute virus of mice, a parvovirus, in complex with the Fab fragment of a neutralizing monoclonal antibody. *J Virol* **81**, 9851-9858.
- Kaufmann, K. B., Buning, H., Galy, A., Schambach, A. & Grez, M. (2013).** Gene therapy on the move. *EMBO Mol Med* **5**, 1642-1661.
- Kelkar, S., De, B. P., Gao, G., Wilson, J. M., Crystal, R. G. & Leopold, P. L. (2006).** A common mechanism for cytoplasmic dynein-dependent microtubule binding

- shared among adeno-associated virus and adenovirus serotypes. *J Virol* **80**, 7781-7785.
- Kim, J. K., Fahad, A. M., Shanmukhappa, K. & Kapil, S. (2006).** Defining the cellular target(s) of porcine reproductive and respiratory syndrome virus blocking monoclonal antibody 7G10. *J Virol* **80**, 689-696.
- Kontou, M., Govindasamy, L., Nam, H. J., Bryant, N., Llamas-Saiz, A. L., Foces-Foces, C., Hernando, E., Rubio, M. P., McKenna, R. & other authors (2005).** Structural determinants of tissue tropism and in vivo pathogenicity for the parvovirus minute virus of mice. *J Virol* **79**, 10931-10943.
- Kopito, R. R. (2000).** Aggresomes, inclusion bodies and protein aggregation. *Trends Cell Biol* **10**, 524-530.
- Koudelka, K. J., Rae, C. S., Gonzalez, M. J. & Manchester, M. (2007).** Interaction between a 54-kilodalton mammalian cell surface protein and cowpea mosaic virus. *J Virol* **81**, 1632-1640.
- Koudelka, K. J., Destito, G., Plummer, E. M., Trauger, S. A., Siuzdak, G. & Manchester, M. (2009).** Endothelial targeting of cowpea mosaic virus (CPMV) via surface vimentin. *PLoS Pathog* **5**, e1000417.
- Kreplak, L., Bar, H., Leterrier, J. F., Herrmann, H. & Aebi, U. (2005).** Exploring the mechanical behavior of single intermediate filaments. *J Mol Biol* **354**, 569-577.
- Ku, N. O., Liao, J. & Omary, M. B. (1998).** Phosphorylation of human keratin 18 serine 33 regulates binding to 14-3-3 proteins. *EMBO J* **17**, 1892-1906.
- Kudchodkar, S. B. & Levine, B. (2009).** Viruses and autophagy. *Rev Med Virol* **19**, 359-378.
- Kuznetsov, Y. G. & McPherson, A. (2011).** Atomic force microscopy in imaging of viruses and virus-infected cells. *Microbiol Mol Biol Rev* **75**, 268-285.
- Kuznetsov, Y. G., Malkin, A. J., Lucas, R. W., Plomp, M. & McPherson, A. (2001).** Imaging of viruses by atomic force microscopy. *J Gen Virol* **82**, 2025-2034.
- Lachmann, S., Rommeleare, J. & Nuesch, J. P. (2003).** Novel PKCeta is required to activate replicative functions of the major nonstructural protein NS1 of minute virus of mice. *J Virol* **77**, 8048-8060.
- Lanier, L. M. & Volkman, L. E. (1998).** Actin binding and nucleation by Autographa californica M nucleopolyhedrovirus. *Virology* **243**, 167-177.
- Le Clainche, C. & Carlier, M. F. (2008).** Regulation of actin assembly associated with protrusion and adhesion in cell migration. *Physiol Rev* **88**, 489-513.
- Lei, S., Tian, Y. P., Xiao, W. D., Li, S., Rao, X. C., Zhang, J. L., Yang, J., Hu, X. M. & Chen, W. (2013).** ROCK is involved in vimentin phosphorylation and rearrangement induced by dengue virus. *Cell Biochem Biophys* **67**, 1333-1342.
- Leopold, P. L., Kreitzer, G., Miyazawa, N., Rempel, S., Pfister, K. K., Rodriguez-Boulan, E. & Crystal, R. G. (2000).** Dynein- and microtubule-mediated translocation of adenovirus serotype 5 occurs after endosomal lysis. *Hum Gene Ther* **11**, 151-165.
- Li, X. & Rhode, S. L., 3rd (1991).** Nonstructural protein NS2 of parvovirus H-1 is required for efficient viral protein synthesis and virus production in rat cells in vivo and in vitro. *Virology* **184**, 117-130.

- Liang, J. J., Yu, C. Y., Liao, C. L. & Lin, Y. L. (2011).** Vimentin binding is critical for infection by the virulent strain of Japanese encephalitis virus. *Cell Microbiol* **13**, 1358-1370.
- Lilienbaum, A., Duc Dodon, M., Alexandre, C., Gazzolo, L. & Paulin, D. (1990).** Effect of human T-cell leukemia virus type I tax protein on activation of the human vimentin gene. *J Virol* **64**, 256-263.
- Liu, Y., Shevchenko, A., Shevchenko, A. & Berk, A. J. (2005).** Adenovirus exploits the cellular aggresome response to accelerate inactivation of the MRN complex. *J Virol* **79**, 14004-14016.
- Locker, J. K., Kuehn, A., Schleich, S., Rutter, G., Hohenberg, H., Wepf, R. & Griffiths, G. (2000).** Entry of the two infectious forms of vaccinia virus at the plasma membrane is signaling-dependent for the IMV but not the EEV. *Mol Biol Cell* **11**, 2497-2511.
- Lofling, J., Michael Lyi, S., Parrish, C. R. & Varki, A. (2013).** Canine and feline parvoviruses preferentially recognize the non-human cell surface sialic acid N-glycolylneuraminic acid. *Virology* **440**, 89-96.
- Lombardo, E., Ramirez, J. C., Garcia, J. & Almendral, J. M. (2002).** Complementary roles of multiple nuclear targeting signals in the capsid proteins of the parvovirus minute virus of mice during assembly and onset of infection. *J Virol* **76**, 7049-7059.
- Lopez-Bueno, A., Rubio, M. P., Bryant, N., McKenna, R., Agbandje-McKenna, M. & Almendral, J. M. (2006).** Host-selected amino acid changes at the sialic acid binding pocket of the parvovirus capsid modulate cell binding affinity and determine virulence. *J Virol* **80**, 1563-1573.
- Lyi, S. M., Tan, M. J. A. & Parrish, C. R. (2014).** Parvovirus particles and movement in the cellular cytoplasm and effects of the cytoskeleton. *Virology* **456-457**, 342-352.
- Lyubchenko, Y. L., Shlyakhtenko, L. S. & Ando, T. (2011).** Imaging of nucleic acids with atomic force microscopy. *Methods* **54**, 274-283.
- Machesky, L. M., Insall, R. H. & Volkman, L. E. (2001).** WASP homology sequences in baculoviruses. *Trends Cell Biol* **11**, 286-287.
- Mani, B., Baltzer, C., Valle, N., Almendral, J. M., Kempf, C. & Ros, C. (2006).** Low pH-dependent endosomal processing of the incoming parvovirus minute virus of mice virion leads to externalization of the VP1 N-terminal sequence (N-VP1), N-VP2 cleavage, and uncoating of the full-length genome. *J Virol* **80**, 1015-1024.
- Maroto, B., Valle, N., Saffrich, R. & Almendral, J. M. (2004).** Nuclear export of the nonenveloped parvovirus virion is directed by an unordered protein signal exposed on the capsid surface. *J Virol* **78**, 10685-10694.
- Marsh, M. & Helenius, A. (2006).** Virus entry: open sesame. *Cell* **124**, 729-740.
- Mattei, L. M., Cotmore, S. F., Tattersall, P. & Iwasaki, A. (2013).** Parvovirus evades interferon-dependent viral control in primary mouse embryonic fibroblasts. *Virology* **442**, 20-27.
- Mattila, P. K. & Lappalainen, P. (2008).** Filopodia: molecular architecture and cellular functions. *Nat Rev Mol Cell Biol* **9**, 446-454.

- McMaster, G. K., Beard, P., Engers, H. D. & Hirt, B. (1981).** Characterization of an immunosuppressive parvovirus related to the minute virus of mice. *J Virol* **38**, 317-326.
- Meckes, D. G., Jr., Menaker, N. F. & Raab-Traub, N. (2013).** Epstein-Barr virus LMP1 modulates lipid raft microdomains and the vimentin cytoskeleton for signal transduction and transformation. *J Virol* **87**, 1301-1311.
- Mercer, J. & Helenius, A. (2008).** Vaccinia virus uses macropinocytosis and apoptotic mimicry to enter host cells. *Science* **320**, 531-535.
- Mercer, J. & Helenius, A. (2012).** Gulping rather than sipping: macropinocytosis as a way of virus entry. *Curr Opin Microbiol* **15**, 490-499.
- Mercer, J., Schelhaas, M. & Helenius, A. (2010a).** Virus entry by endocytosis. *Annu Rev Biochem* **79**, 803-833.
- Mercer, J., Knebel, S., Schmidt, F. I., Crouse, J., Burkard, C. & Helenius, A. (2010b).** Vaccinia virus strains use distinct forms of macropinocytosis for host-cell entry. *Proc Natl Acad Sci USA* **107**, 9346-9351.
- Merino-Gracia, J., Garcia-Mayoral, M. F. & Rodriguez-Crespo, I. (2011).** The association of viral proteins with host cell dynein components during virus infection. *FEBS J* **278**, 2997-3011.
- Miller, C. L. & Pintel, D. J. (2002).** Interaction between parvovirus NS2 protein and nuclear export factor Crm1 is important for viral egress from the nucleus of murine cells. *J Virol* **76**, 3257-3266.
- Miller, M. S. & Hertel, L. (2009).** Onset of human cytomegalovirus replication in fibroblasts requires the presence of an intact vimentin cytoskeleton. *J Virol* **83**, 7015-7028.
- Moisan, E. & Girard, D. (2006).** Cell surface expression of intermediate filament proteins vimentin and lamin B1 in human neutrophil spontaneous apoptosis. *J Leukoc Biol* **79**, 489-498.
- Mooren, O. L., Erickson, E. S., Moore-Nichols, D. & Dunn, R. C. (2004).** Nuclear side conformational changes in the nuclear pore complex following calcium release from the nuclear membrane. *Phys Biol* **1**, 125-134.
- Mor-Vaknin, N., Punturieri, A., Sitwala, K. & Markovitz, D. M. (2003).** Vimentin is secreted by activated macrophages. *Nat Cell Biol* **5**, 59-63.
- Moreau, V., Frischknecht, F., Reckmann, I., Vincentelli, R., Rabut, G., Stewart, D. & Way, M. (2000).** A complex of N-WASP and WIP integrates signalling cascades that lead to actin polymerization. *Nat Cell Biol* **2**, 441-448.
- Mucke, N., Kreplak, L., Kirmse, R., Wedig, T., Herrmann, H., Aebi, U. & Langowski, J. (2004).** Assessing the flexibility of intermediate filaments by atomic force microscopy. *J Mol Biol* **335**, 1241-1250.
- Muller, D. J. & Dufrene, Y. F. (2011).** Atomic force microscopy: a nanoscopic window on the cell surface. *Trends Cell Biol* **21**, 461-469.
- Naeger, L. K., Cater, J. & Pintel, D. J. (1990).** The small nonstructural protein (NS2) of the parvovirus minute virus of mice is required for efficient DNA replication and infectious virus production in a cell-type-specific manner. *J Virol* **64**, 6166-6175.
- Naeger, L. K., Salome, N. & Pintel, D. J. (1993).** NS2 is required for efficient translation of viral mRNA in minute virus of mice-infected murine cells. *J Virol* **67**, 1034-1043.

- Nam, H. J., Gurda-Whitaker, B., Gan, W. Y., Ilaria, S., McKenna, R., Mehta, P., Alvarez, R. A. & Agbandje-McKenna, M. (2006).** Identification of the sialic acid structures recognized by minute virus of mice and the role of binding affinity in virulence adaptation. *J Biol Chem* **281**, 25670-25677.
- Nekrasova, O. E., Mendez, M. G., Chernoiivanenko, I. S., Tyurin-Kuzmin, P. A., Kuczmarski, E. R., Gelfand, V. I., Goldman, R. D. & Minin, A. A. (2011).** Vimentin intermediate filaments modulate the motility of mitochondria. *Mol Biol Cell* **22**, 2282-2289.
- Newsome, T. P., Weisswange, I., Frischknecht, F. & Way, M. (2006).** Abl collaborates with Src family kinases to stimulate actin-based motility of vaccinia virus. *Cell Microbiol* **8**, 233-241.
- Nonnenmacher, M. & Weber, T. (2011).** Adeno-associated virus 2 infection requires endocytosis through the CLIC/GEEC pathway. *Cell Host Microbe* **10**, 563-576.
- Nuesch, J. P. & Rommelaere, J. (2006).** NS1 interaction with CKII alpha: novel protein complex mediating parvovirus-induced cytotoxicity. *J Virol* **80**, 4729-4739.
- Nuesch, J. P., Lachmann, S. & Rommelaere, J. (2005).** Selective alterations of the host cell architecture upon infection with parvovirus minute virus of mice. *Virology* **331**, 159-174.
- Nuesch, J. P., Lachmann, S., Corbau, R. & Rommelaere, J. (2003).** Regulation of minute virus of mice NS1 replicative functions by atypical PKClambda in vivo. *J Virol* **77**, 433-442.
- Nuesch, J. P., Lacroix, J., Marchini, A. & Rommelaere, J. (2012).** Molecular pathways: rodent parvoviruses--mechanisms of oncolysis and prospects for clinical cancer treatment. *Clin Cancer Res* **18**, 3516-3523.
- Ohkawa, T., Volkman, L. E. & Welch, M. D. (2010).** Actin-based motility drives baculovirus transit to the nucleus and cell surface. *J Cell Biol* **190**, 187-195.
- Op De Beeck, A., Sobczak-Thepot, J., Sirma, H., Bourgain, F., Brechot, C. & Caillet-Fauquet, P. (2001).** NS1- and minute virus of mice-induced cell cycle arrest: involvement of p53 and p21(cip1). *J Virol* **75**, 11071-11078.
- Paglino, J. C., Andres, W. & van den Pol, A. N. (2014).** Autonomous parvoviruses neither stimulate nor are inhibited by the type I interferon response in human normal or cancer cells. *J Virol* **88**, 4932-4942.
- Parker, J. S. & Parrish, C. R. (2000).** Cellular uptake and infection by canine parvovirus involves rapid dynamin-regulated clathrin-mediated endocytosis, followed by slower intracellular trafficking. *J Virol* **74**, 1919-1930.
- Parker, J. S., Murphy, W. J., Wang, D., O'Brien, S. J. & Parrish, C. R. (2001).** Canine and feline parvoviruses can use human or feline transferrin receptors to bind, enter, and infect cells. *J Virol* **75**, 3896-3902.
- Parrish, C. R. (2010).** Structures and functions of parvovirus capsids and the process of cell infection. *Curr Top Microbiol Immunol* **343**, 149-176.
- Perides, G., Harter, C. & Traub, P. (1987).** Electrostatic and hydrophobic interactions of the intermediate filament protein vimentin and its amino terminus with lipid bilayers. *J Biol Chem* **262**, 13742-13749.
- Petermann, P., Haase, I. & Knebel-Morsdorf, D. (2009).** Impact of Rac1 and Cdc42 signaling during early herpes simplex virus type 1 infection of keratinocytes. *J Virol* **83**, 9759-9772.

- Plodinec, M., Loparic, M., Suetterlin, R., Herrmann, H., Aebi, U. & Schoenenberger, C. A. (2011).** The nanomechanical properties of rat fibroblasts are modulated by interfering with the vimentin intermediate filament system. *J Struct Biol* **174**, 476-484.
- Porwal, M., Cohen, S., Snoussi, K., Popa-Wagner, R., Anderson, F., Dugot-Senant, N., Wodrich, H., Dinsart, C., Kleinschmidt, J. A. & other authors (2013).** Parvoviruses cause nuclear envelope breakdown by activating key enzymes of mitosis. *PLoS Pathog* **9**, e1003671.
- Quattrocchi, S., Ruprecht, N., Bonsch, C., Bieli, S., Zurcher, C., Boller, K., Kempf, C. & Ros, C. (2012).** Characterization of the early steps of human parvovirus B19 infection. *J Virol* **86**, 9274-9284.
- Radtke, K., Dohner, K. & Sodeik, B. (2006).** Viral interactions with the cytoskeleton: a hitchhiker's guide to the cell. *Cell Microbiol* **8**, 387-400.
- Raykov, Z., Grekova, S. P., Horlein, R., Leuchs, B., Giese, T., Giese, N. A., Rommelaere, J., Zawatzky, R. & Daeffler, L. (2013).** TLR-9 contributes to the antiviral innate immune sensing of rodent parvoviruses MVMP and H-1PV by normal human immune cells. *PLoS One* **8**, e55086.
- Rieder, C. L., Faruki, S. & Khodjakov, A. (2001).** The centrosome in vertebrates: more than a microtubule-organizing center. *Trends Cell Biol* **11**, 413-419.
- Riolobos, L., Reguera, J., Mateu, M. G. & Almendral, J. M. (2006).** Nuclear transport of trimeric assembly intermediates exerts a morphogenetic control on the icosahedral parvovirus capsid. *J Mol Biol* **357**, 1026-1038.
- Risco, C., Rodriguez, J. R., Lopez-Iglesias, C., Carrascosa, J. L., Esteban, M. & Rodriguez, D. (2002).** Endoplasmic reticulum-Golgi intermediate compartment membranes and vimentin filaments participate in vaccinia virus assembly. *J Virol* **76**, 1839-1855.
- Roberts, K. L. & Baines, J. D. (2011).** Actin in herpesvirus infection. *Viruses* **3**, 336-346.
- Ros, C. & Kempf, C. (2004).** The ubiquitin-proteasome machinery is essential for nuclear translocation of incoming minute virus of mice. *Virology* **324**, 350-360.
- Ros, C., Burckhardt, C. J. & Kempf, C. (2002).** Cytoplasmic trafficking of minute virus of mice: low-pH requirement, routing to late endosomes, and proteasome interaction. *J Virol* **76**, 12634-12645.
- Ruiz, Z., D'Abramo, A., Jr. & Tattersall, P. (2006).** Differential roles for the C-terminal hexapeptide domains of NS2 splice variants during MVM infection of murine cells. *Virology* **349**, 382-395.
- Ruiz, Z., Mihaylov, I. S., Cotmore, S. F. & Tattersall, P. (2011).** Recruitment of DNA replication and damage response proteins to viral replication centers during infection with NS2 mutants of Minute Virus of Mice (MVM). *Virology* **410**, 375-384.
- Russell, S. J., Peng, K. W. & Bell, J. C. (2012).** Oncolytic virotherapy. *Nat Biotechnol* **30**, 658-670.
- Sambrook, J. & Russell, D. W. (2001).** *Molecular cloning: a laboratory manual*, 3rd edn, vol. 1. Cold Spring Harbor, N.Y.: Cold Spring Harbor Laboratory Press.
- Satelli, A. & Li, S. (2011).** Vimentin in cancer and its potential as a molecular target for cancer therapy. *Cell Mol Life Sci* **68**, 3033-3046.

- Scaplehorn, N., Holmstrom, A., Moreau, V., Frischknecht, F., Reckmann, I. & Way, M. (2002).** Grb2 and Nck act cooperatively to promote actin-based motility of vaccinia virus. *Curr Biol* **12**, 740-745.
- Schreiner, S., Wimmer, P. & Dobner, T. (2012).** Adenovirus degradation of cellular proteins. *Future Microbiol* **7**, 211-225.
- Schroeder, N., Chung, C. S., Chen, C. H., Liao, C. L. & Chang, W. (2012).** The lipid raft-associated protein CD98 is required for vaccinia virus endocytosis. *J Virol* **86**, 4868-4882.
- Schroer, T. A. (2004).** Dynactin. *Annu Rev Cell Dev Biol* **20**, 759-779.
- Segura-Totten, M. & Wilson, K. L. (2001).** Virology. HIV--breaking the rules for nuclear entry. *Science* **294**, 1016-1017.
- Shoeman, R. L., Huttermann, C., Hartig, R. & Traub, P. (2001).** Amino-terminal polypeptides of vimentin are responsible for the changes in nuclear architecture associated with human immunodeficiency virus type 1 protease activity in tissue culture cells. *Mol Biol Cell* **12**, 143-154.
- Shoeman, R. L., Honer, B., Stoller, T. J., Kesselmeier, C., Miedel, M. C., Traub, P. & Graves, M. C. (1990).** Human immunodeficiency virus type 1 protease cleaves the intermediate filament proteins vimentin, desmin, and glial fibrillary acidic protein. *Proc Natl Acad Sci USA* **87**, 6336-6340.
- Singh, B. B., Patel, H. H., Roepman, R., Schick, D. & Ferreira, P. A. (1999).** The zinc finger cluster domain of RanBP2 is a specific docking site for the nuclear export factor, exportin-1. *J Biol Chem* **274**, 37370-37378.
- Slonska, A., Polowy, R., Golke, A. & Cymerys, J. (2012).** Role of cytoskeletal motor proteins in viral infection. *Postepy Hig Med Dosw (Online)* **66**, 810-817.
- Sodeik, B. (2000).** Mechanisms of viral transport in the cytoplasm. *Trends Microbiol* **8**, 465-472.
- Sodeik, B., Ebersold, M. W. & Helenius, A. (1997).** Microtubule-mediated transport of incoming herpes simplex virus 1 capsids to the nucleus. *J Cell Biol* **136**, 1007-1021.
- Spalholz, B. A. & Tattersall, P. (1983).** Interaction of minute virus of mice with differentiated cells: strain-dependent target cell specificity is mediated by intracellular factors. *J Virol* **46**, 937-943.
- Sripada, S. & Dayaraj, C. (2010).** Viral interactions with intermediate filaments: Paths less explored. *Cell Health and Cytoskeleton* **2**, 1-7.
- Stefanovic, S., Windsor, M., Nagata, K. I., Inagaki, M. & Wileman, T. (2005).** Vimentin rearrangement during African swine fever virus infection involves retrograde transport along microtubules and phosphorylation of vimentin by calcium calmodulin kinase II. *J Virol* **79**, 11766-11775.
- Steinert, P. M. & Parry, D. A. (1985).** Intermediate filaments: conformity and diversity of expression and structure. *Annu Rev Cell Biol* **1**, 41-65.
- Stoffler, D., Goldie, K. N., Feja, B. & Aebi, U. (1999).** Calcium-mediated structural changes of native nuclear pore complexes monitored by time-lapse atomic force microscopy. *J Mol Biol* **287**, 741-752.
- Stolp, B. & Fackler, O. T. (2011).** How HIV takes advantage of the cytoskeleton in entry and replication. *Viruses* **3**, 293-311.

- Strelkov, S. V., Herrmann, H. & Aebi, U. (2003).** Molecular architecture of intermediate filaments. *Bioessays* **25**, 243-251.
- Strunze, S., Trotman, L. C., Boucke, K. & Greber, U. F. (2005).** Nuclear targeting of adenovirus type 2 requires CRM1-mediated nuclear export. *Mol Biol Cell* **16**, 2999-3009.
- Strunze, S., Engelke, M. F., Wang, I. H., Puntener, D., Boucke, K., Schleich, S., Way, M., Schoenenberger, P., Burckhardt, C. J. & other authors (2011).** Kinesin-1-mediated capsid disassembly and disruption of the nuclear pore complex promote virus infection. *Cell Host Microbe* **10**, 210-223.
- Styers, M. L., Kowalczyk, A. P. & Faundez, V. (2005).** Intermediate filaments and vesicular membrane traffic: the odd couple's first dance? *Traffic* **6**, 359-365.
- Styers, M. L., Salazar, G., Love, R., Peden, A. A., Kowalczyk, A. P. & Faundez, V. (2004).** The endo-lysosomal sorting machinery interacts with the intermediate filament cytoskeleton. *Mol Biol Cell* **15**, 5369-5382.
- Suikkanen, S., Saajarvi, K., Hirsimaki, J., Valilehto, O., Reunanen, H., Vihinen-Ranta, M. & Vuento, M. (2002).** Role of recycling endosomes and lysosomes in dynein-dependent entry of canine parvovirus. *J Virol* **76**, 4401-4411.
- Suikkanen, S., Aaltonen, T., Nevalainen, M., Valilehto, O., Lindholm, L., Vuento, M. & Vihinen-Ranta, M. (2003).** Exploitation of microtubule cytoskeleton and dynein during parvoviral traffic toward the nucleus. *J Virol* **77**, 10270-10279.
- Summerford, C. & Samulski, R. J. (1998).** Membrane-associated heparan sulfate proteoglycan is a receptor for adeno-associated virus type 2 virions. *J Virol* **72**, 1438-1445.
- Summerford, C., Bartlett, J. S. & Samulski, R. J. (1999).** AlphaVbeta5 integrin: a co-receptor for adeno-associated virus type 2 infection. *Nat Med* **5**, 78-82.
- Suomalainen, M., Nakano, M. Y., Keller, S., Boucke, K., Stidwill, R. P. & Greber, U. F. (1999).** Microtubule-dependent plus- and minus end-directed motilities are competing processes for nuclear targeting of adenovirus. *J Cell Biol* **144**, 657-672.
- Takai, Y., Ogawara, M., Tomono, Y., Moritoh, C., Imajoh-Ohmi, S., Tsutsumi, O., Taketani, Y. & Inagaki, M. (1996).** Mitosis-specific phosphorylation of vimentin by protein kinase C coupled with reorganization of intracellular membranes. *J Cell Biol* **133**, 141-149.
- Tattersall, P. (1972).** Replication of the parvovirus MVM. I. Dependence of virus multiplication and plaque formation on cell growth. *J Virol* **10**, 586-590.
- Tattersall, P. & Bratton, J. (1983).** Reciprocal productive and restrictive virus-cell interactions of immunosuppressive and prototype strains of minute virus of mice. *J Virol* **46**, 944-955.
- Tattersall, P., Cawte, P. J., Shatkin, A. J. & Ward, D. C. (1976).** Three structural polypeptides coded for by minute virus of mice, a parvovirus. *J Virol* **20**, 273-289.
- Taylor, M. P., Koyuncu, O. O. & Enquist, L. W. (2011).** Subversion of the actin cytoskeleton during viral infection. *Nat Rev Microbiol* **9**, 427-439.
- Teo, C. S. & Chu, J. J. (2014).** Cellular vimentin regulates construction of dengue virus replication complexes through interaction with NS4A protein. *J Virol* **88**, 1897-1913.

- Thiery, J. P. (2002).** Epithelial-mesenchymal transitions in tumour progression. *Nat Rev Cancer* **2**, 442-454.
- Thomas, E. K., Connelly, R. J., Pennathur, S., Dubrovsky, L., Haffar, O. K. & Bukrinsky, M. I. (1996).** Anti-idiotypic antibody to the V3 domain of gp120 binds to vimentin: a possible role of intermediate filaments in the early steps of HIV-1 infection cycle. *Viral Immunol* **9**, 73-87.
- Tiwari, V. & Shukla, D. (2010).** Phosphoinositide 3 kinase signalling may affect multiple steps during herpes simplex virus type-1 entry. *J Gen Virol* **91**, 3002-3009.
- Toivola, D. M., Tao, G. Z., Habtezion, A., Liao, J. & Omary, M. B. (2005).** Cellular integrity plus: organelle-related and protein-targeting functions of intermediate filaments. *Trends Cell Biol* **15**, 608-617.
- Traub, P., Mothes, E., Shoeman, R., Kuhn, S. & Scherbarth, A. (1992).** Characterization of the nucleic acid-binding activities of the isolated amino-terminal head domain of the intermediate filament protein vimentin reveals its close relationship to the DNA-binding regions of some prokaryotic single-stranded DNA-binding proteins. *J Mol Biol* **228**, 41-57.
- Tullis, G. E., Burger, L. R. & Pintel, D. J. (1993).** The minor capsid protein VP1 of the autonomous parvovirus minute virus of mice is dispensable for encapsidation of progeny single-stranded DNA but is required for infectivity. *J Virol* **67**, 131-141.
- Vale, R. D. (2003).** The molecular motor toolbox for intracellular transport. *Cell* **112**, 467-480.
- Valetti, C., Wetzel, D. M., Schrader, M., Hasbani, M. J., Gill, S. R., Kreis, T. E. & Schroer, T. A. (1999).** Role of dynactin in endocytic traffic: effects of dynamitin overexpression and colocalization with CLIP-170. *Mol Biol Cell* **10**, 4107-4120.
- Vallee, R. B., Williams, J. C., Varma, D. & Barnhart, L. E. (2004).** Dynein: An ancient motor protein involved in multiple modes of transport. *J Neurobiol* **58**, 189-200.
- Van den Broeke, C. & Favoreel, H. W. (2011).** Actin' up: herpesvirus interactions with Rho GTPase signaling. *Viruses* **3**, 278-292.
- Ventoso, I., Berlanga, J. J. & Almendral, J. M. (2010).** Translation control by protein kinase R restricts minute virus of mice infection: role in parvovirus oncolysis. *J Virol* **84**, 5043-5051.
- Vicente, D., Cilla, G., Montes, M., Perez-Yarza, E. G. & Perez-Trallero, E. (2007).** Human bocavirus, a respiratory and enteric virus. *Emerg Infect Dis* **13**, 636-637.
- Vihinen-Ranta, M. & Parrish, C. R. (2006).** Cell infection processes of autonomous parvoviruses. In *Parvoviruses*, pp. 157-163. Edited by J. R. Kerr, S. F. Cotmore, M. E. Bloom, R. M. Linden & C. R. Parrish. London, UK: Hodder Arnold.
- Vihinen-Ranta, M., Yuan, W. & Parrish, C. R. (2000).** Cytoplasmic trafficking of the canine parvovirus capsid and its role in infection and nuclear transport. *J Virol* **74**, 4853-4859.
- Wade, R. H. (2009).** On and around microtubules: an overview. *Mol Biotechnol* **43**, 177-191.
- Ward, B. M. (2011).** The taking of the cytoskeleton one two three: how viruses utilize the cytoskeleton during egress. *Virology* **411**, 244-250.
- Weclawicz, K., Kristensson, K. & Svensson, L. (1994).** Rotavirus causes selective vimentin reorganization in monkey kidney CV-1 cells. *J Gen Virol* **75 (Pt 11)**, 3267-3271.

- Welch, M. D. & Way, M. (2013).** Arp2/3-mediated actin-based motility: a tail of pathogen abuse. *Cell Host Microbe* **14**, 242-255.
- Wileman, T. (2006).** Aggresomes and autophagy generate sites for virus replication. *Science* **312**, 875-878.
- Wileman, T. (2007).** Aggresomes and pericentriolar sites of virus assembly: cellular defense or viral design? *Annu Rev Microbiol* **61**, 149-167.
- Williams, W. P., Tamburic, L. & Astell, C. R. (2004).** Increased levels of B1 and B2 SINE transcripts in mouse fibroblast cells due to minute virus of mice infection. *Virology* **327**, 233-241.
- Wu, Z., Miller, E., Agbandje-McKenna, M. & Samulski, R. J. (2006).** Alpha2,3 and alpha2,6 N-linked sialic acids facilitate efficient binding and transduction by adeno-associated virus types 1 and 6. *J Virol* **80**, 9093-9103.
- Xiao, P. J. & Samulski, R. J. (2012).** Cytoplasmic trafficking, endosomal escape, and perinuclear accumulation of adeno-associated virus type 2 particles are facilitated by microtubule network. *J Virol* **86**, 10462-10473.
- Yamauchi, Y. & Helenius, A. (2013).** Virus entry at a glance. *J Cell Sci* **126**, 1289-1295.
- Yasui, Y., Goto, H., Matsui, S., Manser, E., Lim, L., Nagata, K. & Inagaki, M. (2001).** Protein kinases required for segregation of vimentin filaments in mitotic process. *Oncogene* **20**, 2868-2876.
- Ye, G. J., Vaughan, K. T., Vallee, R. B. & Roizman, B. (2000).** The herpes simplex virus 1 U(L)34 protein interacts with a cytoplasmic dynein intermediate chain and targets nuclear membrane. *J Virol* **74**, 1355-1363.
- Yeung, D. E., Brown, G. W., Tam, P., Russnak, R. H., Wilson, G., Clark-Lewis, I. & Astell, C. R. (1991).** Monoclonal antibodies to the major nonstructural nuclear protein of minute virus of mice. *Virology* **181**, 35-45.
- Yoder, A., Yu, D., Dong, L., Iyer, S. R., Xu, X., Kelly, J., Liu, J., Wang, W., Vorster, P. J. & other authors (2008).** HIV envelope-CXCR4 signaling activates cofilin to overcome cortical actin restriction in resting CD4 T cells. *Cell* **134**, 782-792.
- Zadori, Z., Szelei, J., Lacoste, M. C., Li, Y., Gariépy, S., Raymond, P., Allaire, M., Nabi, I. R. & Tijssen, P. (2001).** A viral phospholipase A2 is required for parvovirus infectivity. *Dev Cell* **1**, 291-302.